Mechanistic Studies on Zymogen-Activator and Adhesion Proteins (ZAAPs) as Thrombolytic Drugs and Bacterial Virulence Factors

Sian Huish

Department of Life Sciences,

Imperial College, London

&

Department of Biotherapeutics

NIBSC, Hertfordshire

PhD, September 2015

Abstract

Streptokinase (SK), expressed by Lancefield Group A, C and G β-haemolytic Streptococci and Staphylocoagulase (SCG), expressed by S. *aureus*, are bacterial virulence factors which belong to a family of proteins known as Zymogen-activator and adhesion proteins (ZAAPs). SK and SCG are responsible for the non-proteolytic activation of plasminogen and prothrombin, respectively. Understanding of SK activity is exclusively based on the Group C (GCS) S. *equisimilis* H46a SK, a 'clot buster' or thrombolytic used in the treatment of Myocardial Infarction (MI), which exhibits no fibrin specificity. SK is the most used thrombolytic worldwide.

Here, detailed kinetic studies in purified assay systems explored the mechanistic variation between a recombinant H46a SK (rSK H46a) and a Group A Streptococcal SK (M1GAS), most typically isolated in invasive human infection. This work demonstrates a fibrin specific mechanism for M1GAS SK and proposes a kinetic model for M1GAS SK plasminogen activation, to compliment the "Trigger and Bullet" hypothesis for H46a SK by Bock and colleagues.

This work has relevance to the use of SK variants, with enhanced fibrin specificity, for improvement of thrombolytic therapies. Cardiovascular diseases such as myocardial infaraction and ischaemic stroke are significant casues of mortality, particularly in the developing world. Access to Alteplase, an expensive recombinant tPA and the only licensed treatment for stroke, is limited and there is interest in the use of SK for this purpose. Furthermore, microbial resistance is an increasing health burden, as demonstrated by programs such as the Longitude prize. Exploring the mechanisms of bacterial virulence factors at the molecular level such as this could provide rationale for the development of much-needed new antimicrobial technologies.

Acknowledgements

Firstly, I wish to thank my supervisors, Dr Craig Thelwell and Dr Colin Longstaff (NIBSC) and Prof. Neil Fairweather (Imperial College, London) for this opportunity, and their guidance. Thank you to Craig for all the scientific and not quite so scientific conversations, and the countless hours of training. Thank you to Colin (you're one of a kind!) for your time and for sharing so much of your knowledge and expertise. I have learnt so much from you both, for which I am so very grateful.

I would also like to thank all my friends at NIBSC, particularly in Haemostasis, for their endless encouragement and advice. A special thanks to Sarah, Stella, John and Helen who provided extra support on innumerable occasions. Thank you also to Dr Huw Williams and Prof. Tony Cass (Imperial College, London), my progress review panel.

Thank you to my family - Mum, Dad, Nan, Leah and Ellie, who have given me unconditional love, clarity and a retreat whenever I needed. Thank you to Thivya (the strongest person I know) and Kumi (the wisest and kindest), two of my closest friends who encourage my good and bad sides in equal measure, and most importantly, understand everything without me saying a word.

Lastly, my biggest thanks goes to Ben, for which there really are no words. We made it to the end, together. I love you.

Sian Huish

London, September 2015

'Nobody said it was easy. No one ever said it would be this hard.' Lyrics from *The Scientist*, by Coldplay.

'For the things we have to learn before we can do, we learn by doing.' from *The Nicomachean Ethics*, by Aristotle.

Table of contents

Contents of figures

Contents of tables

Abbreviations

Acronym	Phrase
AmpR	Ampicillin resistance gene
DTT	Dithiothreitol
EDQM	European Directorate for the Quality of Medicines
EP	European Pharmacopeioa
FDP	Fibrin degradation products
GAS	Group A Streptococci
GCS	Group C Streptococci
Glu-Pg	Glu-plasminogen
GST	Glutathione *S*-transferase
HSA	Human Serum Albumin
IC_{50}	Inhibitory concentration that is 50% the maximal
IU	International units
k_{cat}	Catalytic constant
K_D	Dissociation constant
kDa	Kilodalton
K_M	Michaelis constant
LB	Luria-Bertani media
Lys-Pg	Lys-plasminogen
M1GAS	M1 serotype Group A Streptococci
M1GAS SK	Streptokinase from the M1 type Group A Steptococci
OD	Optical density
PAM	Plasminogen-binding Group A Streptococcal M protein
PCI	Percutaneous coronary intervention
PCR	Polymerase chain reaction
Pg	Plasminogen
Pm	Plasmin
pNA	*p*-nitroaniline
rEK	Recombinant enterokinase

rSK	Recombinant Streptokinase
rSK H46a	Recombinant Streptokinase from Group C S. *equisimilis* H46a
rSK M1GAS	Recombinant Streptokinase from M1 Group A S. *pyogenes*
SAK	Staphylokinase
SCG	Staphylocoagulase
scuPA	Single chain urokinase
SD	Standard deviation
SDS-PAGE	Sodium dodecyl sulfate polyacrylamide gel electrophoresis
SEM	Standard error of the mean
SK	Streptokinase
STSS	Streptococcal toxic shock syndrome
tPA	Tissue-type plasminogen activator
uPA	Urokinase
V	velocity
V_{max}	Maximal velocity
WHO	World Health Organisation
YFP	Yellow fluorescent protein
ZAAPs	Zymogen-activator and adhesion proteins

Statement of originality

I confirm, in this statement of originality, that the work presented here and entered for PhD examination is entirely my own, except where appropriately referenced. The total word count of this thesis is 36,787 excluding references and appendices.

Chapter 1: Introduction

1.1 An overview of haemostasis and fibrinoysis

Haemostasis, the prevention of blood loss, and fibrinolysis (clot breakdown) are a delicate equilibrium necessary to ensure continuous blood flow, thus preventing ischaemia and maintaining a functional vascular system, whilst avoiding excess blood loss following blood vessel damage (Marder, 2012). Haemostasis is generally divided into primary and secondary haemostasis. Primary haemostasis is the formation of a platelet plug, the initial step to prevent blood loss, with secondary haemostasis the act of blood coagulation (Clemetson, 2012). There are two main triggers of coagulation - the extrinsic and the intrinsic pathways. The extrinsic pathway is initiated by tissue damage which causes tissue factor release, whereas the intrinsic pathway is initiated by contact with negatively charged surfaces, including the surface of platelets (Marder, 2012).

Many steps in the coagulation and fibrinolysis pathways involve conversion of inactive zymogens to active serine proteases, thus forming an amplifying cascade; an idea first proposed in 1964 (Davie and Ratnoff, 1964). Overall, the main intention of the coagulation cascade is the generation of thrombin, which among other functions such as FXIII and platelet activation catalyses the hydrolysis of fibrinogen to form fibrin, the protein framework of blood clots (Figure 1.1) (Davie, 2003).

Fibrinolysis, initiated by plasminogen conversion to plasmin, counteracts the effect of the coagulation cascade, to subsequently breakdown the fibrin clot (Cesarman-Maus and Hajjar, 2005). The sophisticated feedback loops of the coagulation and fibrinolysis factors maintain healthy blood flow with essential input from platelets providing further regulation.

As well as maintaining blood flow and preventing blood loss, coagulation is critical for mammalian response to pathogenic invasion. Fibrin clots help to trap pathogens preventing their entry into the blood (see section 1.8 for further information).

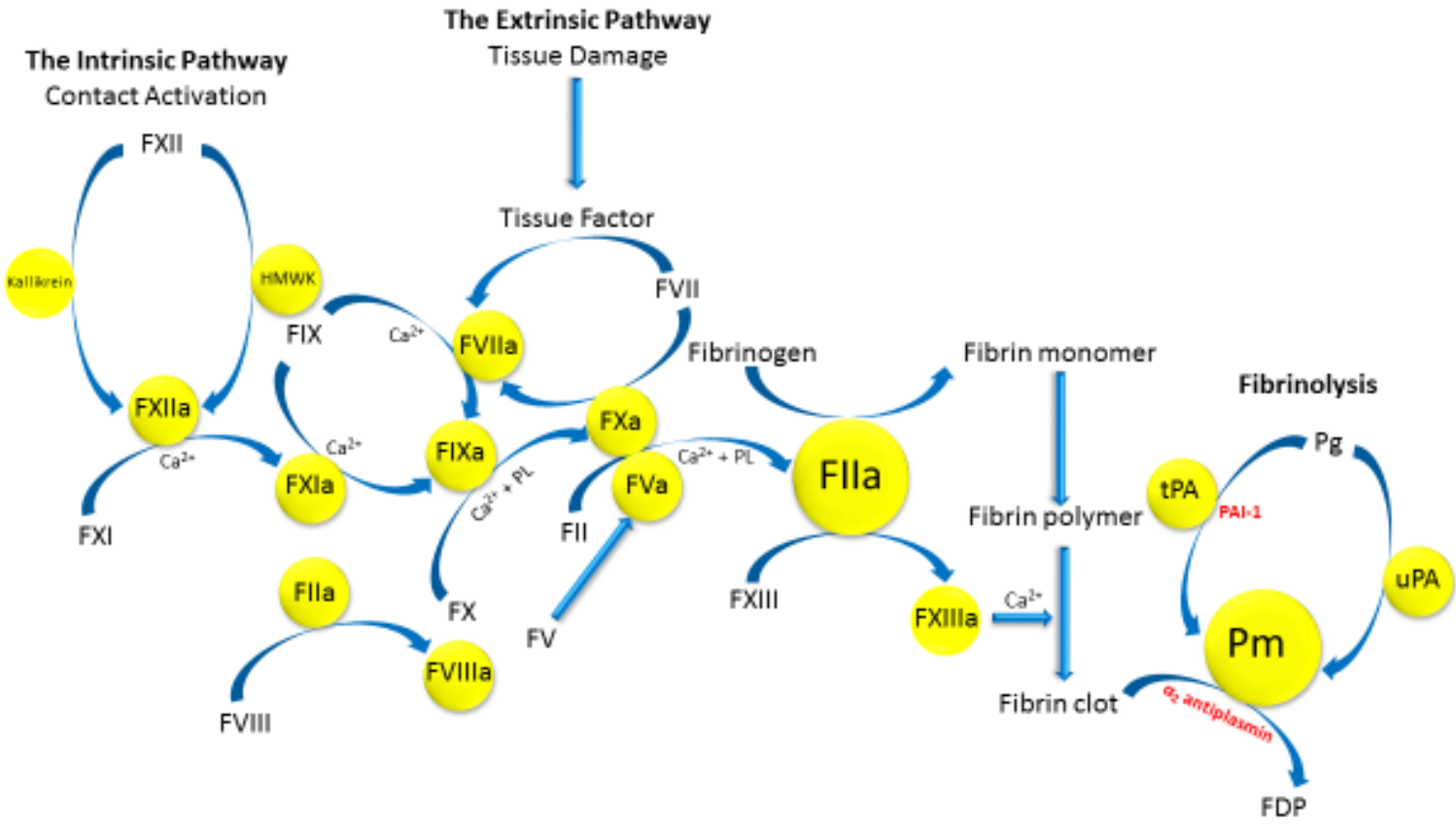

Figure 1.1 A simplified coagulation cascade. The coagulation cascade culminates in the activation of prothrombin, to the serine protease thrombin, and thus the initiation of fibrin formation. Thrombin also activates FXIII to FXIIIa which cross-links fibrin to stabilise the clot. Plasminogen is activated to the serine protease plasmin by physiological plasminogen activators tPA and uPA to promote fibrinolysis, the dissolution of fibrin into fibrin degradation products.

1.2 Fibrinogen and fibrin formation

Fibrinogen is a large (340 kDa) soluble glycoprotein dimer circulating in human blood and extracellular fluids (Chapin and Hajjar, 2015). Though considered inert in circulation, fragments made in a variety of ways can enhance plasminogen activation, and fibrinogen has been shown to enhance the activity of urokinase (uPA) and tPA (Thelwell and Longstaff, 2007, Bringmann et al., 1995a).

Fibrinogen consists of three polypeptide chains termed Aα, Bβ and γ (Henschen et al., 1983) which fold to form a central E structural domain, two D regions and αC domains (Medved and Nieuwenhuizen, 2003). The E domain contains fibrinopeptide A and fibrinopeptide B. Thrombin initially cleaves at Arg^{17}-Gly^{18} on the Aα chain and then at Arg^{14}-Gly^{15} on the Bβ polypeptide, to releases fibrinopeptide A first, and then fibrinopeptide B, from the fibrinogen molecule to initiate fibrin formation (Medved and Nieuwenhuizen, 2003). This cleavage exposes knobs 'A' and 'B' located on the E domain, allowing them to fit into holes 'a' and 'b' respectively, located in the D region, of other fibrinogen molecules. It is the removal and arrangement of fibrinopeptide A first that promotes protofibril formation and their lateral overlapping (Medved and Nieuwenhuizen, 2003). The cleavage to release fibrinopeptide B, which occurs subsequently, promotes lateral association of protofibrils (Yang et al., 2000). The release of fibrinopeptide B is combined with dissociation of the αC domains within the molecule from the central domain, promoting aggregation (Nieuwenhuizen, 2001, Undas and Ariens, 2011).

Aside from cleaving fibrinogen, thrombin can activate the transglutaminase factor XIII (FXIIIa), which cross-links the fibrin polymers during fibrin formation via a ε(γ-glutamyl)lysine bond thus supporting the fibrin structure and elasticity (Chapin and Hajjar, 2015, Undas and Ariens, 2011, Duval et al., 2014, Hethershaw et al., 2014). FXIIIa also cross-links the plasmin inhibitor α_2-antiplasmin to fibrin strands during fibrin clot formation, to further protect from fibrinolysis (Pisano et al., 1968, Fraser et al., 2011).

1.3 Plasminogen, plasmin and fibrinolysis

Fibrinolysis is the process of fibrin breakdown to promote clot dissolution. A key event in fibrinolysis is the activation of plasminogen to plasmin, a broad-specificity serine protease responsible for fibrin hydrolysis (Chapin and Hajjar, 2015). Plasminogen, a 92 kDa zymogen, consists of an amino-terminal peptide sequence, five structural domains known as kringles and a catalytic domain (serine protease) (Longstaff and Kolev, 2015).

The zymogen circulates in human plasma at high concentrations (180-200 µg/ml), in a soluble form, termed Glu-Pg owing to the amino-terminal glutamic acid residue (Lahteenmaki et al., 2001). Glu-Pg is closed conformation and thus resistant to activation (Horrevoets et al., 1995). Published crystal structures of full-length human Glu-Pg have recently become available, providing further insight into the intramolecular interactions involved (Law et al., 2012, Xue et al., 2012). The kringle domains of plasminogen contain lysine binding sites (LBS) which facilitate binding with fibrin and helps to incorporate plasminogen into clots as they form (Lucas et al., 1983). Fibrin binding also alters Glu-Pg conformation to a more open and easily activated form (Horrevoets et al., 1995). Limited exposure of inactive plasminogen to plasmin upon activation, results in cleavage of the Lys^{76}-Lys^{77} peptide bond and release of the amino-terminal peptide sequence. This newly formed plasminogen, known as Lys-Pg, is more readily activated (Horrevoets et al., 1995, Lucas et al., 1983).

Plasmin consists of two-chains, a heavy chain (65 kDa), and a light chain (25 kDa) which contains the active site, linked by two disulfide bonds (Cesarman-Maus and Hajjar, 2005). The active serine protease initially catalyses the generation of C-terminal lysine residues to increase binding of plasminogen and the plasminogen activator, tPA to further promote plasmin generation (Cesarman-Maus and Hajjar, 2005). Hydrolysis of fibrin through cleavage of several sites generates multiple degradation products including D-dimer, leading to clot dissolution (Figure 1.1). Plasmin activity is inhibited by α_2-antiplasmin, but binding to fibrin protects plasmin from α_2-antiplasmin inactivation (Schneider and Nesheim, 2004).

1.4 Physiological plasminogen activators and their regulation of fibrinolysis

Physiological plasminogen activators include the proteases tissue-type plasminogen activator (tPA) and urokinase (uPA). tPA and uPA function *via* proteolytic cleavage of the Arg^{561}-Val^{562} bond of plasminogen, allowing Val^{562} to form a salt bridge with Asp^{740} and creating the active plasmin enzyme (Wang et al., 1999). As with plasminogen, lysine binding sites in the kringle domains, and also a finger domain, promote tPA binding to fibrin (Longstaff et al., 2011).

Fibrinogen has been demonstrated to bind and stimulate tPA activation of plasminogen in several studies (Lucas et al., 1983, Thelwell and Longstaff, 2007, Bringmann et al., 1995b). Additionally, tPA activation of plasminogen in the presence of fibrinogen has been shown to exhibit a template profile (Thelwell and Longstaff, 2007). However, other studies have seen stimulation of activity in the presence of fibrin only, concluding that fibrinogen does not bind to plasminogen or the plasminogen activator, tPA. It is therefore hypothesised that tPA and plasminogen binding sites are only exposed through the conversion of fibrinogen to fibrin (Nieuwenhuizen, 2001, Nieuwenhuizen et al., 1988).

Plasmin generation is promoted by a positive feedback mechanism whereby the active protease cleaves single-chain tPA (sctPA) and singe-chain uPA (scuPA) to generate two chain versions (tctPA and tcuPA respectively), thereby enhancing plasminogen activation in solution (Cesarman-Maus and Hajjar, 2005). Studies have demonstrated though that in the presence of fibrinogen and fibrin, tctPA and sctPA exhibit similar activities (Thelwell and Longstaff, 2007)

It is important to note the different mechanisms by which plasminogen activation can occur. Although the vast majority of intravascular fibrinolysis is catalysed by tPA, mouse models have demonstrated that uPA may also play a role (Bugge et al., 1996). Binding of the lysine analogue tranexamic acid to lysine binding sites on the plasminogen molecule serves to open up the closed conformation of Glu-Pg and enhance its activation by uPA, suggesting uPA is more sensitive to the open conformation. This effect is not observed with tPA, whose mechanism as outlined above relies more on its colocalisation with fibrin or fibrinogen (Silva

et al., 2012). Under physiological conditions, plasminogen activation by both tPA and uPA is inhibited by plasminogen activator inhibitor 1 (PAI-1) (Thelwell and Longstaff, 2007).

1.5 Bacterial plasminogen activators

To counter host defence systems, bacteria have evolved mechanisms to hijack mammalian haemostasis in order to enable their dissemination. Many pathogenic bacteria employ the use of bacterial-derived or host physiological plasminogen activators (Sun, 2006).

The key importance of plasminogen and it's activation to plasmin, in the degradation of fibrin, is exploited by several bacteria who have evolved to produce plasminogen activators. For example, the Pla protein is a plasminogen activator protease, like the serine proteases tPA and uPA (Bergmann and Hammerschmidt, 2008). It is found on the outer membrane of *Yersinia pestis,* the bacteria responsible for the bubonic plague. Pla is shown to be critical in Y. *pestis* virulence; dramatically reducing the number of bacteria required to kill the host (Degen et al., 2007).

In contrast to this, streptokinase (SK) is an indirect non-proteolytic activator of plasminogen secreted by Lancefield gram-positive group A, C and G β-haemolytic *Streptococci* (Huang et al., 1989). The SK protein consists of 414 amino acid residues and is divided into three domains termed α (residues 1-146), β (147-290) and γ (291-414) (Wang et al., 1998). Our understanding of SK functionality comes exclusively from studies on the well-characterised mechanism of the group C H46a S*. equisimilis* SK, which behaves very differently from the physiological and bacterial plasminogen activators described before. The protein has no intrinsic enzymatic activity of its own, instead binding to plasminogen to form a 1:1 stoichiometric complex (Wang et al., 1999). Upon binding and complex formation, Ile^{1} is theorised to act as a substitute for Val^{562} of plasminogen, working as a counterion and forming a salt bridge to Asp^{740}, which induces a conformational change generating an active site in the bound plasminogen molecule (Wang et al., 2000).

The N-terminal region of SK is shown to be critical for SK activity and SK mutants lacking residues 1-59 are incapable of plasminogen activation in solution, becoming fibrin specific (Sazonova et al., 2004, Reed et al., 1999).

However, overall H46a SK demonstrates no fibrin specificity or stimulation, and thus understanding of the mechanism of SK activity is based upon this view. In particular, Ile^{1} of SK is necessary for the conversion of the inactive SK-Pg complex to SK-Pg* (active plasminogen activator complex) (Wang et al., 2000, Wang et al., 1999). SK also forms a tight complex with plasmin, for which it has a higher affinity than plasminogen (Boxrud et al., 2000). The formation of the SK-Pm* active complex modifies the substrate specificity of plasmin towards the activation loop of free plasminogen (Bajaj and Castellino, 1977). The SK-Pg* and SK-Pm* complexes are both plasminogen activators, converting free plasminogen into plasmin, through cleavage of the Arg^{561}-Val^{562} bond; as with the physiological plasminogen activators (Figure 1.4). This ability to act as plasminogen activators is not a property possessed by plasminogen or plasmin when not in complex with SK, and both SK-Pg* and SK-Pm* activity cannot be regulated by physiological plasmin inhibitors α_2-antiplasmin (D'Costa and Boyle, 2000, Cole et al., 2011). Coevolution of SK and plasminogen in a battle of survival between host and pathogen has ensured that SK's are extremely species specific, with variants from human pathogens exhibiting poor activation potential of other animal plasminogens (Gladysheva et al., 2003).

Staphylokinase (SAK), secreted by Staphylococcal bacteria, is another non-proteolytic plasminogen activator with many similarities in mechanism to SK. SAK also forms a plasminogen activator complex, inducing a conformational change, and generating an active site in the bound plasminogen molecule through insertion of its N-terminal residues. However, unlike H46a SK, SAK requires binding to fibrin for its activity, (Bergmann and Hammerschmidt, 2008).

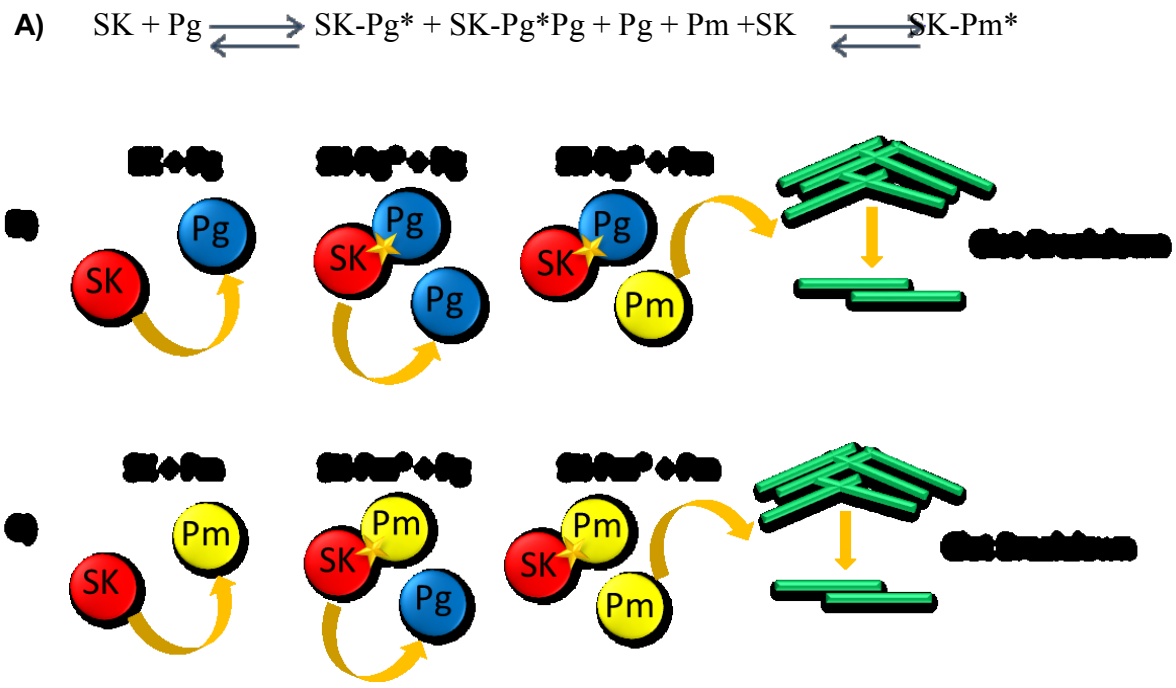

Figure 1.2 A schematic of Streptokinase (SK) interactions with Plasminogen (Pg) and Plasmin (Pm). A) Representative schematic for SK interaction with plasminogen and plasmin. B) SK binds plasminogen in a 1:1 stoichiometric complex inducing a conformational change and generating an active site. The active site can bind and cleave further plasminogen molecules converting them to the active serine protease plasmin. C) SK preferentially binds plasmin and the SK-Pm* complex acts as a plasminogen activator too. The plasmin generated hydrolyses fibrin to promote clot breakdown (fibrinolysis).

1.6 Zymogen activator adhesion proteins (ZAAP's) and molecular sexuality

The plasminogen activators SK, and SAK, secreted by *Staphylococcus* bacteria including *S. aureus*, belong to a family of bacterial proteins and virulence factors known as the zymogen-activator and adhesion proteins (ZAAPs) (Panizzi et al., 2004). This group includes the prothrombin activator staphylocoagulase (SCG), also secreted by S*. aureus* (Friedrich et al., 2003).

ZAAPs interactions with the human host fibrinolytic (SK, SAK) and blood coagulation (SCG) systems, respectively, have been demonstrated to help establish infection (Figure 1.3) (Panizzi et al., 2004). The family of proteins function to promote the activation of their respective zymogens through the mechanism of 'molecular sexuality', where activation is non-proteolytic and achieved by complex formation inducing a conformational change and the generation of an active site (Panizzi et al., 2004). The concept of 'molecular sexuality' was first proposed by Bode and Huber in 1976 (Bode and Huber, 1976). ZAAP's share conserved N-terminal sequences which mimic sequences crucial for activation in trypsin (Ile-Val-Gly) and chymotrypsin (Ile-Val-Asn). These N-terminal sequences insert into activation pockets on their respective zymogens to promote activation (Panizzi et al., 2004, Bode and Huber, 1976). The best characterised of these is the mechanism of plasminogen activation by SK (Figure 1.3).

1.7 Staphylocoagulase and prothrombin activation

SCG, a zymogen activator-adhesion protein (ZAAP), is an indirect, non-proteolytic activator of prothrombin secreted by Staphylococcus aureus (Panizzi et al., 2004). The SCG protein is divided into N-terminal D1-D2 domains which bind prothrombin, a linker region and the fibrinogen-binding C-terminal domain (Friedrich et al., 2003, McAdow et al., 2012). In a manner analogous to plasminogen activation by SK, the N-terminal Ile^{1}-Val^{2}-Thr^{3} of SCG is shown to insert into the Ile^{16} 'activation' pocket of prothrombin and form a salt bridge with $Asp^{194,}$ as demonstrated by X-ray crystallography (Friedrich et al., 2003). The formation of this salt bridge acts as a substitute for the N-terminal Ile formed following physiological cleavage

of prothrombin, and is the fundamental concept of the molecular sexuality mechanism (Friedrich et al., 2003, Bode and Huber, 1976).

SCG binding to prothrombin causes a conformational change in the zymogen, inducing a functional active site. Like SK, the N-terminal of SCG is important for zymogen activation with Ile^1 and Val^2 shown to be critical (Friedrich et al., 2003), and the bacterial protein has no intrinsic enzymatic activity of its own. SCG has been shown to form active 'staphylothrombin' complexes with both prothrombin (SCG-prothrombin) and thrombin (SCG-thrombin) to specifically cleave fibrinogen to make fibrin (Panizzi et al., 2004). The SCG-prothrombin complex demonstrates ~2 fold greater amidolytic activity than SCG-thrombin, but overall the efficiency against fibrinogen is indistinguishable compared to human thrombin (Friedrich et al., 2006). As with SK and SAK, S. *aureus* SCG activity is species specific, with poor potential as a bovine prothombin activator (Friedrich et al., 2006). The key difference between SK function and SCG is that the staphylothrombin complexes act directly on the thrombin substrate fibrinogen, whereas SK-Pm* and SK-Pg* complexes act as plasminogen activators.

Staphylothrombin does not activate Factor V, Factor VIII or many other physiological substrates of thrombin (Hendrix et al., 1983), but there is conflicting evidence wih regard to staphylothrombin interaction with FXIII (McAdow et al., 2012, Panizzi et al., 2004). Staphylothrombin do not appear to be regulated by physiological thrombin inhibitors (Kawabata et al., 1986) with the formation of the activator complex shielding thrombin from antithrombin inhibition (Hendrix et al., 1983). However, the therapeutic thrombin inhibitors argatroban (Hijikata-Okunomiya and Kataoka, 2003) and dabigatran have been shown to inhibit SCG-prothrombin activity (Vanassche et al., 2010). Dabigatran has also been demonstrated to reduce S. *aureus* virulence and sepsis in *in vivo* models (Vanassche et al., 2011, McAdow et al., 2011), as well as staphylothrombin initiated platelet aggregation (Vanassche et al., 2013).

Both SCG-prothrombin and SCG-thrombin bind to fibrinogen with high affinity *via* an alternative mechanism from that of thrombin alone, forming a pentameric complex consisting

of two SCG-(pro)thrombin complexes and one fibrinogen molecule (Panizzi et al., 2006). Despite understanding of staphylothrombin interaction with fibrinogen and the mechanism of fibrin formation, there is little understanding of the properties of the fibrin product formed.

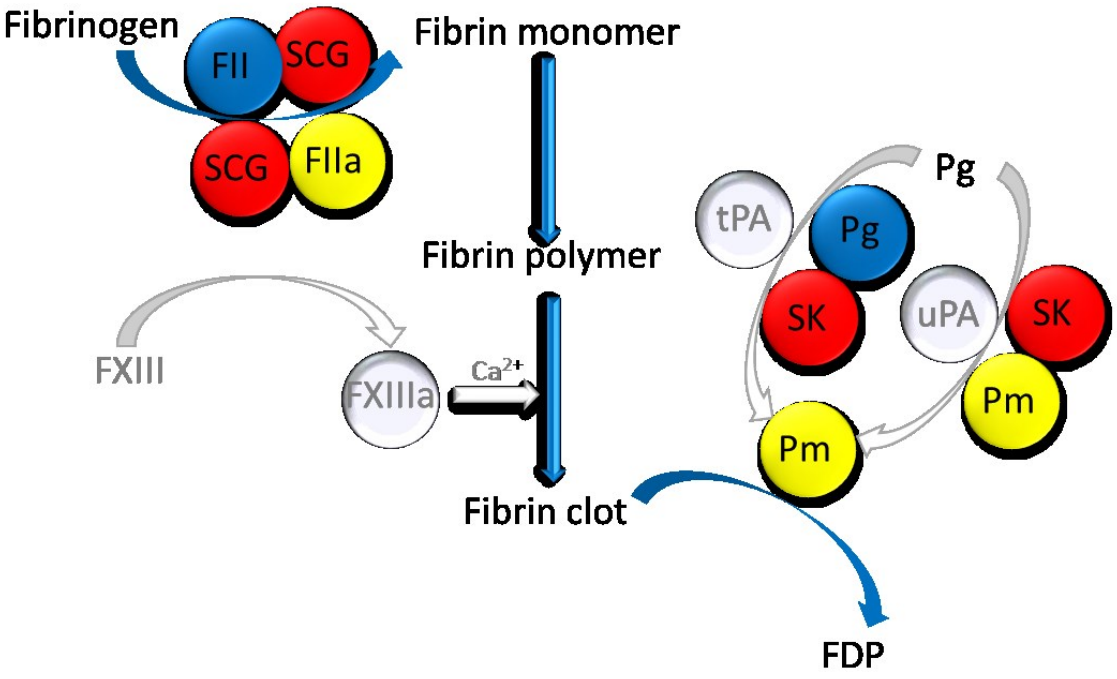

Figure 1.3 The interaction of SCG and SK with the mammalian haemostasis system. SCG secreted by S. *aureus* binds to prothrombin and thrombin to form staphylothrombin complexes that promote fibrin formation to enable bacterial immune evasion. SK from Streptococcal species bind plasminogen and plasmin to form plasminogen activator complexes that promote the generation of plasmin. The plasmin generated by SK activity hydrolyses the fibrin clot to promote bacterial dissemination in the host.

1.8 Haemostasis, mammalian defences and bacterial virulence

Coagulation plays an important part in mammalian defence against invading pathogens. The fibrin networks of clots encapsulate, kill and block entry of invading pathogens, providing a physical barrier to pathogenic entry and dissemination (Loof et al., 2014, Shannon et al., 2010). There is extensive evidence detailing the interaction between pathogenic bacteria and the coagulation system of their human host. In particular, the binding of peptides released during thrombin catalysis of fibrinogen to bacterial fibrinogen-binding surface receptors has been demonstrated to reduce the number of colony forming units (CFU's) and aid the killing of Group A Streptococci, Group B Streptococci and S. *aureus* (Pahlman et al., 2013). Whilst the presence of FXIIIa has been demonstrated to facilitate entrapment of E. *coli* and S. *aureus,* with FXIIIa-deficient clots losing this capacity (Wang et al., 2010) as well as the killing and trapping of S. *pyogenes* within the fibrin networks of the clot, through cross-linking of the bacterial fibrinogen-binding surface protein M1 to fibrin strands (Wang et al., 2010, Loof et al., 2011). FXIII has also been shown to prevent establishment of S. *pyogenes* infection in a murine model. Here the bacteria were localised to within fibrin clots in wild-type mice (i.e. in the presence of FXIII), but had disseminated beyond the initial site of infection in FXIII-deficient mice (Loof et al., 2012).

To counteract host defences, evolutionary advantage has ensured that many bacterial species including Staphylococci and Streptococci studied in this work, display cell surface proteins that bind coagulation factors, including plasminogen and fibrinogen, as well as secrete plasminogen activators to influence haemostasis and fibrinolysis (Sun, 2006). These interactions with fibrinogen or plasminogen are an effective way to localise plasmin activity to the bacterial surface (Takada and Takada, 1989a). They also allow bacteria to degrade host fibrinogen, extracellular matrix and tissues to facilitate dissemination and establish invasive infection (Bergmann and Hammerschmidt, 2008).

Understanding the interaction between bacterial proteins and haemostatic proteins at the molecular level could also prove useful for the development of new antimicrobial technologies

to help fight infection. There is an increasingly pressing need for advancements in this area given the rising instance of microbial resistance to available antibiotics, and few suitable developments (*Longitude Prize Open*, 2015).

1.8.1 Haemostasis and Streptococcal virulence

Both Group C (GCS) and Group A Streptococci (GAS) are capable of human diseases but it is GAS, in particular the M1GAS serotype, that is the predominant isolate in severe invasive Streptococcal infections (Steer et al., 2009, Ekelund et al., 2005, Cole et al., 2011). *S. pyogenes*, an M1GAS, is a strict human pathogen, responsible for diseases such as impetigo and pharyngitis, as well as life-threatening conditions including Streptococcal toxic shock syndrome (STSS) and necrotizing fasciitis (Walker et al., 2005). It has an extensive portfolio of interaction with the human coagulation and fibrinolysis, reviewed recently by (Loof et al., 2014, Bisno et al., 2003).

S. *pyogenes* displays several surface proteins which bind human coagulation factors including plasminogen, fibrinogen, FV, FXI and FXII and hijack the human coagulation system to promote infection (Herwald et al., 2003). The interaction of streptococcal strains with the host plasminogen activation system is particularly important in establishing invasive systemic disease (Cole et al., 2006), and bacterial virulence is increased by SK-dependent interaction with plasminogen (Khil et al., 2003).

Subgroups of M1GAS are known to have different plasminogen activation characteristics whereby some strains require the presence of fibrinogen in order to both bind and activate plasminogen (McArthur et al., 2008, McKay et al., 2004a). Group A Streptococci fall distinctly into three phylogenetic clusters, cluster 1, cluster 2a and cluster 2b, with distinctive surface proteins (Figure 1.4) (McArthur et al., 2008). Cluster 2b can bind plasminogen through the surface-bound PAM molecule. PAM is not present in cluster 2a bacteria, including the S. *pyogenes* strain studied in this project, which instead have evolved fibrinogen binding potential through expression of the M1 protein, the M protein most commonly connected with invasive

Streptococcal infection (Steer et al., 2009). Cluster 1 Group A Streptococci produce both fibrinogen and plasminogen binding receptors different from PAM and M1 (McArthur et al., 2008). A hypothesis by the McArthur group suggests that with all GAS bacteria, regardless of which cluster, SK and plasminogen can interact with fibrinogen to form a tri-molecular complex (Figure 1.4, (McArthur et al., 2008)). However, there is no direct evidence studying these proteins in isolation to support this. Plasminogen acquisition to GAS *via* plasminogen and fibrinogen binding to cell surface receptors, is shown to be a crucial factor of establishing systemic infection (McKay et al., 2004). (Sun et al., 2012) inhibited SK gene expression in GAS bacteria to demonstrate that SK deficiency improves the survival of infected mice.

The relationship between GAS interaction with human haemostasis and their pathogenesis has never been investigated with regard to mechanistic details of SK functionality. It is entirely plausible that the mechanistic variety of the specific receptors of each Streptococcal strain which bind haemostatic proteins contributes at least in part to differences in their observed pathogenesis.

1.8.2 Haemostasis and S. *aureus* virulence

S. *aureus* is responsible for diseases including infective endocarditis, sepsis and osteomyelitis as well superficial soft tissue infections (McAdow et al., 2012). SCG is a known virulence factor contributing to the survival of S. *aureus* in the bloodstream, implemented in the promotion of sepsis, colonisation of tissues and abscess formation, a defining feature of S. *aureus* infection (Cheng et al., 2010, DeDent et al., 2012). Specifically, S. *aureus* mediated fibrin formation through SCG activation of prothrombin has been shown to reduce activation of leucocytes (Vanassche et al., 2011) and promote platelet aggregation and S. *aureus* platelet interactions (Vanassche et al., 2012). SCG interaction with fibrinogen is known to be crucial in abscess formation (Cheng et al., 2009) and has been detected in the pseudocapsule of mouse renal abscess models (Cheng et al., 2010). Murine endocarditis model have also demonstrated that prothrombin binding to SCG serves to incorporate the zymogen into the bacterial vegetations

(Panizzi et al., 2011). SCG distribution is restricted to the host facing peripheral layers of the structures in both instances. SCG has also been implemented in the establishment of catheter related S. *aureus* infections (Vanassche et al., 2013). It has been proposed that S. *aureus* may use the fibrin produced *via* SCG activity as a protective coat allowing immune evasion as it disseminates throughout its host (Vanassche et al., 2011, McAdow et al., 2012, Cheng et al., 2011). Despite detailed understanding of SCG in virulence models, little attention has been paid to understanding the protein and it's interaction with the haemostastic system at the molecular level.

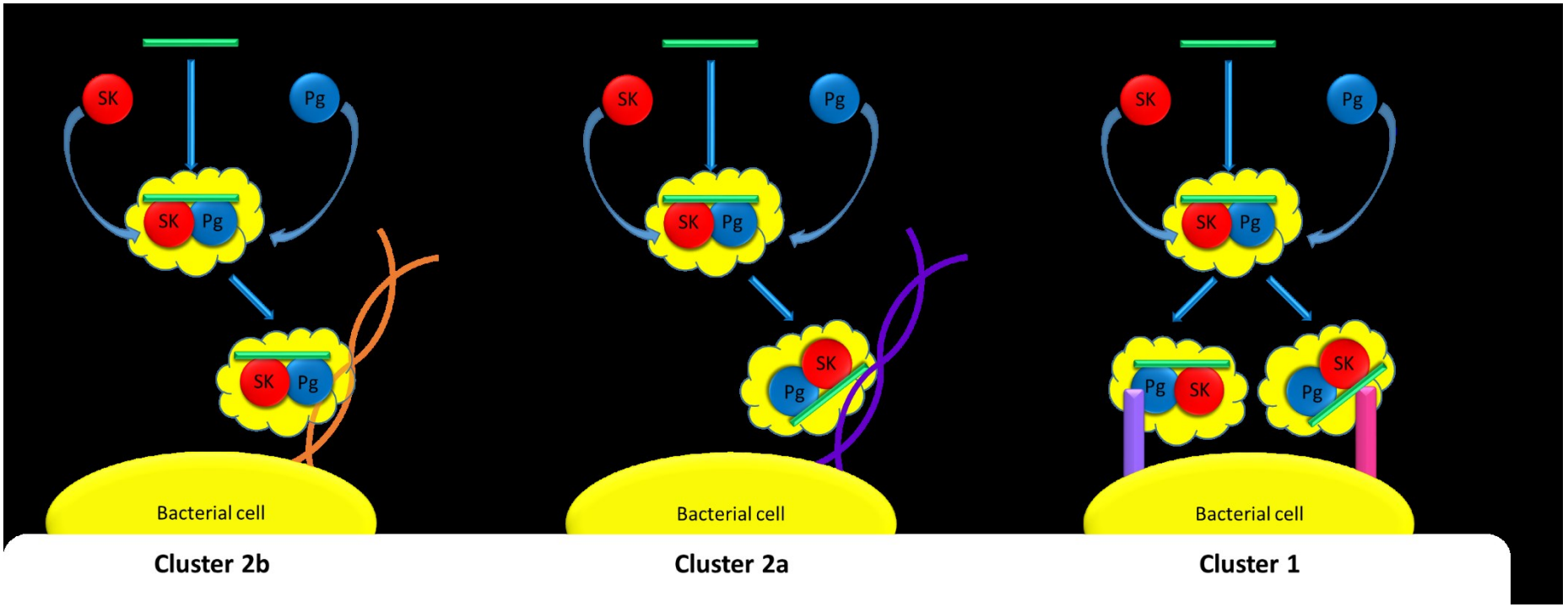

Fig 1.4 Proposed mechanisms for the cell surface acquisition of plasmin activity by Group A Streptococcal Clusters 1, 2a and 2b (adapted from (McArthur et al., 2008). Phylogenetic analysis of group A streptococcal bacteria revealed three distinct clusters (1, 2a and 2b). Each displays a characteristic cell surface proteins that bind plasminogen and/or fibrinogen. A) Cluster 2b display PAM, a plasminogen receptor. B) Cluster 2a display M1, a fibrinogen receptor. C) Cluster 1 display plasminogen and fibrinogen receptors but not PAM or M1.

1.9 Myocardial infarction and history of thrombolytics

Cardiovascular disease, including myocardial infarction (MI) or heart attack, is the leading cause of death in the world (McKay et al., 2004b). The disease is often a result of blood clots, and so 'clot buster's' or thrombolytics are employed as therapeutics administered for the dissolution of blood clots in the treatment of acute myocardial infarction (Collen and Lijnen, 2005). The efficiency of SK as a plasminogen activator resulted in its use as a first generation thrombolytic drug along with the physiological plasminogen activator, uPA (Parry et al., 2000). SK is still the most widely used thrombolytic in the world (Armstrong and Collen, 2001).

The SK protein used in the therapeutic is derived exclusively from the Group C H46a *S. equisimilis* strain. This strain was originally chosen for the production of therapeutic SK because it expressed high levels of SK but no erythrogenic toxins. This was an advantage when fermenting large culture volumes as required to manufacture the thrombolytic, proving much safer than more pathogenic alternatives (Kunamneni et al., 2007). However, H46a SK has no proven advantage over other SK strains with regard to plasminogen activation potential. In particular, first generation thrombolytics, are not fibrin specific, causing systemic plasminogen activation, and depletion of many coagulation factors (Longstaff and Thelwell, 2005). This is a major concern with thrombolytics, often resulting in bleeding complications (Dundar et al., 2003).

Accordingly, the rationale for the development of second generation thrombolytics was fibrin specificity. The objective of more fibrin-targeted plasminogen activation was to improve the clot-busting potential and reduce the incidence of bleeding complications seen with systemic SK and uPA (Verstraete, 2000). Recombinant tPA (Alteplase) with fibrin-binding domains replaced the use of first generation alternatives after demonstrating improvements compared to SK for haemorrhagic stroke and mortality in the international randomised GUSTO trial (Investigators, 1993). However, the short half life meant large therapeutic doses were needed,

and as such systemic activation and bleeding complications were still a problem, and better alternatives were needed (Collen and Lijnen, 1991, Verstraete, 2000).

To further enhance the fibrin specificity of tPA, improve the half life and increase resistance to inhibitors, recombinant variants with domain deletions such as reteplase and tenectaplase were designed, and the third generation of thrombolytics was founded (Longstaff and Thelwell, 2005). This group also includes desmotoplase, a plasminogen activator, discovered in Vampire bat saliva, that shares similarities with tPA but offers increased fibrin specificity (Medcalf, 2012, Verstraete, 2000).

Overall, despite improved technologies and significant effort, thrombolytics have not performed as well as would have been expected with reducing bleeding complications and mortality (Armstrong and Collen, 2001, Verstraete, 2000). As such, the treatment of MI has largely moved beyond thrombolytics in developed countries, with percutaneous coronary intervention (PCI) considered vastly superior (Armstrong et al., 2003).

Whilst the treatment of myocardial infarction has moved away from the use of SK in developed countries, its use is licensed in Europe. It also remains an inexpensive and easily produced thrombolytic for use in less developed nations, where cardiovascular disease is an increasingly significant concern (Feigin, 2007). Thrombolytics are an essential treatment for ischaemic stroke, with Alteplase (tPA) the only licensed therapeutic available (Longstaff and Kolev, 2015). Investigating the mechanism of SK variants from bacterial strains other than S. *equisimilis,* for which very little understanding exists, may provide understanding which could improve the effectiveness of the thrombolytic.

1.10 Project aims

The aim of this project is to investigate the details of the 'molecular sexuality' mechanisms by which the ZAAPs, SK and SCG activate the zymogens, plasminogen and prothrombin, respectively.

For SK, this includes characterisation of plasminogen binding, determination of activation kinetics, and study of regulation of activity by fibrinogen and fibrin. In particular, this work will investigate the mechanism of plasminogen activation and fibrinolysis by M1GAS SK, as relative to H46a SK from GCS, used in the thrombolytic, very little is known about the M1GAS SK structure/function relationship. The SK from S. *pyogenes* shares 88.4% amino acid sequence identity with the GCS SK used in the thrombolytic but it is only recently that differences in plasminogen activation between SK from Streptococcal strains has been investigated. Increased understanding of the mechanistic variation between SK from different Streptococcal species will aid our understanding of bacterial virulence, potentially providing rationale for new improved antmicrobial therapeutics. It will also aid improvement of thrombolytic therapies, for the treatment of myocardial infarction and ischaemic stroke.

With regard to SCG, the aim is to clone and express a full-length native N-terminal recombinant SCG protein and investigate the physical properties of the fibrin product and its fibrinolysis, by both physiological and bacterial plasminogen activators of which very little is known. There is currently limited understanding of the benefit to S. *aureus* in producing both staphylokinase, which aims to degrade fibrin clots, and staphylocoagulase which serves to induce fibrin formation. It is therefore an aim of this project to begin to understand the interplay between the two virulence factors and how their interaction with the human host haemostatic system may promote their dissemination and establishment of infection.

Chapter 2: Investigating plasminogen activation by rSK H46a and rSK MIGAS

2.1 Introduction

Until recently understanding of activation of plasminogen by SK was based almost exclusively on kinetic studies of the SK from H46a strain of S. *equisimilis,* which displays no fibrin specificity (Chibber et al., 1985, Takada and Takada, 1989b). This SK is used in the therapeutic treatment of myocardial infarction. Accordingly, all SK was considered to have no fibrin specificity. Recent studies into SK from cluster 2b have begun to elucidate differences in mechanisms (Zhang et al., 2012, Zhang et al., 2013). However, there is still limited understanding of the association between differences in Streptococcal pathogenicity and mechanistic variation among SK.

Group A Streptococci (GAS) are more commonly associated with invasive disease in humans than Group C Streptococci (Ekelund et al., 2005, Cole et al., 2011). Furthermore, the M protein serotype most typically associated with invasive GAS disease is M1, a fibrinogen binding surface receptor (Johansson et al., 2010). Despite the pathogenicity of GAS, very little is known about the structure/function relationship of GAS SK, a known virulence factor.

To begin to address this, the work herein investigates the activity of GCS S. *equisimilis* H46a strain SK and SK from GAS M1 type S. *pyogenes* using recombinant variants. In particular, given the expression of M1, examining the effect of fibrinogen and fibrin may provide some useful insights into the mechanism of plasminogen activation by M1GAS SK, particularly in comparison to H46a SK. Furthermore, a recent study by (Loof et al., 2012), demonstrated that the trapping of S. *pyogenes* within fibrin clots was linked to the FXIIIa-mediated cross-linking of M1 to fibrinogen. FXIIIa is also known to cross-link the plasmin inhibitor α_2-antiplasmin to fibrin strands within the clot (Fraser et al., 2011). However, the fibrinolysis of FXIIIa cross-linked fibrin by S. *pyogenes* SK and the combined effect of FXIIIa and α_2-antiplasmin on this M1GAS SK is unknown, and hence is a focus of this mechanistic study.

Previous work has shown that the conserved N-terminal residues of SK are critical for plasminogen activation (Wang et al., 2000, Wang et al., 1999). Many expression systems in E. *coli* require the addition of a Met 'start' codon at the N-terminus to enable protein expression. However, this residue is inefficiently cleaved in E. *coli* post-translation modifications and has been demonstrated to affect SK function, leaving it unable to activate plasminogen (Thelwell and Longstaff, 2014). With this in mind, a SUMOstar fusion protein expression system was used to express rSK H46a and rSK M1GAS. A SUMOstar expression system allows preservation of the native N-terminal sequence in the final product, thus minimising any changes in function. Cleavage of the SUMOstar tag by SUMOstar protease recognises the tertiary structure of the SUMOstar tag ensuring no unwanted residues are left at the N-terminus preserving the native SK sequence (Malakhov et al., 2004). Other advantages of the system include simple purification from cell lysate and removal of the SUMOstar protease, and SUMOstar tag following cleavage, by Ni-affinity chromatography utilising the 6xHis tag within the SUMOstar fusion protein and protease.

2.2 Experimental Procedures

2.2.1 Materials, equipment and software for recombinant protein expression and purification

LB media powder, B-per, Lysozyme, DNAse I (Thermo Scientific, Massachusetts, USA)

0.5-3 ml Dialysis cassettes, Coomassie Plus reagent (Pierce, Rockford, IL)

NuPAGE Novex precast gel system, 4-12% Bis-Tris polyacrylamide gel, MES running buffer, Sample reducing agent, Sample buffer, Molecular weight standard, SimplyBlue safety stain, His-Trap columns (Life Technologies, Renfrewshire, UK)

SUMOstar Expression kits (LifeSensors, Pennsylvania, USA)

T7 Express *lysY E. coli* (New England Biolabs, Hertfordshire, UK)

Amino-acid analysis (Alta-Bioscience, Birmingham, UK)

0.2 micron filters, Ampicillin, IPTG, Imidazole, DTT, NiNTA agarose (Sigma Aldrich, St Louis, Missouri, USA)

Propylene columns (Qiagen, Manchester, UK)

AKTA Purifier (GE Healthcare, Buckinghamshire, UK)

Vector NTI (Thermo Fisher, Paisley, UK)

2.2.2 Recombinant protein expression and purification

Recombinant SK (rSK) rSK H46a, rSK M1GAS were expressed as N-terminal SUMOstar fusion proteins from transformed glycerol stocks (15% (v/v)) of T7 Express *lysY E. coli* provided by C. Thelwell (personal communication). Cells were transformed with a construct of pETBlue-1, a vector for T7 lac promoter IPTG-inducible expression of proteins, the sequence for SUMOstar fusion protein (including a 6xHis affinity tag) and the appropriate SK variant (Figure 2.1).

2.2.2A Expression of recombinant proteins in E. coli

Overnight cultures of *E.* coli containing the expression plasmid were diluted 1:50 into fresh LB media supplemented with 100 µg/ml ampicillin, and incubated at 37°C with shaking to an OD 600 nm of 0.4-0.6. Protein expression was induced by the addition of IPTG to a final concentration of 0.4 mM for a further 2-3 hours. Cells were harvested by centrifugation (3000 x g for 15 min) then lysed chemically using 4 ml of B-PER reagent per gram of cells. The B-PER was supplemented with DNase I (2 µl per ml of B-PER to give a final concentration of 5 U/ml), lysozyme (2 µl per ml of B-PER to give a final concentration of 0.1 mg/ml) and 1x Halt protease inhibitor cocktail according to the manufacturer's instructions. The soluble protein fraction was recovered by centrifugation (20000 x g for 20 min).

2.2.2B Purification of his-tagged proteins

His-tagged proteins were purified from culture lysates by Ni-affinity chromatography using a 1 ml HisTrap HP column equilibrated with 20 mM Tris-HCl, 0.5 M NaCL, 40 mM imidazole, pH 7.7 at room temp on an AKTA Purifier. All buffers and culture lysates were vacuum filtered through a 0.2 µM filter and degassed before use, and applied to the column at a flow rate of 1 mL min^{-1}. Culture lysates were supplemented with 40 mM imidazole to limit non-specific binding of bacterial proteins and applied to the HisTrap column. The column was washed with 15 ml equilibration buffer supplemented with 40 mM imidazole and bound proteins were eluted

from the column in 0.5 ml fractions against a 10 ml imidazole gradient of 40 mM – 600 mM. Protein elution was monitored using a UV detector (280 nm) and fractions containing the recombinant fusion protein (assessed visually using SDS page) were pooled.

2.2.2C Cleavage of SUMOstar fusion tag

Pooled fractions of purified proteins were dialysed against protease cleavage buffer (20 mM Tris-HCL, pH 8.0. containing 1.5 M NaCl) using 0.5-3ml dialysis cassettes. Dialysis was at 4 °C initially for 4 hours in 1 L, followed by 2 L overnight, with continuous stirring. The SUMOstar fusion tag was cleaved using SUMOstar protease according to the manufacturer's protocol. Cleavage was typically achieved over 4 hours at 30°C in the presence of 2 mM DTT and was confirmed by SDS-PAGE, although overnight incubation were sometimes necessary for rSK H46a. The SUMOstar tag and protease were bound to Ni-NTA agarose by mixing for 1 hour at room temperature and the cleaved purified protein was recovered by filtration through an empty column.

2.2.2D SDS-page and coomassie staining

Presence of recombinant proteins in peak fractions following Ni-affinity chromatography, molecular weights of proteins, estimations of purity and confirmation of SUMOstar cleavage, were checked visually by SDS-PAGE and Coomassi'e staining relative to molecular weight markers. Visualisation of proteins by SDS PAGE was performed using the NuPAGE Novex precast gel system. Proteins were incubated with sample buffer and reducing agent at 70 °C for 10 min according to the manufacturer's instructions. Samples were loaded and run on 4-12% Bis-Tris polyacrylamide gel alongside SeeBlue Plus2 pre-stained molecular weight marker (10 µl) as directed by the manufacturer using NuPAGE MES buffer. Gels were stained with SimplyBlue SafeStain for 1 hour and destained overnight in H_2O.

2.2.2E Determining protein concentration

Protein concentrations were determined by amino-acid analysis or using Coomassie Plus reagent relative to a standard curve of full-length SK quantified by amino acid analysis.

2.2.2F Batch pooling

Several preparations were made and pooled together for each recombinant protein and all assays carried out on the same pooled batch.

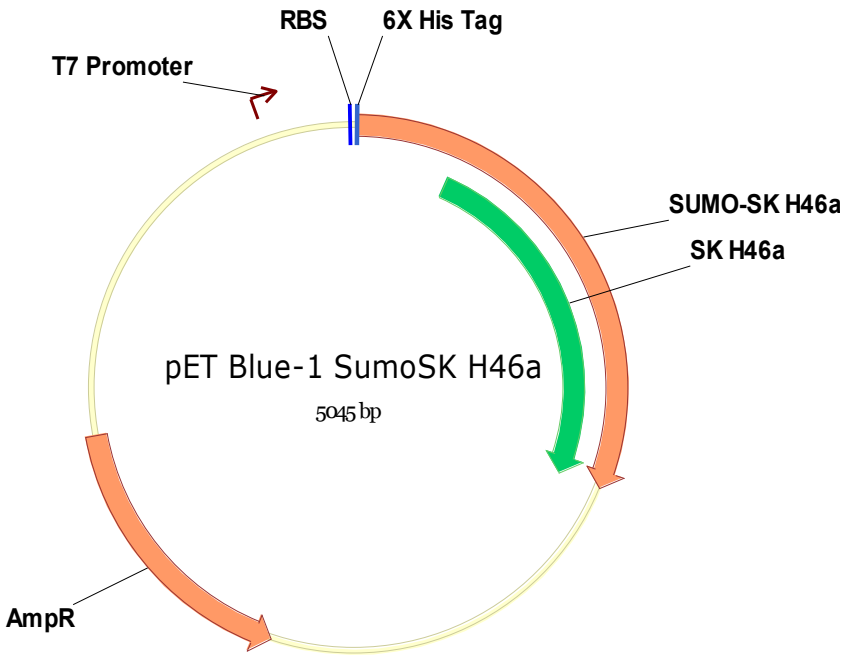

Figure 2.1 Expression vector construct pET Blue- 1 SumoSK H46a. Map of example expression vector construct created in Vector NTI (Invitrogen) showing the T7 promoter, the ribosome binding site (RBS), ampicillin resistance gene (AmpR), the SUMOstar SK H46a fusion protein sequence (SUMO-SK H46a) and 6 x His-tag used for purification. An equivalent construct was designed for expression of SUMOstar SK M1GAS, SUMOstar SK H46a del1-59 and SUMOstar SK M1GAS del1-59.

2.2.3 Material and software for SK activity assays

2.2.3A Materials

Buffer A - 0.5 M Tris pH 8.4 at 37 °C. Stored at 2-8 °C for 6 months.

Buffer B – 10 mM Tris HCL 100 mM NaCl 0.01% Tween 20. Store at 2-8 °C for 1 week.

Buffer C – Buffer B + 1mg/ml Human Serum Albumin (HSA). Store at 2-8 °C for 3 days.

Buffer D – 40 mM Tris-HCL 100 mM NaCl 0.01% Tween 20. Store at 2-8 °C for 1 week.

Blocking buffer – 0.05M Tris HCL, 0.01% Tween 20, pH 8.4 at 37 °C.

All laboratory chemicals used to make buffers were from Sigma Aldrich, St Louis, Missouri, USA.

Fibrinogen (Calbiochem, Merck Millipore, Billerica, Massachusetts, USA) - reconstituted in Buffer B to give stock solution of 50 mg/ml, and flash frozen in liquid nitrogen in small aliquots and stored at -40 °C. All dilutions for reaction set ups were in buffer B also.

Glu-Plasminogen (Glu-Pg) (Quadratech, Surrey, UK) - Reconstituted to 1mg/ml in H_20, flash frozen in small aliquots in liquid nitrogen and stored at -40 °C. All dilutions for reactions were made in buffer C.

Lys-Plasminogen (Lys-Pg) (Immuno, Vienna, Austria) – Reconstituted to 1 mg/ml in H_20, flash frozen in small aliquots in liquid nitrogen and stored at -40 °C. All dilutions for reactions were made in buffer C.

WHO 2nd IS Thrombin (01/578) – Reconstituted in 1 ml H_20, flash frozen in small aliquots in liquid nitrogen and stored at -40 °C. All dilutions for reactions were made in buffer C.

WHO 3rd IS SK (00/464) – reconstituted in 1ml H_20, flash frozen in small aliquots in liquid nitrogen and stored at -40 °C. All dilutions for reactions were made in buffer C.

rSK H46a, rSK M1GAS, rSK H46a (del1-59), rSK M1GAS (del 1-59) (see section 2). Flash frozen in liquid nitrogen and stored in small aliquots at -40 °C. All dilutions for reaction set up were made in buffer C.

S-2251, H-D-Val-L-Leu-L-Lys-pNA (Chromogenix, Milan, Italy) – reconstituted in 15 ml H_2O, to give a 3 mM stock solution. Stored at 2-8 °C, stable for several months.

Microtitre plates (Greiner, Kremsmunster, Austria) – all microtitre plates were blocked with 200 µL blocking buffer for 2 hours at 37 °C and washed 2x with 200 µL H_20 before use.

2.2.3B Software Packages

GraphPad Prism (GraphPad Software, San Diego, California, USA)

SoftMax Pro v5.0 (Molecular Diagnostics, Sunnydale, California, USA)

Microsoft Excel (Redmood, Washington, USA)

R script (R Foundation, Vienna, Austria)

Combistats (EDQM, Strasbourg, France)

2.2.4 SK Activity Assays

The methods below describe the measurement of SK activation of plasminogen in the Glu- and Lys- forms in solution and in the presence of fibrinogen and fibrin. Initially, the variants were investigated in each assay system with fixed concentrations of Plasminogen, thrombin and fibrinogen. The assays were then adapted to look at the effect of fibrinogen concentration, plasminogen concentration, FXIIIa cross-linked fibrin, tranexamic acid and α_2-antiplasmin.

2.2.4A Plasminogen activation by SK in solution (Figure 2.2A)

Rates of plasminogen activation by recombinant SK variants were determined using the chromogenic substrate for plasmin, S-2251 based on the European Pharmacopeoial method for assigning potencies to therapeutic SK (Europe, 2008b). A range of SK dilutions made in

buffer C were mixed with a solution of Glu- or Lys- Pg and S-2251, in blocked 96 well microtitre plates. The SK concentrations were such that the rates for rSK H46a and rSK M1GAS activity were similar to the WHO 3rd IS SK (00/464) and produced a linear dose response. Final concentrations were Glu- or Lys- Pg (100 nM) and S-2251 (0.6 mM) in a total reaction volume of 100 µl. The plasmin generated cleaves S-2251 to release *p*-nitroaniline (pNA) which was monitored by measuring absorbance change at 405 nm in 30 s intervals, for 90 min at 37 °C. Each assay included 4 SK doses with 4 replicates for each sample. Initial rates of plasminogen activation were calculated from the slopes of plots where the substrate (S-2251) and plasminogen were less than 10% consumed absorbance versus time squared using an R program (The R Foundation) script (Silva et al., 2012) written by C. Longstaff (personal communication) based on equations (1), (2) and (3) (Longstaff et al., 1995).

$$OD_{405} = \frac{\epsilon}{2}\beta\nu t^2 \quad (1)$$

$$\beta = \frac{k_{cat(S\text{-}2251)}[S\text{-}2251]}{K_{M(S\text{-}2251)} + [S\text{-}2251]} \quad (2)$$

$$\nu = \frac{k_{cat}[SK][Pg]}{K_M + [Pg]} \quad (3)$$

2.2.4B Plasminogen activation by SK in the presence of fibrinogen (Figure 2.2B)

Rates of plasminogen activation were determined as in 2.2.4A, but with the addition of fibrinogen (3.0 mg/ml).

2.2.4C Plasminogen activation by SK in the presence of fibrin (Figure 2.2C)

Fibrin clots (60 µl) were made in blocked microtitre plates by incubating thrombin (20 nM) with fibrinogen (3.0 mg/ml) containing Glu- or Lys- Pg (100 nM), for 30 mins at 37°C. 40 µl solution containing SK and S-2251 (reaction concentration 0.6 mM) were added to the surface of pre-formed fibrin clots, thus SK activates plasminogen on the surface of the clot, bound to fibrin (Longstaff and Whitton, 2004). All dilutions were made in buffer D, so as to produce clear clots

which would not affect the absorbance readings from pNA generation. As with the chromogenic solution assay, pNA generation was monitored by measuring absorbance at 405 nm at 30 s intervals for 90 mins at 37 °C, and rates of plasminogen activation were calculated from transformed plots of absorbance versus time squared using an R program script written by Colin Longstaff, personal communication.

2.2.4D Fibrinolysis (Figure 2.2D)

Fibrin clots were made in blocked microtitre plate wells by adding a solution of fibrinogen (3.0 mg/ml) containing Glu- or Lys- Pg (100 nM) (60 µl) to a 40 µl solution of thrombin (20 nM) and SK (refer to Figure 2.3). Each assay contained 4 doses and 4 replicates for each SK variant. Absorbance at 405 nm was measured at 30 s intervals for 5 hours at 37 °C using plate reader software SoftMax Pro v5.0 to monitor clotting and lysis through changes in fibrin clot opacity.

The raw, kinetic data was exported from Softmax Pro plate reader software as a text file. An R program script, written by Colin Longstaff (Personal communication, see appendix 1) was used to determine the time at maximum absorbance (complete clotting) and time at lowest absorbance (complete lysis), to allow calculation of the time to 50% lysis (Figure 2.3). The script is capable of determining several parameters from the raw kinetic data such as max absorbance, time to max absorbance, time to complete lysis, time to % lysis. Time to 50% lysis from start of reaction is commonly used as a measure of fibrinolysis and as such was chosen in this instance as a parameter by which to compare the variants.

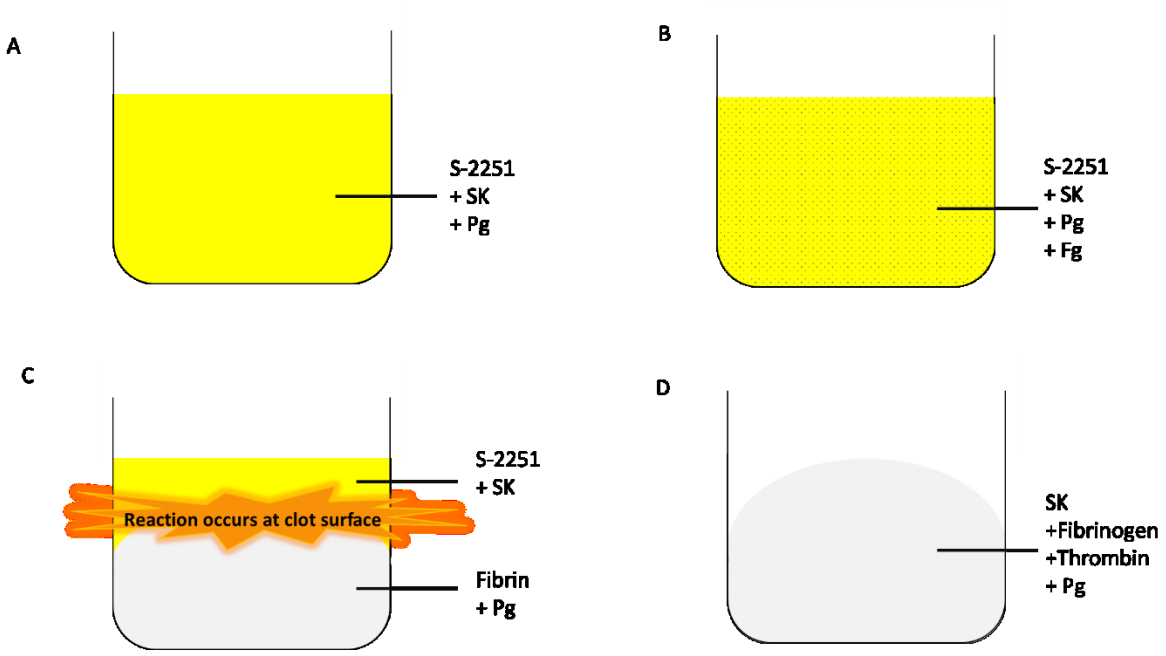

Figure 2.2 Assay systems used to determine rates of plasminogen activation and fibrinolysis by rSK H46a and rSK M1GAS. Assays were performed in 96 well microtitre plates, with each image representing the reaction in one well for each of the four assay systems (2.2.4A-D). Plasminogen activation by SK against the chromogenic substrate for plasmin (S-2251) was measured by monitoring absorbance change at 405 nm in solution (a), in the presence of fibrinogen (b) and at the surface of a pre-formed fibrin clot to measure the activity in the presence of fibrin (c). Fibrinolysis rates were measured by absorbance change at 405 nm in the absence of a chromogenic substrate (d). In this instance, the change in absorbance corresponds to the changes in clot turbidity as the fibrin clot forms and lyses.

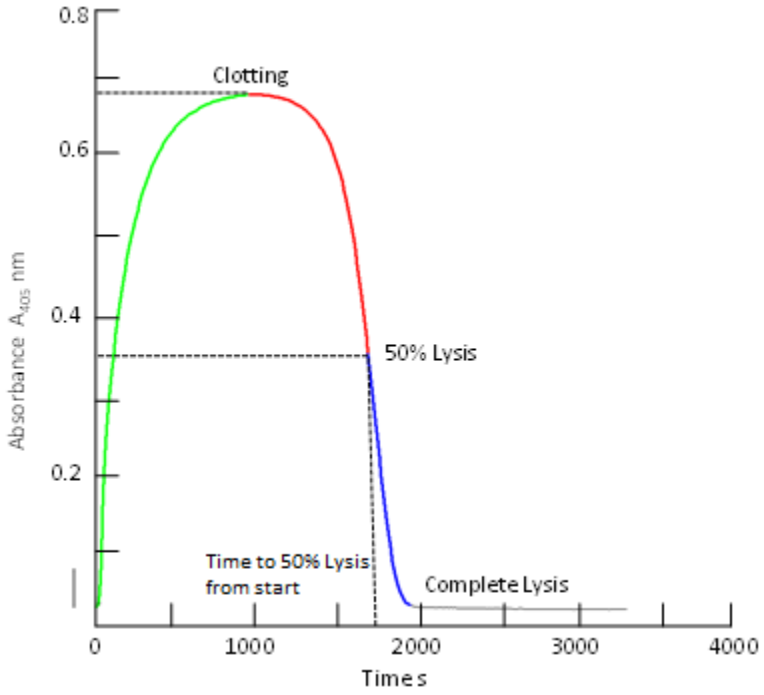

Figure 2.3 Typical clot lysis profile from a fibrinolysis assay (Section 2.2.4D and Figure 2.2D). Change in absorbance at 405 nm represents lysis and clotting and was used to calculate the time at maximum absorbance at 405 nm (complete clotting) and time at lowest absorbance (complete lysis), to determine the time to 50% lysis from the start of the reaction, as a measure of SK activity.

2.2.4E Data analysis – parallel line bioassay

rSK activity in each assay system was calculated in International Units (IU) relative to the WHO 3rd International Standard for SK (00/464), a commercial thrombolytic SK from H46a strain. In these assay systems, multiple SK dose responses for all variants were successfully fitted to a parallel line bioassay according to chapter 5.3 of the European Pharmacopoeia with the software Combistats (EDQM) (Europe, 2008a). Combistats is a statistical analysis program for biological dilution or potency assays. Thus, potencies (IU/ml) were reported with 95% confidence limits and statistical assessment of linearity of dose responses and parallelism between standard (00/464) and test SK dose responses. If non-linearity and non-parallelism were determined to be significant at the 5% significance level, the assay was deemed invalid and potency could not be determined. Protein concentrations determined by amino acid analysis were used to calculate specific activities, expressed in terms of IU/μg protein for each SK variant.

2.2.5 Investigating the effect of fibrinogen concentration on plasminogen activation by rSK H46a and rSK M1GAS

To investigate the effect of fibrinogen further, the solution assay with fibrinogen (Section 2.2.4B and Figure 2.2B) was adapted to measure plasminogen activation rates by rSK H46a and rSK M1GAS over a fibrinogen concentration range (0 -10 mg/ml). 4 replicates of each fibrinogen concentration and at least 3 independent experiments were carried out for each of the plasminogen activators. SK doses for the variants were determined so as to produce the same rates of pNA generation based on activity in solution i.e. in the presence of 100 nM Glu-Pg and 0.6 mM S-2251, without fibrinogen. All reaction volumes were 100 µl.

Rates were calculated as in 2.2.4A. Percentage activity compared to in solution (i.e. no fibrinogen) was determined in Microsoft Excel and plotted against a log fibrinogen concentration range in GraphPad prism, to establish the stimulatory effect of fibrinogen on the

rSK variants. The activity for rSK H46a with Lys-Pg was also subtracted from all activities to account for the stimulation by formation of a SK-Pg complex and thus determine the effect of fibrinogen.

2.2.6 Investigating the combined effect of fibrinogen and plasminogen on plasminogen activation by rSK H46a and rSK M1GAS

To investigate the effect of fibrinogen further, the solution assay with fibrinogen (as described in Section 2.2.4B and Figure 2.2B) was adapted to measure plasminogen activation rates by rSK H46a and rSK M1GAS over a fibrinogen/ plasminogen concentration matrix. 12 fibrinogen concentrations (0 -10 mg/ml) increasing across a 96 well microtitre plate and 8 concentrations of Glu-Pg (0 – 1.6 μM) down the plate, were incubated with 0.6 mM S-2251 and a fixed concentration of plasminogen activator, to produce a matrix of 96 different reactions. All reactions were 100 μL and a minimum of 3 independent experiments were carried out for each of the plasminogen activators, tPA (included to allow comparison), rSK H46a and rSK M1GAS. The plasminogen activator doses were determined so as to produce the similar rates of pNA generation based on activity in solution i.e. in the presence of 100 nM Glu-Pg and 0.6 mM S-2251, without fibrinogen. pNA generation was monitored by measuring absorbance change at 405 nm at 30 s intervals for 90 min at 37 °C.

Rates were calculated as in section 2.2.4A. An R script (Colin Longstaff, personal communication, see appendix 2) was used to produce surface contour plots and heat maps to allow comparison and an overview of tPA, rSK H46a and rSK M1GAS activity across the fibrinogen/plasminogen matrix.

2.2.7 Investigating the effect of plasminogen concentration on fibrinolysis by rSK H46a and rSK M1GAS

The fibrinolysis assay (section 2.2.4D and Figure 2.2D) was adapted to incorporate a range of plasminogen concentrations (0.0 - 1.6 μM Glu-Pg). The amount of tPA (included to allow comparison), rSK H46a and rSK M1GAS was adjusted to ensure similar activities were achieved for all the plasminogen activators with 100 nM Glu-Pg. As such, tPA (0.6 nM), rSK H46a (0.3 nM) and rSK M1GAS (0.02 nM) were used. A minimum of 3 independent experiments were carried out.

2.2.8 Investigating the effect of tranexamic acid on plasminogen activation by rSK H46a and rSK M1GAS

The solution assay (section 2.2.4A and Figure 2.2A) was adapted to include tranexamic acid (0 – 2.5 mM). 3 independent experiments with 4 replicates of each tranexamic acid concentration were carried out for a fixed SK dose. The SK concentration for each variant was determined such that similar rates of pNA generation were seen without tranexamic acid. As such, tPA (0.6 nM), rSK H46a (0.3 nM) and rSK M1GAS (0.02 nM) were used

2.2.9 Investigating the combined effect of tranexamic acid and fibrinogen on plasminogen activation by rSK H46a and rSK M1GAS

The solution assay with fibrinogen (section 2.2.4B and Figure 2.2B) was adapted to include 12 fibrinogen concentrations (0 – 10 mg/ml) across the plate and 8 tranexamic acid concentrations (0 – 2.5 mM**)** down the plate; to produce a matrix of 96 different reactions. All reactions included 0.6 mM S-2251 and a fixed concentration of plasminogen activator. 3 independent experiments were performed for each plasminogen activator with 100 nM Glu- and Lys- Pg. The plasminogen activator doses were determined so as to produce the similar rates of pNA generation based on activity in solution i.e. in the presence of 100 nM Glu-Pg

and 0.6 mM S-2251, without fibrinogen or tranexamic acid. As such rSK H46a (0.3 nM) and rSK M1GAS (0.02 nM) were used.

2.2.10 Investigating the effect of tranexamic acid on fibrinolysis by rSK H46a and rSK M1GAS

The fibrinolysis assay (section 2.2.4D and Figure 2.2D) was adapted to incorporate a range of tranexamic acid concentrations (0 – 2.5 mM). The amount of tPA (included to allow comparison), rSK H46a and rSK M1GAS was adjusted to ensure similar activities were achieved for all the plasminogen activators with no tranexamic acid. As such, tPA (0.6 nM), rSK H46a (0.3 nM) and rSK M1GAS (0.02 nM) were used. A minimum of 3 independent experiments were carried out.

2.2.11 Investigating fibrinolysis by rSK H46a and rSK M1GAS of FXIIIa cross-linked fibrin

The fibrinolysis assay (section 2.2.4D and Figure 2.2D) was adapted to incorporate FXIIa cross-linked fibrin. FXIII was pre-activated to FXIIIa via incubation with thrombin (100 nM) and 5 mM $CaCl_2$ solution for 30 min at 37 °C. Reactions were made with and without FXIIIa at a concentration of 2 IU/ml (i.e. twice the normal concentration in plasma).

2.2.12 Investigating the effect of α_2-antiplasmin on fibrinolysis by rSK H46a and rSK M1GAS

The fibrinolysis assay (section 2.2.4D and Figure 2.2D) was adapted to incorporate α_2-antiplasmin at a fixed concentration of 20 nM. A minimum of 3 independent experiments were carried out.

2.2.13 Investigating the effect of α_2-antiplasmin on fibrinolysis of FXIIIa cross-linked fibrin by rSK H46a and rSK M1GAS

The fibrinolysis assay (section 2.2.4D and Figure 2.2D) was adapted to incorporate FXIIa cross-linked fibrin and α_2-antiplasmin (20 mM). FXIII was preactivated and used as described in 2.2.11.

2.3 Results

2.3.1 Expression and purification of recombinant SK variants in E. coli

Recombinant SK from *S. equisimilis* (rSK H46a) and *S pyogenes* (rSK M1GAS) were expressed in *E. coli* as N-terminal SUMOstar fusion proteins. This system allows simple purification by Ni-affinity chromatography utilising the 6xHis tag within the SUMOstar fusion sequence. SK SUMOstar fusion proteins were cleaved by SUMOstar protease. The protease cleaves precisely at the junction between the tag and the SK sequence leaving no unwanted amino acids and preserving the N-terminal Ile essential for SK function.

The final purification step removes the SUMOstar tag and protease by Ni-affinity leaving the purified SK in solution (Figure 2.4). Typically *E.coli* cultures yielded 200-500 μg cleaved protein per litre of culture. SDS-page of each variant under reducing conditions confirmed a discrete band, consistent with the expected size relative to MW markers, of 47 kDa. No other bands were present on the gel indicating good purity. For each variant several batches of protein were expressed and pooled and total protein concentration determined by amino acid analysis, sufficient to carry out all the studies in this project. Each combined batch was diluted to a working concentration to facilitate appropriate dilution regimes for the activity assays and stored as frozen aliquots to negate the effect of any batch to batch variation by preventing repeated freeze/thaw cycles.

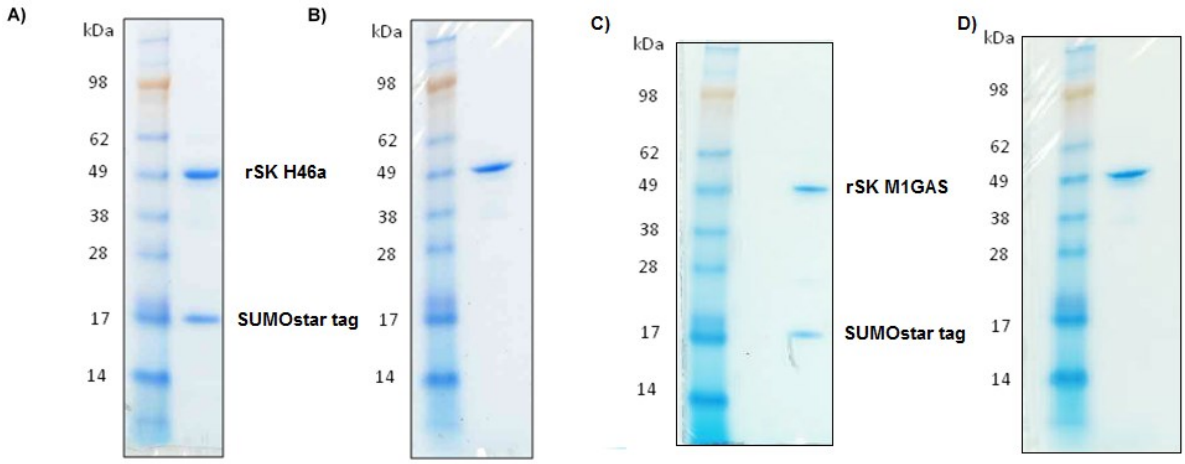

Figure 2.4 SDS-PAGE of rSK H46a and rSK M1GAS to check for SUMOstar fusion protein cleavage and purification. Gels were loaded with 500 ng protein and stained with Coomassie reagent. Molecular weight markers were included in each gel for reference. A) and C) Indicates presence of rSK H46a and rSK M1GAS protein respectively (47 kDa) and cleaved SUMOstar tag (according to the manufacturer's protocol 15-20 kDa) after incubation with SUMOstar protease. B) and D) Presence of rSK H46a and rSK M1GAS respectively after SUMOstar tag removed by Ni-NTA agarose column filtration.

2.3.2 The effect of fibrinogen and fibrin on plasminogen activation by rSK H46a and rSK M1GAS

Four different assay systems were used to investigate the kinetic activities of rSK H46a and rSK M1GAS. Plasminogen activation was measured in solution; in the presence of fibrinogen; in the presence of fibrin; and in a fibrinolysis assay. For each assay system, rSK H46a and rSK M1GAS potencies were calculated relative to the WHO 3rd IS for SK (00/464), in IU/ml, from multiple SK doses using a parallel line bioassay analysis. To compare SK activity between the different assay systems specific activities (expressed as IU/μg protein) were calculated based on the protein concentration determined for each rSK preparation.

2.3.2A Glu-Pg activation by rSK H46a and rSK M1GAS in solution

To investigate SK activity in solution i.e. with no fibrin(ogen) present, the current EP method for assigning potencies to therapeutic SK was used. Initial plasminogen activation rates were measured against the chromogenic substrate for plasmin, S-2251. The results show rSK M1GAS has approximately 5-fold lower specific activity than rSK H46a, 12.4 IU/μg compared to 58.2 IU/μg respectively (Figure 3.2).

2.3.2B Glu-Pg activation by rSK H46a and rSK M1GAS in presence of fibrinogen

The solution plasminogen activation assay was adapted to investigate SK activity in the presence of fibrinogen (3 mg/ml). Potency estimates for rSK H46a and rSK M1GAS were calculated relative to the IS (00/464) in the same was as with the original assay, using initial plasminogen activation rates against S-2251.

In the presence of fibrinogen, the specific activity determined for rSK H46a was found to be lower than in the solution assay (39.0 IU/μg and 58.2 IU/μg respectively). Conversely, the specific activity of rSK M1GAS was higher in the presence of fibrinogen (20.2 IU/μg) compared to the solution assay (12.4 IU/μg) (Figure 3.2). When the activities of rSK H46a and rSK

M1GAS in fibrinogen were compared, rSK H46a was 2-fold higher than rSK M1GAS (39.0 IU/µg vs 20.2 IU/µg), however this is smaller than the 5-fold difference observed in solution.

The apparent inhibition of activity for rSK H46a may be explained by the competition between the chromogenic substrate and fibrinogen for the active site of plasmin. The higher activity observed for rSK M1GAS in the presence of fibrinogen appears to overcome any competitive inhibition to have an overall stimulatory effect.

2.3.2C Glu-Pg activation by rSK H46a and rSK M1GAS in presence of fibrin

The relative activities of rSK H46a and rSK M1GAS were investigated in the presence of fibrin. As with the solution and fibrinogen assays, initial plasminogen activation rates were determined using S-2251, however in this system the reaction occurs at the surface of a pre-formed fibrin clot. This approach is intended to be representative of the mechanism of action for therapeutic SK during thrombolytic therapy. Fibrin clots were made in microtitre plates using physiological concentrations of fibrinogen (3 mg/ml) and thrombin (20 nM), incorporating plasminogen throughout. The ionic strength of the buffer used in the reaction was optimised to ensure the clots were transparent; thus preventing clot turbidity from affecting absorbance readings at 405 nm.

Specific activities for rSK H46a and rSK M1GAS were derived from potency estimates calculated relative to the WHO 3rd IS for SK (00/464). The presence of fibrin appeared to have no measurable effect on the activity of rSK H46a (61.6 IU/µg) compared to the solution assay (58.2 IU/µg). For rSK M1GAS however the activity in fibrin was calculated to be 74.0 IU/µg, which is approximately 7-fold higher than the specific activity of rSK-M1GAS calculated in the solution assay (12.2 IU/µg) (Figure 2.5).

2.3.2D Effect of Glu-Pg activation by rSK H46a and rSK M1GAS on fibrinolysis

The relative activities of rSK H46a and rSK M1GAS were investigated with Glu-Pg in a purified fibrinolysis assay system. Fibrin clot lysis activity was measured by following absorbance

readings to monitor changes in clot turbidity corresponding to clot formation and lysis. Fibrinolysis rates were calculated as the time to 50% lysis from start of reaction. Specific activities were determined for rSK H46a and rSK M1GAS, based on potency estimates made relative to the WHO IS (00/464), and the activity of rSK-M1GAS (168.3 IU/µg) was calculated to be more than two-fold higher than rSK H46a (72.8 IU/µg).

The relative activities of rSK-H46a and rSK M1GAS in the four assay systems is summarised in Figure 2.5 and Table 2.1. While rSK H46a shows only small changes in activity in the presence of fibrin, and inhibition in the presence of fibrinogen, rSK M1GAS activation of plasminogen appears to be stimulated by fibrin. The presence of fibrin in the fibrin-bound plasminogen activation assay system shows a 7- fold increase in rSK M1GAS activity and there is up to a 15- fold increase in the fibrinolysis assay system compared to the solution assay where no fibrin(ogen) is present. rSK M1GAS activity is also stimulated in the presence of fibrinogen approximately 2- fold.

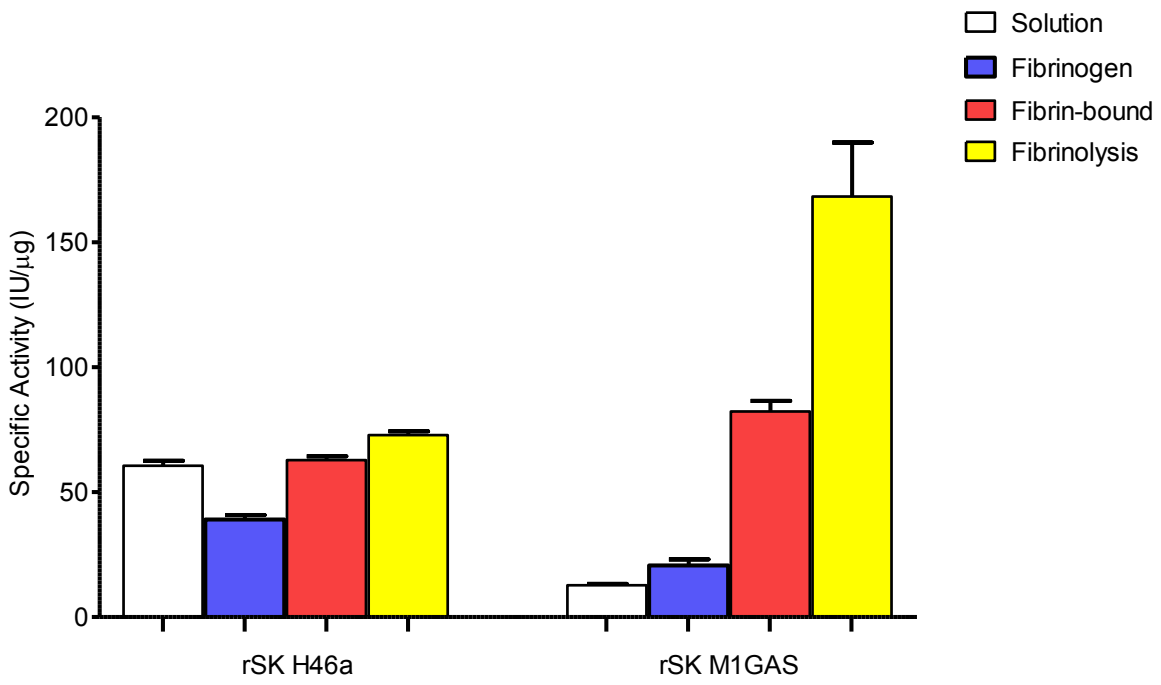

Figure 2.5 The effect of fibrinogen and fibrin on SK activity against Glu-Pg. Specific activity (IU/µg) of rSK H46a and rSK M1GAS were determined in solution (EP method), in the presence of fibrinogen, in the presence of fibrin and in a fibrinolysis assay using Glu-Pg relative to the WHO 3rd IS SK (00/464) to determine the effect of fibrin(ogen). Error bars show standard deviation of a minimum of 3 independent experiments (see Table 2.1).

2.3.3 Lys-Pg activation by rSK H46a and rSK M1GAS

For each of the four assay systems, Glu-Pg was substituted with Lys-Pg, a more readily activated plasminogen form with an open conformation. Any relative differences between Glu- and Lys- Pg could shed light on the mechanism of action of the SK variants such as whether SK variants induce different conformational changes in plasminogen or alter fibrinogen binding.

Lys-Pg activation and fibrinolysis rates were faster in all four assay systems than with Glu-Pg (data not shown); however the relative specific activities of rSK H46a and rSK M1GAS in IU/µg were comparable. The results for the solution plasminogen activation assay show rSK M1GAS has approx. 4-fold lower specific activity than rSK H46a; 54.6 IU/µg compared to 14.0 IU/µg, respectively. In the presence of fibrin (fibrin-bound plasminogen activation assay), rSK M1GAS activity increased, compared to in solution, to 67.0 IU/µg and was similar to rSK H46a 59.2 IU/µg. This equates to an approximate 5-fold increase in specific activity of rSK M1GAS in the presence of fibrin. In the fibrinolysis assay, rSK M1GAS shows approx. three-fold higher activity than rSK H46a (176.3 IU/µg vs. 60.4 IU/µg) (Table 2.1).

Overall, the comparison of rSK H46a and rSK M1GAS activation of Glu- and Lys- Pg demonstrates that the differences seen are due to the binding of SK-Pg complexes with fibrinogen and fibrin.

Table 2.1 Effect of fibrin on SK activity against Glu-Pg and Lys-Pg. Specific activity (IU/µg) of rSK H46a and rSK M1GAS were determined for plasminogen activation in solution (EP method), in the presence of fibrinogen, at the surface of a fibrin clot and in a fibrinolysis assay, using Glu-Pg and Lys-Pg. (N =) number of independent assays.

	Glu-Pg				Lys-Pg			
	rSK H46a		rSK M1GAS		rSK H46a		rSK M1GAS	
	Specific Activity (IU/µg)	(N =)	Specific Activity (IU/µg)	(N =)	Specific Activity (IU/µg)	(N =)	Specific Activity (IU/µg)	(N =)
Solution plasminogen activation	58.2	6	12.4	6	54.6	8	14.0	8
Solution assay + fibrinogen	39.0	3	20.6	3	54.0	2	25.0	2
Fibrin-bound plasminogen activation assay	61.6	7	74.0	7	59.2	7	67.0	7
Fibrinolysis assay	72.8	5	168.3	5	60.4	7	176.3	7

2.3.4 Investigating the effect of fibrinogen concentration on plasminogen activation by rSK H46a and rSK M1GAS

As demonstrated in Table 2.1 and Figure 2.5, fibrin(ogen) stimulates rSK M1GAS activation of Glu- and Lys-Pg. Fibrinogen is the soluble precursor of fibrin. It forms a homogeneous system, making it easier to study in activity assays than insoluble fibrin and as such is useful when investigating fibrin stimulation of plasminogen activation.

The effect of fibrinogen on the activation of plasminogen by rSK H46a and rSK M1GAS was further investigated by determining plasminogen activation rates for Glu- and Lys- Pg across a fibrinogen concentration range. The aim was to understand the relative fibrinogen binding capacity of the SK variants in complex with plasminogen. Plasminogen and SK concentrations were kept constant to represent physiological concentration and ensure the rates of plasminogen activation by rSK H46a and rSK M1GAS were equivalent in solution (i.e. without fibrinogen).

The height of the peak at the optimum fibrinogen concentration represents the stimulatory effect. For rSK M1GAS, fibrinogen binding is shown to be necessary for stimulation of plasminogen activation. Across the concentration range, Glu-Pg activation by rSK M1GAS was stimulated to a maximum of approx. 300% compared to in solution (Figure 2.6). In comparison, rSK H46a showed minimal stimulation up to physiological fibrinogen concentration (3mg/ml) of a 150%, and inhibition at this point and above.

SK activation of Lys-Pg by rSK M1GAS showed the same profile, and maximal stimulation of activity at around physiological fibrinogen concentration of 3 mg/ml. (Figure 2.6). In contrast, the small stimulation of rSK H46a activity in the presence of Glu-Pg was lost in the presence of Lys-Pg, suggesting that Glu-Pg bound to fibrinogen undergoes a conformational change, making it more easily activated by SK. However, the open conformation of Lys-Pg means binding to fibrinogen does not undergo any increased activation when bound to rSK H46a,

and therefore the profile of Lys-Pg across the fibrinogen concentration represents the stimulation and inhibition by fibrinogen binding only.

Subtracting the rates for rSK H46a activation of Lys-Pg from the other rates is therefore useful for demonstrating the extent to which the rSK variants are stimulated by fibrinogen across the concentration range (Figure 2.7). When this subtraction is taken into account, there is no stimulation of rSK H46a by fibrinogen but rSK M1GAS still shows a 6–fold increase in activity with Glu-Pg and 5-fold with Lys-Pg, relative to in solution.

As demonstrated in these experiments, rSK M1GAS stimulation displays a bell-shape curve of plasminogen activation against a log concentration of fibrinogen; typical of a template model. In a template model an increase in template concentration, in this instance fibrinogen, leads to an increase in plasminogen activation rates up to an optimum template concentration. Binding of the rSK M1GAS-Pg* complex and plasminogen to fibrinogen, brings activator and substrate into close proximity to facilitate activation. As the template concentration increases above the optimum, the activator and substrate are more likely to bind different template molecules and the stimulatory effect is lost. No such effect is seen for rSK H46a in the presence of fibrinogen.

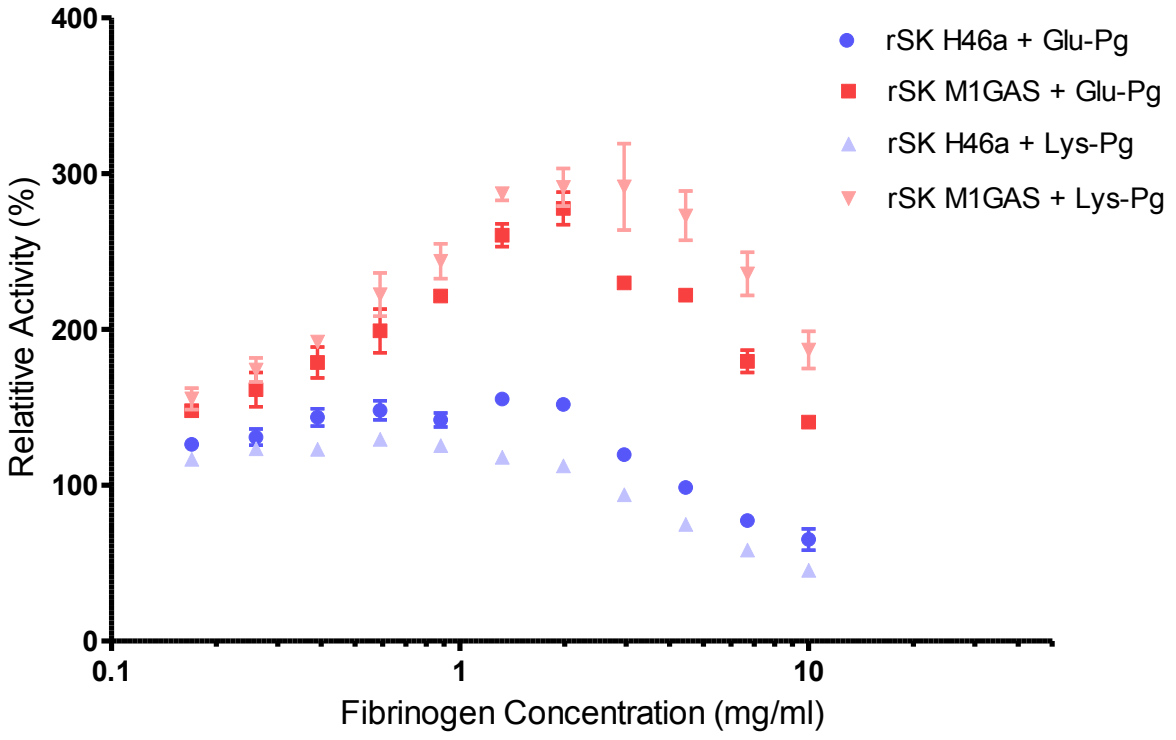

Figure 2.6 The effect of fibrinogen on rSK H46a and rSK M1GAS activation of Glu- and Lys- Pg. rSK H46a and rSK M1GAS activity against Glu- and Lys– Pg by were measured over a range of fibrinogen concentrations (0 – 10 mg/ml). Rates are represented as relative activity (%) to that with no fibrinogen and plotted against a log fibrinogen concentration (mg/mL). Error bars show SEM of 4 replicates.

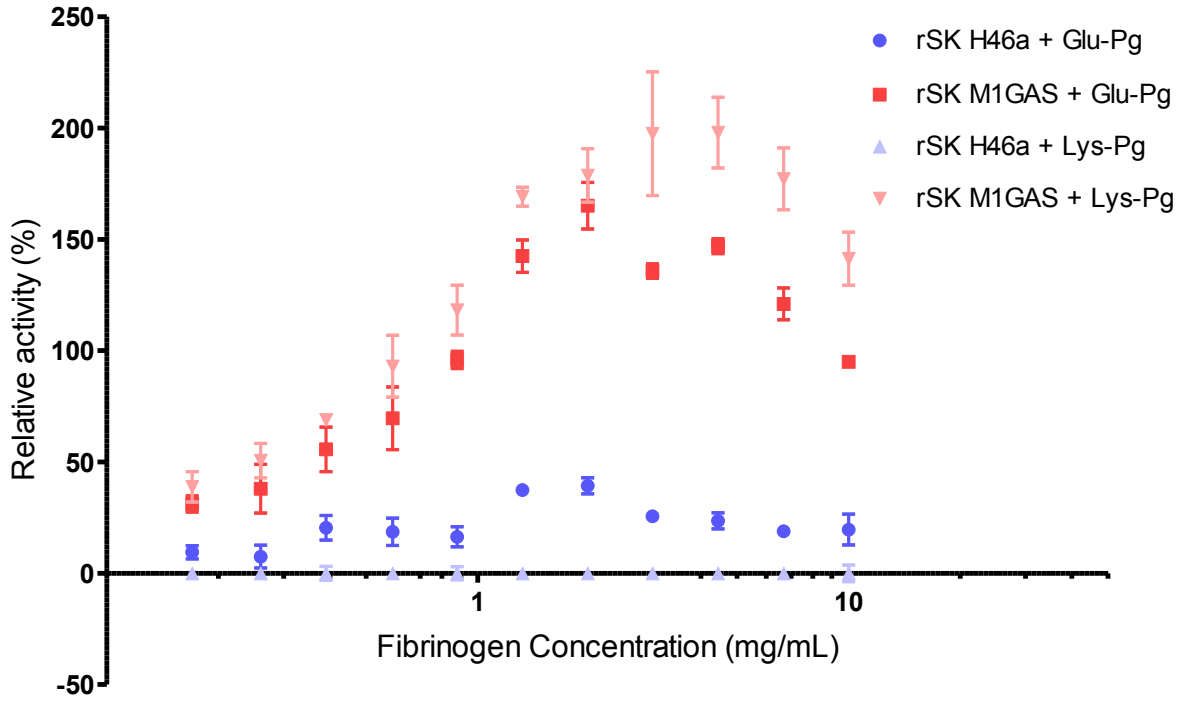

Figure 2.7 The stimulation of rSK M1GAS by fibrinogen. The stimulation of rSK H46a and rSK M1GAS was measured over a range of fibrinogen concentrations. The activity of rSK H46a in the presence of Lys-Pg was considered a baseline for conformational activation i.e. stimulation which could not be attributed to fibrinogen binding, and therefore subtracted from the rates for rSK H46a and rSK M1GAS activity with Glu-Pg, as well as rSK M1GAS activity with Lys-Pg. Rates are represented as relative activity (%) to that seen with no fibrinogen before subtraction of rSK H46a Lys-Pg activity, and plotted against a log fibrinogen concentration (mg/mL). Error bars show SEM of 4 replicates.

Fibrinogen is also known to be a template for plasminogen activation by tPA, which displays the characteristic bell-shaped curve across a fibrinogen range demonstrated above for rSK M1GAS (Thelwell and Longstaff, 2007). A solution assay matrix of increasing fibrinogen concentration across the plate and increasing plasminogen concentration down the plate was used to further investigate the template model demonstrated by rSK M1GAS, and to compare activity of rSK H46a and rSK M1GAS with that of tPA.

Increasing the plasminogen and/or fibrinogen concentration is seen to increase the rate of tPA activation of plasminogen, and to a much lesser extent rSK M1GAS, but changes in fibrinogen and plasminogen concentrations have very minimal effect on rSK H46a as demonstrated in the surface plots shown in Figure 2.8. rSK H46a activity reaches a maximum of 2.5-fold stimulation, but this is only at a plasminogen concentration much greater than seen in physiological conditions (1.6 μM). Maximal stimulation of rSK M1GAS is seen to be at around physiological fibrinogen (3 mg/mL), and is similar for tPA.

In summary rSK M1GAS requires binding to fibrinogen to stimulate plasminogen activation. In contrast, rSK H46a shows equivalent activity in solution based and fibrin-based assay systems with inhibition in assays with fibrinogen.

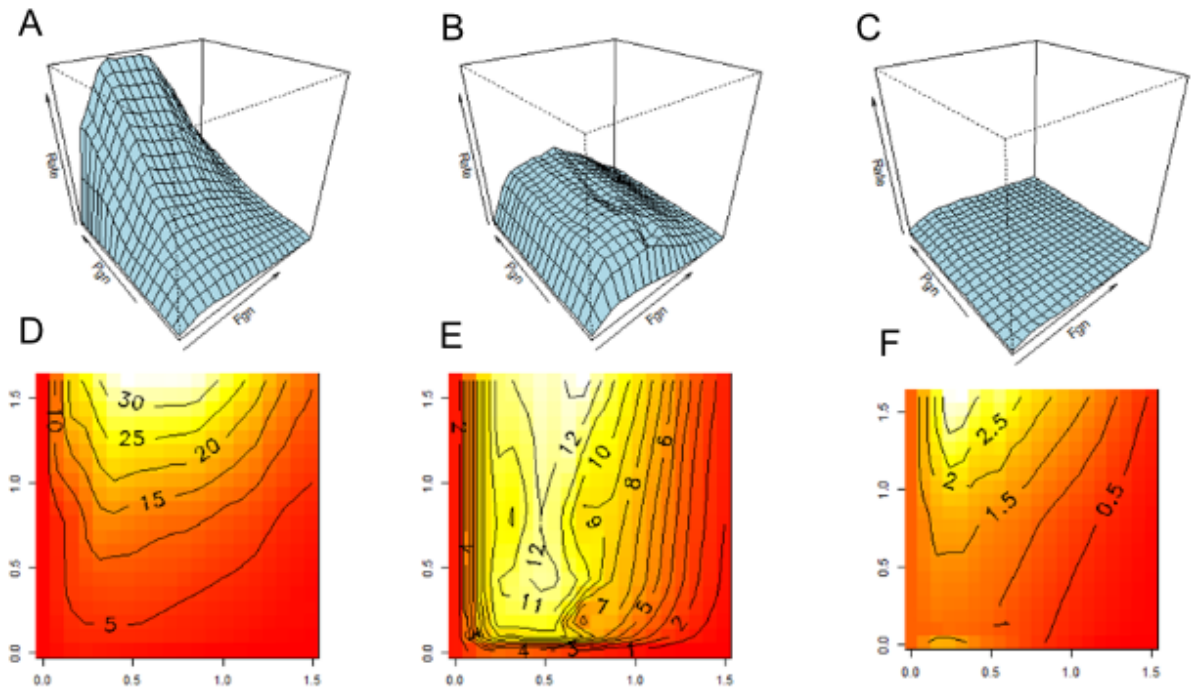

Figure 2.8 The effect of plasminogen and fibrinogen concentration on plasminogen activation by tPA, rSK M1GAS and rSK H46a. 3D Surface contour plots (A for rSK M1GAS, B for tPA and C for rSK H46a) and corresponding heat maps (D, E and F) were generated to represent the activity, and allow comparison, of tPA, rSK H46a and rSK M1GAS, across a plasminogen/fibrinogen concentration matrix. The heat map isobars represent fold stimulation, with the fibrinogen concentration (0 – 15 mg/mL) along the X axis and the plasminogen concentration (0 – 1.6 µg/mL) along the Y axis. The colour gradient from white, through yellow and orange, to red represents maximal to minimal rate of stimulation, corresponding to height on the 3D surface contour plots.

2.3.5 Investigating the enzyme kinetics of plasminogen activation by rSK H46a and rSK M1GAS in a fibrin clot lysis assay

Although fibrinogen is shown to stimulate rSK M1GAS activity, there is a greater stimulation in the presence of fibrin (Figure 2.5). As such, the effect of rSK H46a and rSK M1GAS on fibrinolysis was investigated further in a fibrinolysis assay. Varying the concentration of fibrinogen or thrombin used would alter the clot structure and fibrin formed, thereby affecting the stability of the clot, as well as making it difficult to interpret results. Instead, fibrinolysis by tPA, rSK H46a and rSK M1GAS was measured across a plasminogen concentration range. In all instances, the plasminogen activator concentration was adjusted to produce similar clot lysis times. Figure 2.9 shows these results with data expressed as lysis rate (1/time to 50 % lysis) versus plasminogen concentration. This allowed results to be fitted to the Michaelis Menten equation and provide estimates for the apparent K_M and V_{max} values which are summarised in Table 2.2.

In this assay system the K_M (0.08 – 0.11 μM) and V_{max} (1.06 – 1.42 μM s^{-1}) values did not differ significantly between the 3 plasminogen activators, but the amount of rSK M1GAS (0.02 nM) required for this activity was approximately 15 and 24-fold lower than the rSK H46a (0.3 nM) and tPA (0.6 nM) respectively. Normalising the V_{max}/K_M to account for the differences in concentrations gives values of 25.8 s^{-1} , 43.2 s^{-1} and 629.0 s^{-1} for tPA, rSK H46a and rSK M1GAS activity respectively (Table 2.2). Thus, in the presence of fibrin, rSK M1GAS on a mole for mole basis, is much more potent than rSK H46a or tPA.

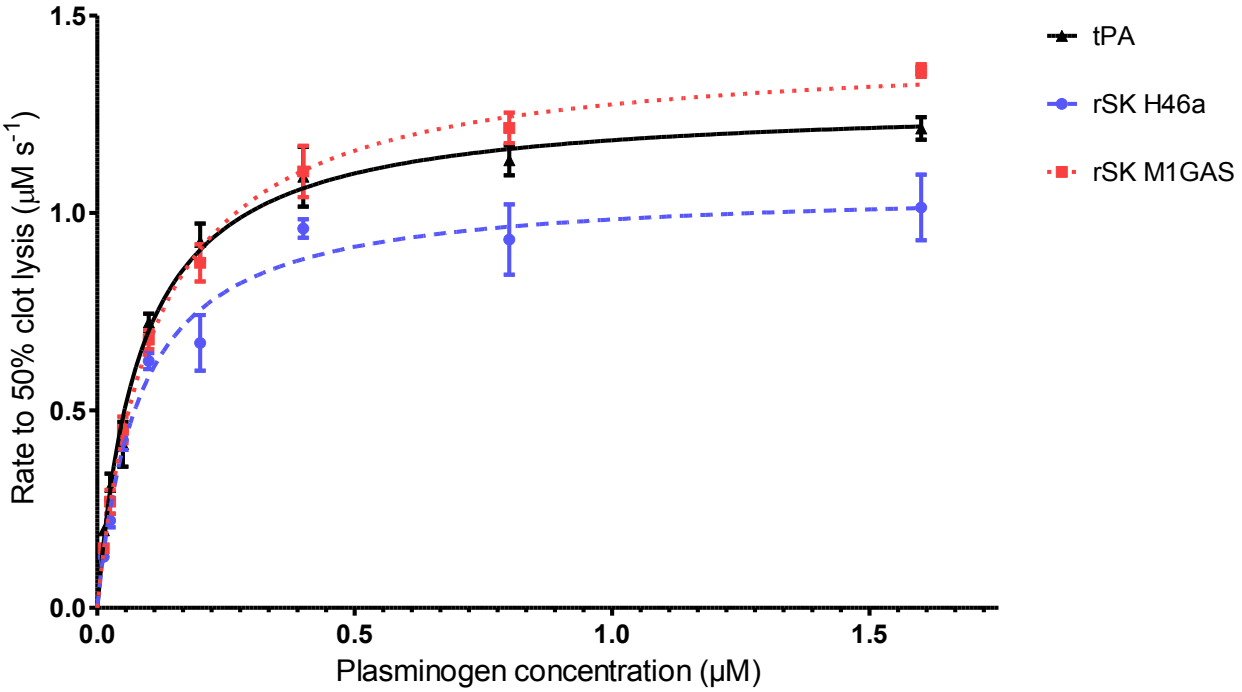

Figure 2.9 The effect of plasminogen concentration on tPA, rSK H46a and rSK M1GAS mediated fibrinolysis. Fibrinolysis by tPA, rSK H46a and rSK M1GAS was investigated across a plasminogen concentration range (0- 1.6 µM). Concentrations of each plasminogen activator were chosen to give similar activities at 100 nM Glu-Pg. Error Bars represent SEM of 4 replicates.

Table 2.2 Comparison of kinetic parameters for tPA, rSK H46a and rSK M1GAS mediated fibrinolysis. Kinetic parameters V_{max} and K_M, were determined for fibrinolysis by tPA, rSK H46a and rSK M1GAS. A normalised V_{max}/K_M value was determined for each variant to allow comparison based on the enzyme concentration (E_0) necessary to produce similar kinetic rates.

	V_{max} (μM s^{-1})	K_M (μM)	E_0 (nM)	Normalised V_{max}/K_M (s^{-1})
tPA	1.28	0.08	0.60	25.8
rSK H46a	1.06	0.08	0.30	43.2
rSK M1GAS	1.42	0.11	0.02	629.0

2.3.6 The effect of tranexamic acid on SK H46a and rSK M1GAS activity.

Tranexamic acid, a lysine analogue, inhibits plasminogen binding to fibrin(ogen) by competing for the lysine-binding sites in the plasminogen kringle domains. It is useful in studying mechanisms of plasminogen activation by SK as it also interrupts the SK-plasminogen complex by disrupting SK-binding to the plasminogen kringle domains. To investigate any differences in rSK H46a and rSK M1GAS binding to plasminogen through lysine-binding sites, the chromogenic solution assay (2.3.2A) was adapted to include a range of tranexamic acid concentrations and the results are shown in Figure 2.10. The rSK concentrations were adjusted to give equivalent rates of activity in the absence of tranexamic acid, and the results were expressed as a percentage of this result for each SK. The activity of rSK M1GAS was far more sensitive to low tranexamic acid concentrations than rSK H46a in solution, with a much sharper loss in activity across the concentration range.

The effect of tranexamic acid on rSK H46a and rSK M1GAS activity was further investigated across a fibrinogen range in the presence of both Glu- and Lys-Pg (Figure 2.11). Here, once again, the activity of rSK M1GAS was more sensitive to lower tranexamic acid concentrations than rSK H46a, depicted by the comparative IC_{50} values of 14.5 μM for rSK M1GAS and 465 μM for rSK H46a.

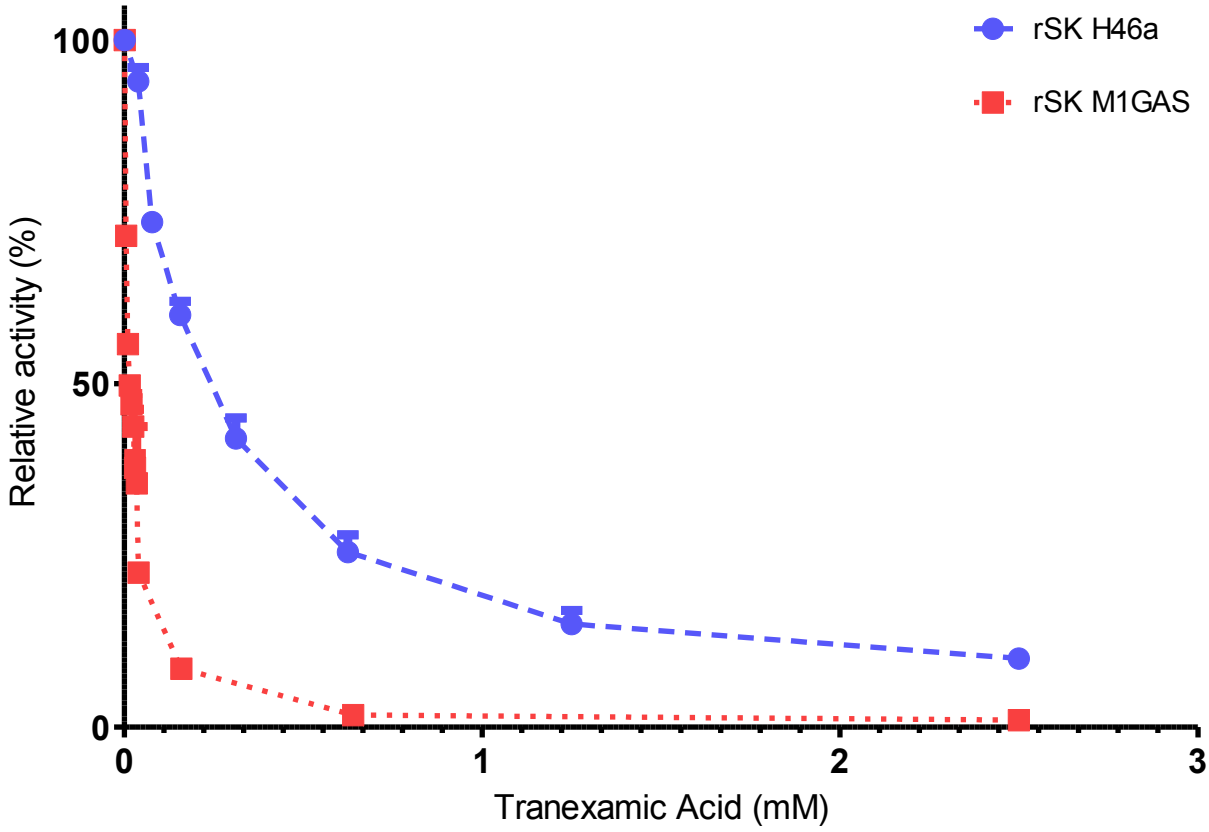

Figure 2.10 The relative effect of tranexamic acid on rSK H46a and rSK M1GAS activity in solution. Plasminogen activation by rSK H46a and rSK M1GAS was determined across a tranexamic acid concentration range (0 – 2.5 mM) using the chromogenic substrate for plasmin, S-2251. Activity is represented as % relative to plasminogen activation with no tranexamic acid present. Error bars represent the SEM of 4 replicates.

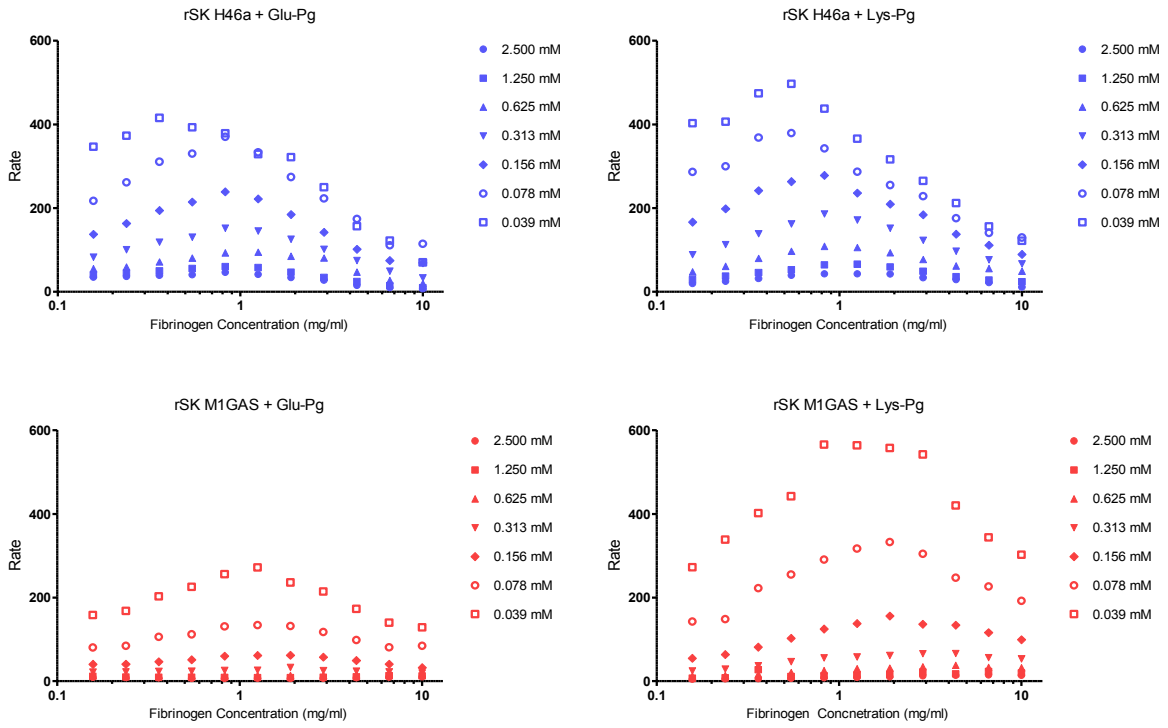

Figure 2.11 The combined effect of tranexamic acid and fibrinogen concentration on rSk H46a and rSK M1GAS. The rates of S-2251 substrate turnover by rSK H46a and Glu-Pg (top left), rSK H46a and Lys-Pg (top right), rSK M1GAS and Glu-Pg (bottom left), rSK M1GAS and Lys-Pg (bottom right) were investigated in a tranexamic acid (0-2.5 mM) and fibrinogen (0-10 mg/mL) concentration matrix.

Fibrinolysis with tPA, rSK H46a and rSK M1GAS was also investigated across the tranexamic acid concentration range (Figure 2.12). Whilst all three plasminogen activators showed the same sigmoidal curve, rSK H46a was less affected by increased concentration of tranexamic acid than tPA and rSK M1GAS, which were indistinguishable across the range. Here, the IC_{50} for rSK H46a is 327 μM whilst for rSK M1GAS it is 133 μM.

Whilst fibrinogen stimulates rSK M1GAS activity, this work has demonstrated there is a greater effect in the presence of fibrin (Figure 2.5). Figure 2.13 further demonstrates the difference fibrinogen and fibrin has on rSK M1GAS. Tranexamic acid is seen to have a much greater inhibitory effect on fibrinogen than fibrin; demonstrating that rSK M1GAS binding of fibrin is stronger than fibrinogen (IC_{50} 133 μM vs. 14.5 μM respectively). In comparison, there is very little difference in the binding of rSK H46a to fibrinogen and fibrin (IC_{50} of 465 μM vs 327 μM).

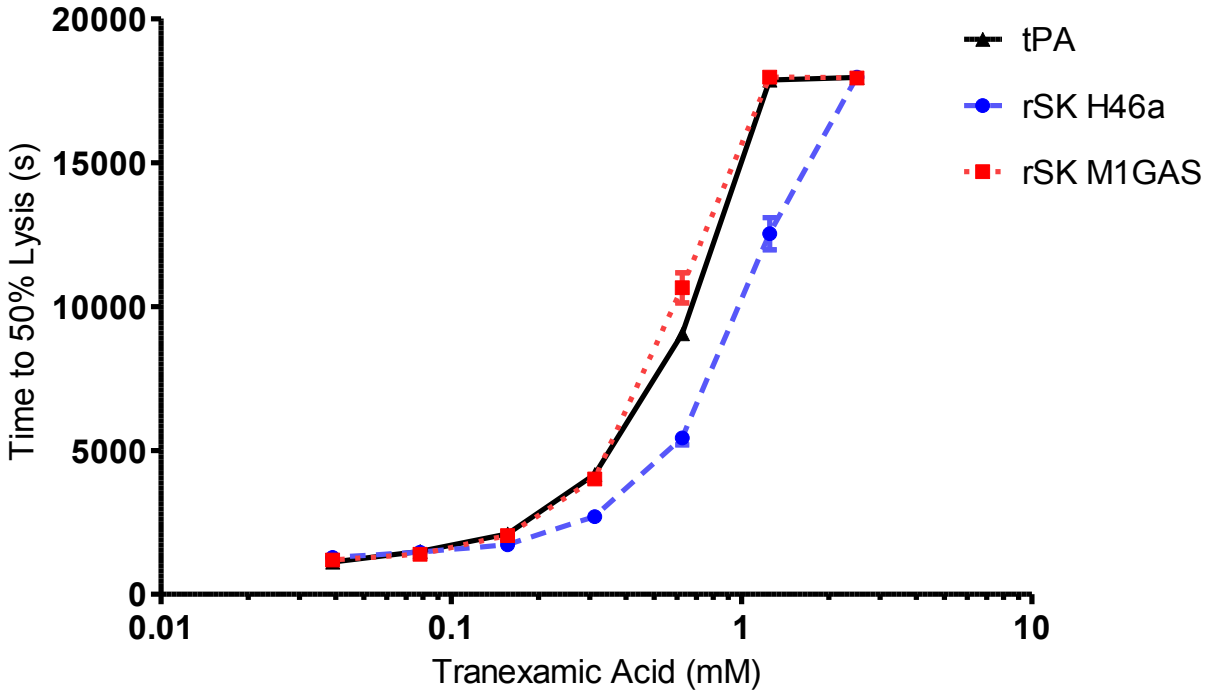

Figure 2.12 The effect of tranexamic acid on tPA, rSK H46a and rSK M1GAS mediated fibrinolysis. Time to 50% fibrinolysis (s) by tPA, rSK H46a and rSK M1GAS was investigated across a tranexamic acid concentration range (0 - 2.5 mM). Concentrations of each plasminogen activator were chosen to give similar activities with no tranexamic acid present to facilitate comparison. Error Bars represent SEM of 4 replicates.

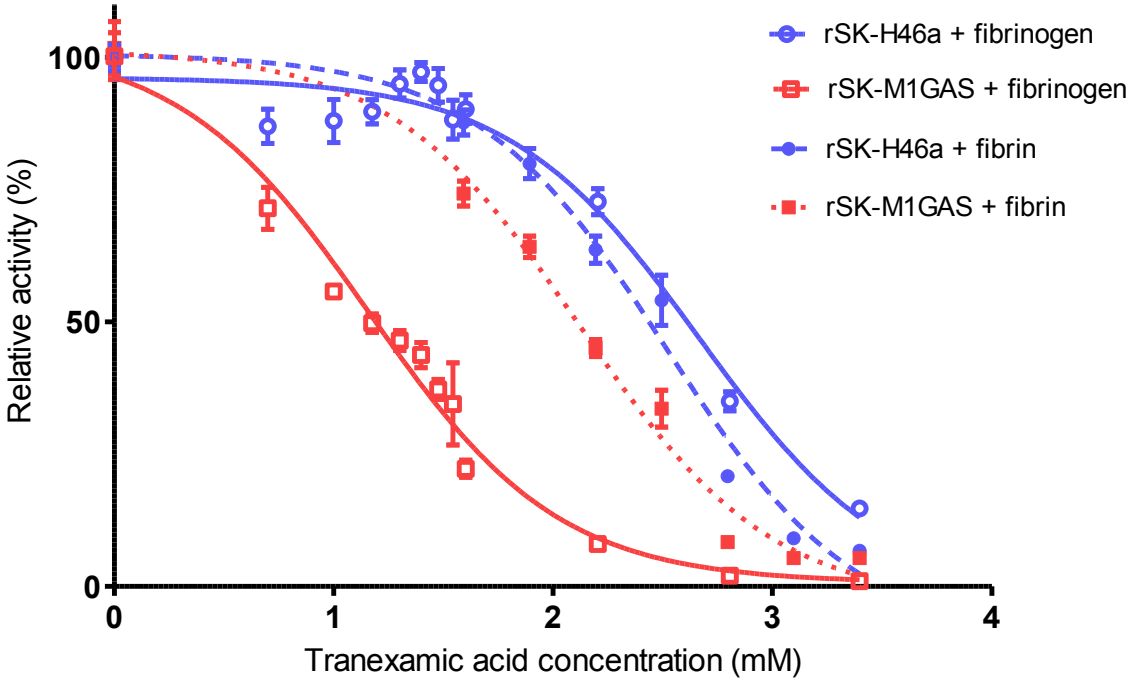

Figure 2.13 A comparison of the effect of tranexamic acid on rSK H46a and rSK M1GAS activity in the presence of fibrinogen and fibrin. The activity of rSK H46a and rSK M1GAS in fibrinogen and fibrin across a tranexamic acid concentration range was calculated relative to the corresponding activity in solution (i.e. no tranexamic acid present). The results were used to compare the relative effect of fibrinogen and fibrin on the two variants.

2.3.7 The effect of FXIII and α_2-antiplasmin on fibrinolysis by rSK H46a and rSK M1GAS

In physiological conditions, fibrin is cross-linked by activated FXIII (FXIIIa) to increase the stability of the fibrin clot and limit degradation (Chapin and Hajjar, 2015). FXIIIa has also been demonstrated to act as part of the innate immunity against S. *pyogenes*, actively trapping the bacteria in the fibrin clot by cross-linking the M1 protein to fibrin (Loof et al., 2011, Loof et al., 2012). However, no studies have demonstrated the effect of FXIIIa and cross-linked fibrin on SK activation of plasminogen and subsequent fibrinolysis.

To investigate this, plasminogen activation by rSK H46a and rSK M1GAS and the subsequent fibrinolysis of FXIIIa cross-linked fibrin was compared to that of untreated fibrin. Physiological concentrations of fibrinogen, thrombin and FXIIIa were used to ensure the fibrin formed was representative of that in bacterial invasion *in vivo*. FXIII was preactivated to FXIIIa by incubation with thrombin.

Initially, studies with WHO 3rd IS SK (00/464) were used to determine the effect inclusion of FXIIIa has on clot lysis profiles. As seen in Figure 2.14, a different clot lysis profile was observed, compared to clots with no FXIII. This was represented by a lower maximum absorbance, indicating a change in clot turbidity as a result of the altered fibrin structure. The same assay set-up was replicated in the presence of rSK H46a and rSK M1GAS. However, despite the differing fibrin structure, the specific activities of rSK H46a and rSK M1GAS were unaffected, with time to complete lysis of FXIIIa cross-linked fibrin equivalent to that of untreated fibrin in all instances (Figure 2.15).

A)

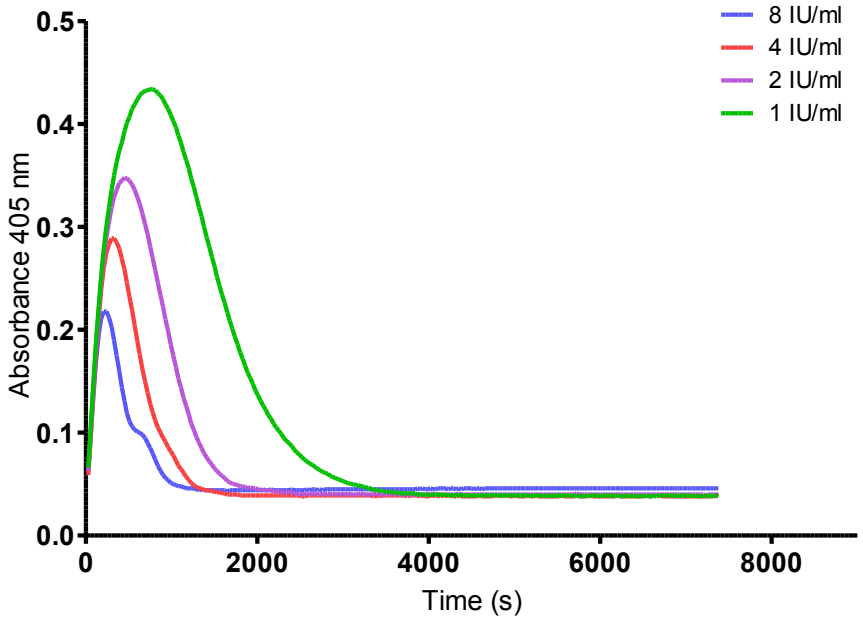

B)

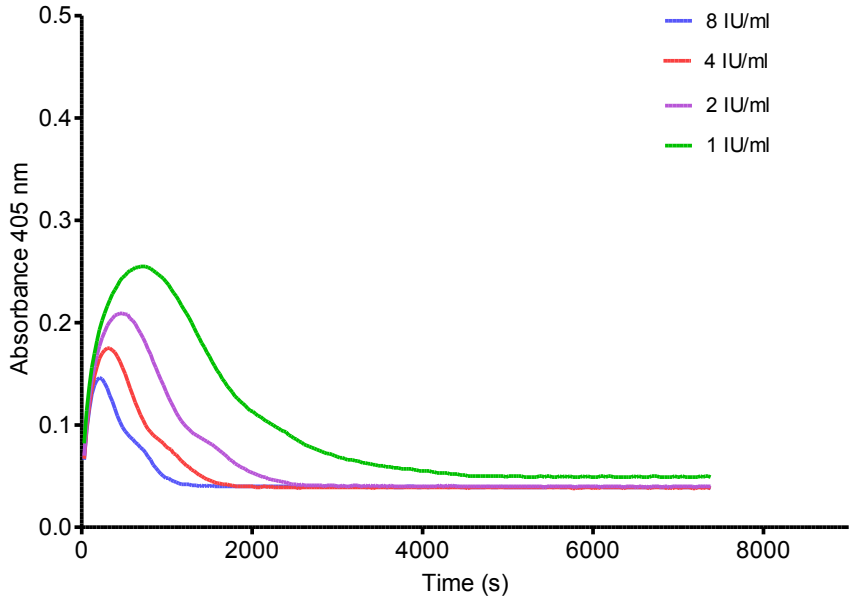

Figure 2.14 The effect of FXIIIa on clot formation absorbance at 405 nm. Typical clotting and lysis curves shown are for WHO 3rd IS SK (00/464) in the presence (A) or absence (B) of 2 IU/ml FXIIIa over a range of SK concentrations (1,2,4 and 8 IU/ml) to show the change in maximum absorbance at 405 nm and hence change in fibrin clot structure through FXIIIa cross-linking.

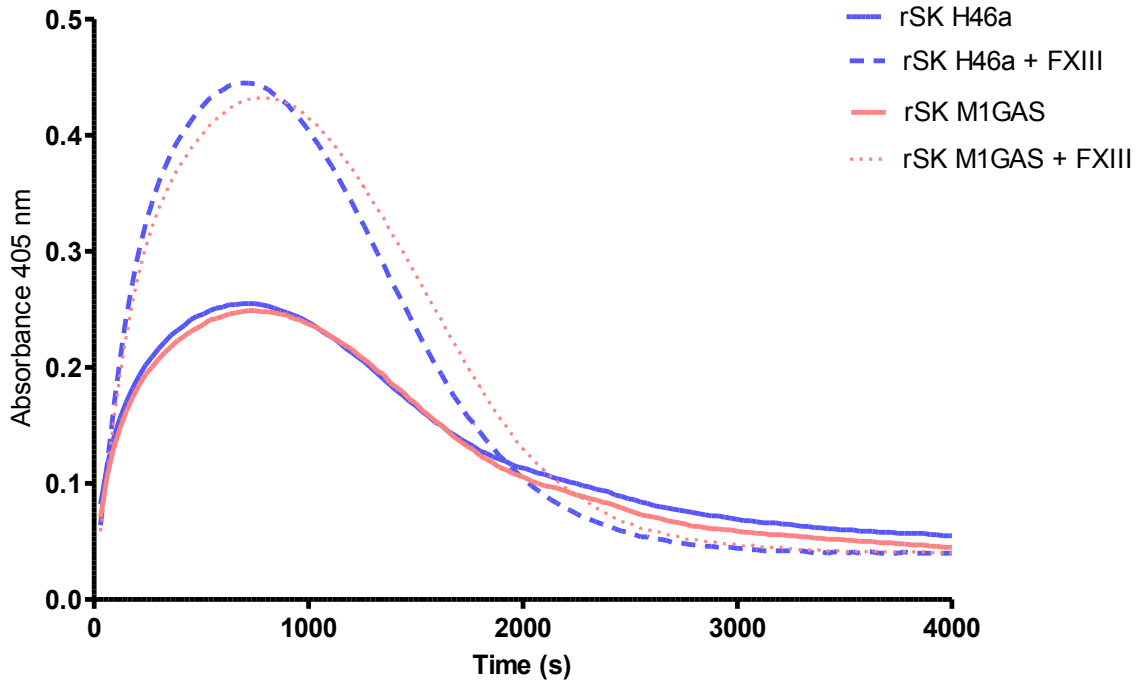

Figure 2.15 The effect of FXIIIa cross-linked fibrin on rSK H46a- and rSK M1GAS-mediated fibrinolysis. Fibrinolysis mediated by rSK H46a and rSK M1GAS was investigated in the presence of activated FXIII. Lysis profiles for each variant with and without 2 IU/ml FXIIIa were determined by measuring absorbance at 405 nm. Typical profiles are shown here.

Under normal physiological conditions, FXIIIa cross-links α_2-antiplasmin into fibrin clots to prevent clot degradation (Fraser et al., 2011). As such, the effect of α_2-antiplasmin on fibrinolysis facilitated by rSK H46a and rSK M1GAS was investigated.

Fibrinolysis rates were determined for rSK H46a and rSK M1GAS in the presence of α_2-antiplasmin. Though the α_2-antiplasmin was shown to increase fibrinolysis time, as with FXIIIa cross-linked fibrin there appeared to be no difference in effect on rSK H46a or rSK M1GAS activity (Figure 2.16).

To further investigate the combined effect FXIIIa and α_2-antiplasmin may have on rSK H46a and rSK M1GAS promotion of fibrin degradation, the fibrinolysis assay was replicated in the presence of both. This was compared concurrently to FXIIIa alone to investigate any changes in fibrinolysis by rSK H46a and rSK M1GAS. Again, as with α_2-antiplasmin alone, fibrinolysis times were increased but there was no observed effect on rSK H46a and rSK M1GAS activity (Figure 2.17).

Overall, rSK M1GAS does not appear to have any advantage with regard to fibrinolysis of FXIIIa cross-linked fibrin, when compared to rSK H46a. Furthermore, there is no protection from inhibition by the plasmin inhibitor α_2-antiplasmin.

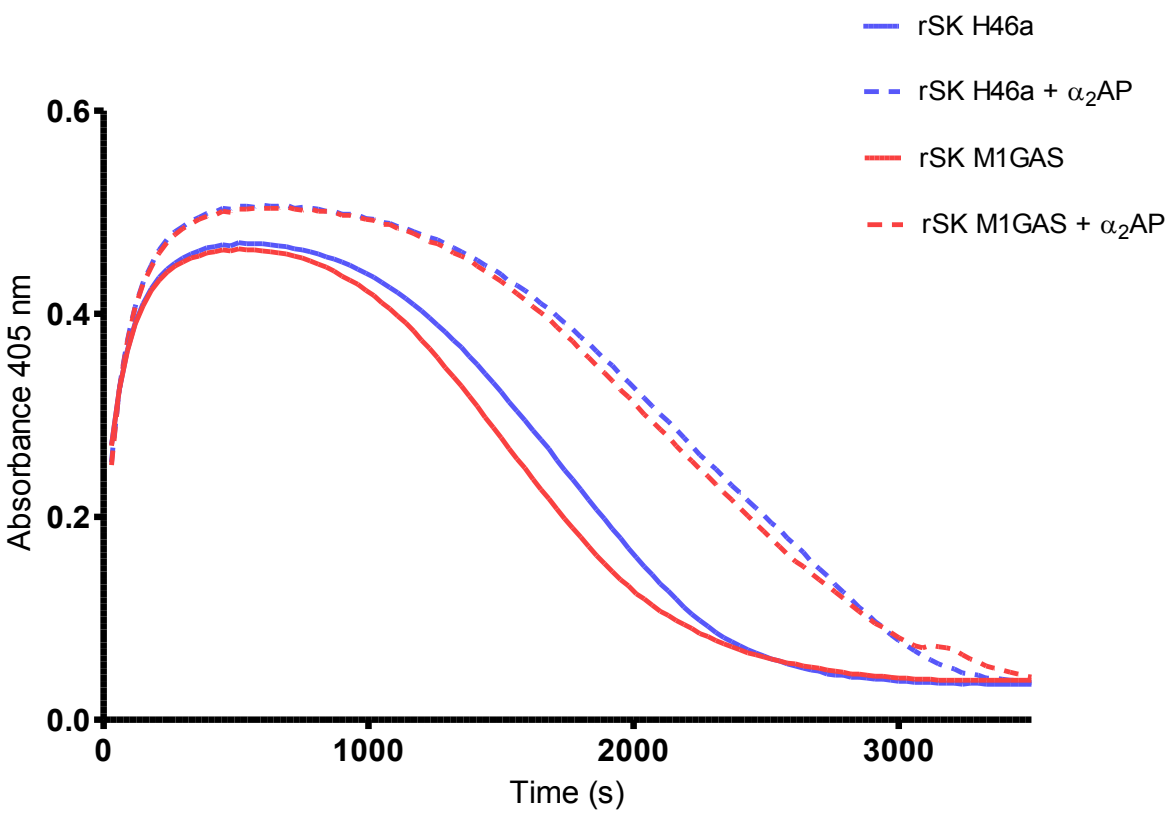

Figure 2.16 The effect of α_2-antiplasmin (α_2-AP) on rSK H46a- and rSK M1GAS- mediated fibrinolysis. Fibrinolysis mediated by rSK H46a and rSK M1GAS was investigated in the presence of α_2-antiplasmin. Lysis profiles for each variant with and without α_2-antiplasmin were determined by measuring absorbance at 405 nm. Typical profiles are shown here.

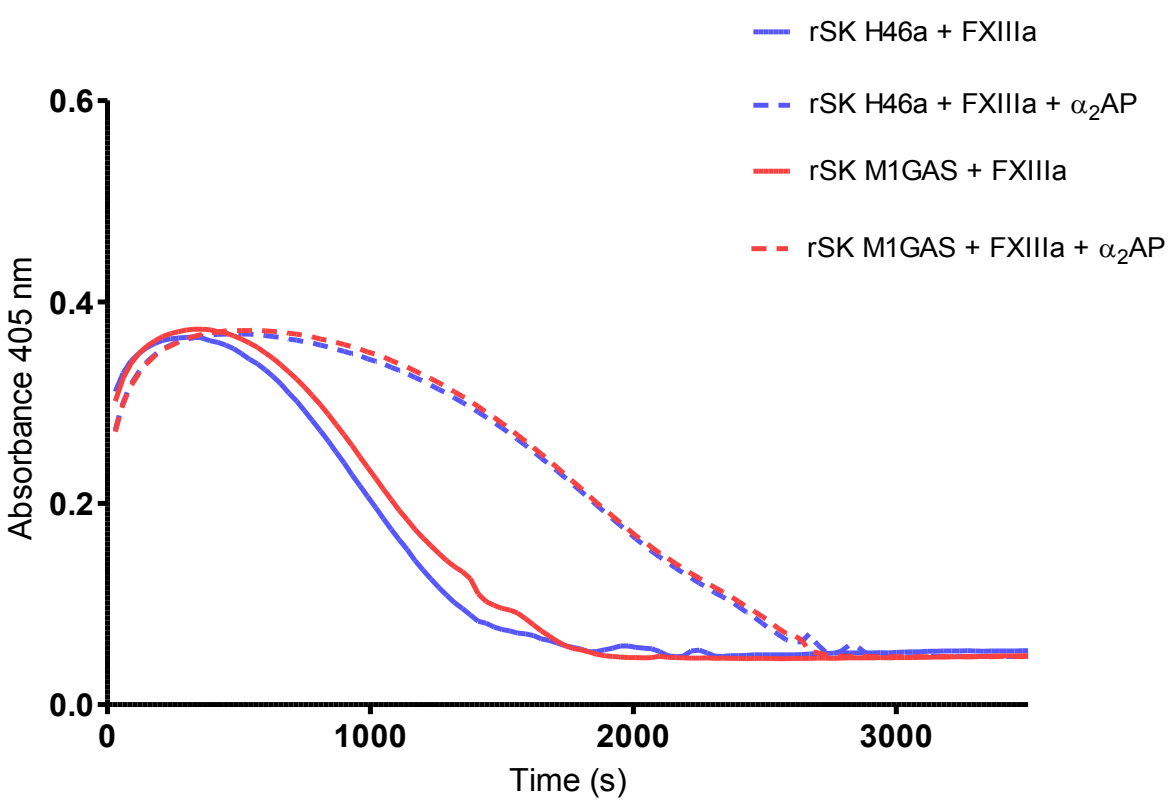

Figure 2.17 The combined effect of FXIIIa and α_2-antiplasmin (α_2-AP) on rSK H46a- and rSK M1GAS– mediated fibrinolysis. Fibrinolysis mediated by rSK H46a and rSK M1GAS was investigated in the presence of activated FXIII and α_2-antiplasmin. Profiles of rSK H46a and rSK M1GAS mediated fibrinolysis of FXIII cross-linked fibrin with and without α_2-antiplasmin were determined by measuring absorbance at 405 nm. Typical profiles are shown here.

2.4 Discussion

This work demonstrates that in contrast to the H46a SK used in the therapeutic SK, M1GAS SK is stimulated by fibrinogen, and to an even greater extent fibrin. Maximal stimulation of rSK M1GAS by fibrinogen in these assays is seen to be at around physiological fibrinogen (3 mg/mL), and is similar for tPA, suggesting that fibrinogen binding is likely to regulate the activity of rSK M1GAS *in vivo*.

The plasmin generated by rSK H46a and rSK M1GAS activity will bind both fibrinogen and the chromogenic substrate, S-2251, so competitive inhibition of S-2251 turnover will be present. With rSK H46a, these means a loss of activity compared to in solution, as demonstrated in Figure 2.5. Whilst this competitive inhibition is still present with rSK M1GAS, the stimulation through binding of fibrinogen more than overcomes the competitive inhibition resulting in a higher activity.

The template effect, demonstrated by the studies with a fibrinogen concentration range (Figures 2.6 and 2.7) suggest that fibrinogen binds the M1GAS SK activator complex (SK-Pg*) in addition to the substrate plasminogen, resulting in a ternary complex as hypothesised by McArthur *et al.* (McArthur et al., 2008). The binding may be *via* manipulation of binding sites on the plasminogen molecule during formation of the activator complex. Alternatively it may be *via* distinct sites on the SK molecule itself, but further studies would need to be conducted in order to accurately determine the mechanisms of binding.

Overall, from the studies with FXIIIa cross-linked fibrin and α_2-antiplasmin (Figures 2.15, 2.16 and 2.17), the different mechanism of M1GAS SK identified in this chapter does not appear to offer any advantage over H46a SK with regard to the mechanism of pathogenesis proposed by Loof *et al.* (Loof et al., 2011, Loof et al., 2012).

A difference between rSK H46a and rSK M1GAS activity is seen across a tranexamic acid range in solution which demonstrates that the complex formation of rSK M1GAS and plasminogen is more reliant on lysine binding sites than the rSK H46a-Pg complex (Figure

2.12). This also suggests that the differences between the SK variant activities in the presence of fibrinogen and fibrin across a tranexamic acid concentration range (Figure 2.13) is at least in part due to the effect of the lysine analogue on rSK M1GAS complex formation with plasminogen; not simply just the binding of the complex and plasminogen to fibrin(ogen). Despite this, the rSK M1GAS-Pg complex also exhibits stronger binding to fibrin than fibrinogen. This is presumably due to differences in binding sites for the rSK M1GAS-Pg complex with fibrinogen and fibrin, again through lysine binding sites. There is no observed difference in activity between rSK H46a plasminogen activation in the presence of fibrinogen and fibrin.

Chapter 3: Investigating the effect of rSK H46a and rSK M1GAS on plasmin

3.1 Introduction

As well as binding plasminogen, SK can also form an activator complex with plasmin (Pm), for which it has a higher affinity (Boxrud et al., 2000, Boxrud and Bock, 2000). Binding to plasmin is known to alter the enzyme specificity towards the activation site of plasminogen; promoting further plasmin generation (Bhattacharya et al., 2012). Some studies have looked at plasmin kinetics in complex with rSK H46a as well as the role of the N-terminus (Bean et al., 2005, Verhamme and Bock, 2008), but as with plasminogen less is known about the differences between SK variants. Investigating the kinetics of plasmin in complex with rSK H46a and rSK M1GAS will aid understanding of the more complicated mechanism of plasminogen activation. Any differences in mechanism between rSK H46a and rSK M1GAS with plasmin may point to different mechanisms in the pathways of plasminogen activation.

The crystal structure of human plasminogen has been determined (Law et al., 2012, Xue et al., 2012), as has the crystal structure of the catalytic domain of plasmin in complex with SK from group C H46a S. *equisimilis* (Wang et al., 1998), but no such equivalent for SK from group A M1 streptococci, such as S. *pyogenes,* is available. Though details of the molecular structure of the plasmin in complex with rSK M1GAS are lacking, it may be possible to model the structure by comparing sequences of rSK H46a and rSK M1GAS.

Microplasmin (μPm) is the active site and linker sequence of plasmin only, lacking the kringle domains where many of the fibrinogen binding sites and SK interaction occurs (Takada and Takada, 1989a). This plasmin derivative is most like the catalytic domain used to determine the crystal structure of the complex with H46a S. *equisimilis* (Wang et al., 1998). Kinetic studies using microplasmin may be more readily interpreted with reference to the crystal structure without potential interference of other domains in plasmin that are absent in microplasmin. In this chapter, the effect of H46a and M1GAS SK binding on plasmin and microplasmin activity was investigated. Initially solution based Michaelis-Menten kinetics were

employed to understand how the active site is manipulated by SK binding. The addition of fibrinogen and fibrin to the assays with plasmin provides information on the interaction of SK with the kringle domains and how this affects fibrin(ogen) binding and the kinetics of plasmin generation.

3.2 Experimental Procedures

3.2.1 Materials and software

3.2.1a Materials

Buffer A - 0.5 M Tris pH 8.4 at 37 °C. Stored at 2-8 °C for 6 up to months.

Buffer B – 10 mM Tris HCL 100 mM NaCl 0.01% Tween 20. Store at 2-8 °C for up to 1 week.

Buffer C – Buffer B + 1mg/ml HSA. Store at 2-8 °C for up to 3 days.

Blocking buffer – 0.05M Tris 0.1% Tween 20 pH 8.4 at 37 °C.

All laboratory chemicals used to make buffers were from Sigma Aldrich, St Louis, Missouri, USA.

Fibrinogen (Calbiochem, Merck Millipore, Billerica, Massachusetts, USA) - reconstituted in Buffer B to give stock solution of 50 mg/ml, and flash frozen in liquid nitrogen in small aliquots and stored at -40 °C. All dilutions for reactions were made using buffer B.

WHO 3rd IS Plasmin (97/536) – reconstituted in 1 ml H_2O, flash frozen in liquid nitrogen in small aliquots and stored at -40 °C. All dilutions for reactions were made in buffer C.

Microplasmin (μPm) (Thrombogenics, Leuven, Belgium) – flash frozen in small aliquots in liquid nitrogen and stored at -40 °C. All dilutions for reactions were made using buffer C.

WHO IS Thrombin (01/578) – flash frozen in small aliquots in liquid nitrogen and stored at -40 °C. All dilutions for reactions were made using buffer C.

rSK H46a, rSK M1GAS, rSK H46a (del1-59), rSK M1GAS (del 1-59) (see chapter 2) were flash frozen in liquid nitrogen and stored in small aliquots at -40 °C. All dilutions for reactions were made using buffer C.

S-2251, H-D-Val-L-Leu-L-Lys-pNA (Chromogenix, Milan, Italy) – reconstituted in 15 ml H_2O, to give a 3 mM stock solution. Stored at 2-8 °C, stable for several months.

Microtitre plates (Greiner, Kremsmunster, Austria) – all microtitre plates were blocked with 200 µL blocking buffer for 2 hours at 37 °C and washed 2x with 200 dH_20 before use.

3.2.1b Software

GraphPad Prism (GraphPad Software, San Diego, California, USA)

SoftMax Pro v5.0 (Molecular Diagnostics, Sunnydale, California, USA)

Microsoft Excel (Redwood, Washington, USA)

R Core Team (2012). R: A language and environment for statistical computing. R Foundation for Statistical Computing, Vienna, Austria. ISBN 3-900051-07-0, URL: http://www.R-project.org/.

Combistats (EDQM, Strasbourg, France)

3.2.2 Plasmin and microplasmin activity against S-2251

3.2.2a Amidolytic activity of plasmin and microplasmin in solution

Amidolytic activity of plasmin alone and plasmin in complex with rSK H46a, rSK M1GAS, rSK H46a del 1-59 and rSK M1GAS del 1-59 was determined in solution against the chromogenic substrate for plasmin, S-2251. K_M and k_{cat} values were then calculated for each complex. Amidolytic activity of microplasmin and the kinetic parameters k_{cat} and K_M were also determined against S-2251 alone and in complex with rSK H46a and rSK M1GAS.

In all instances, 1.35 nM final concentration plasmin or microplasmin, diluted using buffer C, with and without a two-fold molar excess of SK was used. A two-fold molar excess was determined as sufficient to complex all plasmin with SK by preliminary experiments where an increase in amidolytic rate was seen between a 1:1 and 1:2 Pm:SK ratio, but no further increase demonstrated for 1:3. The Plasmin SK solutions were added to a range of eight S-2251 concentrations (0.02 - 2.25 mM in final reaction mixtures), diluted in dH_2O. All reactions

were 120 µl total volume and carried out in 96 well microtitre plates. All microtitre plates were incubated at 37 °C using a heated block. pNA generation was monitored by measuring absorbance change at 405 nm at 30 s intervals for 60 min at 37 °C.

Reactions were measured for 60 min with changes in absorbance at 405 nm corresponding to substrate hydrolysis and pNA generation. Plots of rates of absorbance versus time (mOD min^{-1}) were created by plate reader software, SoftMax Pro v5.0, where substrate was < 10% depleted and therefore initial rates were at a maximum. The data were exported to Excel and initial rates of pNA generation (M s^{-1}) were calculated using the extinction coefficient (ε) of a 1 M solution under these conditions of 2500 OD M^{-1}. The extinction coefficient was determined under these experimental conditions following complete hydrolysis of a range of S-2251 concentrations with excess enzyme.

Initial rates (Ms^{-1}) were plotted against substrate (S-2251) concentration and fitted to the Michaelis-Menten equation in order to determine values for the kinetic parameters V_{max} and K_M (equation 4) using GraphPad Prism 5. Three independent experiments with two replicates for each variant per plate were carried out.

$$v = \frac{V_{max}[S]}{K_M + [S]} \quad (4)$$

In this equation, v stands for velocity as a molar concentration of pNA generated per second and V_{max} is the maximal velocity of the reaction. K_M is the substrate concentration at which half the maximal velocity (V_{max}) is achieved. [S] is the molar substrate concentration.

$$k_{cat} = \frac{V_{max}}{E_0} \quad (5)$$

k_{cat} values were calculated as demonstrated in equation 5 with the total plasmin concentration representing the active enzyme E_0, in this instance 1.35 nM calculated from the amount of active enzyme for the 3rd WHO IS for plasmin as determined by active-site titration (Longstaff and Gaffney, 1991). Activity of plasmin SK and microplasmin SK complexes was compared

using $k_{cat}/K_{M,}$ the specificity constant. The microplasmin concentration was taken as advised on the manufacturer's insert.

3.2.2b Amidolytic activity of plasmin and microplasmin with fibrinogen

The assay outlined above for determining the plasmin and microplasmin activity in solution alone and in complex with rSK H46a and rSK M1GAS was modified to study the complexes in the presence of fibrinogen (3 mg/mL).

3.2.3 Fibrinolysis

The following assays were used to measure fibrinolysis by plasmin in complex with rSK H46a and rSK M1GAS.

3.2.3a Fibrinolysis assay with plasmin

In order to measure fibrinolysis by plasmin in complex with rSK H46a and rSK M1GAS, fibrin clots were made in microtitre plate wells by adding a solution of fibrinogen (final concentration in reaction 2.8 mg/ml) (60 µl) to a 40 µl solution of thrombin (final concentration in reaction 20 nM) and Pm-SK complex, or plasmin alone. Each assay contained 4 doses (3-25 nM) and 4 replicates for each plasmin variant. As before, a two-fold molar excess of SK was used. All concentrations are for final reaction.

Absorbance at 405 nm was measured for 5 hours to monitor changes in fibrin clot turbidity with increases in absorbance corresponding to clotting and subsequent decreases corresponding to lysis.

The raw, kinetic data were exported from Softmax Pro plate reader software as a text file. An R program script (Silva et al., 2012), written by Colin Longstaff (Personal communication, see appendix 1) was used to determine the time at maximum absorbance (complete clotting) and time at lowest absorbance (complete lysis), to allow calculation of the time to 50% lysis (Figure 2.2). The script is capable of determining several parameters from the raw kinetic data such

as max absorbance, time to max absorbance, time to complete lysis, time to any chosen % lysis. Time to 50% lysis from start of reaction is a standard measure of fibrinolysis and as such was chosen in this instance as a parameter by which to compare the variants. Values for time to 50% lysis were then fitted to a parallel line bioassay using Combistats as outlined in section 2.2.4e.

3.2.3b Physical fibrinolysis assay

Fibrinolytic activity of plasmin, with and without a two-fold molar excess of SK was determined using an assay based on the European Pharmacopoeia method for determining lysis times of tPA (Alteplase) (Sands et al., 2004, Sands et al., 2002). Briefly, fibrin clots were made in glass tubes by adding a solution of 0.5 mL fibrinogen (final concentration in reaction 1.24 mg/mL) to 0.1 mL thrombin (final concentration in reaction 20 nM) solution containing plasmin (6.3 nM or 25 nM). After 30 s, clots were visible at which point a glass bead was added to each tube. Lysis was defined as the time taken for the bead to pass through the clot to reach the bottom of the tube. Timing started from when the fibrinogen solution and thrombin/plasmin solution were mixed and was timed using a stopwatch. Assays contained 2 replicates and a range of concentrations for plasmin alone and in complex with rSK H46a and rSK M1GAS.

Relative lysis times for plasmin in complex to rSK H46a and rSK M1GAS compared to plasmin alone were plotted in GraphPad Prism. To determine whether lysis times were significantly different ($P < 0.05$) to plasmin alone, a student t test was performed in GraphPad Prism.

3.2.4 Data Collection and analysis for microtitre plate assays

All microtitre plate reactions were measured using a SpectraMax M5 plate reader and SoftMax Pro v5.0. All reactions were measured at 37 °C in 30 s intervals at 405 nm.

3.3 Results

3.3.1 Amidolytic activity of plasmin in complex with rSK H46a and rSK M1GAS

K_M, k_{cat} and k_{cat}/K_M were determined for plasmin and plasmin in complex with rSK H46a, rSK M1GAS to explore the mechanism of stimulation of plasmin activity. K_M, k_{cat} and k_{cat}/K_M were also determined for plasmin in complex with 1-59 deletion mutants of rSK H46a and rSK M1GAS to investigate whether N-terminal interactions of SK, known to be critical for plasminogen activation, are involved.

Fitting to the Michaelis-Menten equation is shown in Figure 3.1. The values determined for K_M, k_{cat} and k_{cat}/K_M from this are presented in Table 3.1. Figure 3.3 shows k_{cat}/K_M for plasmin in complex with all the variants.

Both plasmin rSK H46a and plasmin rSK M1GAS complexes increased plasmin enzyme specificity constant (k_{cat}/K_M) against S-2251, ≈ 2-fold compared with k_{cat}/K_M plasmin enzyme activity alone (Figure 3.3). No increase in activity was seen for plasmin rSK H46a del 1-59 complex and plasmin rSK M1GAS del 1-59 complex, both being comparable to plasmin. This indicates that the increase in activity is due to interaction between plasmin and the N-terminus of both rSK H46a and rSK M1GAS. Without the first 59 amino acids, the interaction between plasmin and SK is potentially lost, or ineffective.

Though the rSK H46a and rSK M1GAS both show ≈ 2- fold increase in k_{cat}/K_M, their respective k_{cat} and K_M were significantly different, as seen in Table 3.1. The k_{cat} value for plasmin rSK H46a complex was 2-fold higher than observed for all other plasmin rSK complexes and plasmin alone; whereas the K_M for the plasmin rSK M1GAS complex was 0.20 mM compared to ≈0.40 mM for all other complexes.

In summary, full-length H46a and M1GAS SK stimulate plasmin as shown by k_{cat}/K_M. In both instances, the N-terminal amino acids (1-59) are required. However, although H46a and M1GAS SK both stimulate plasmin activity to a similar extent closer examination of the K_M and

k_{cat} values show the mechanism to be different. H46a SK alters plasmin activity by increasing k_{cat}, whereas M1GAS SK relies on improvements in K_M for the substrate S-2251.

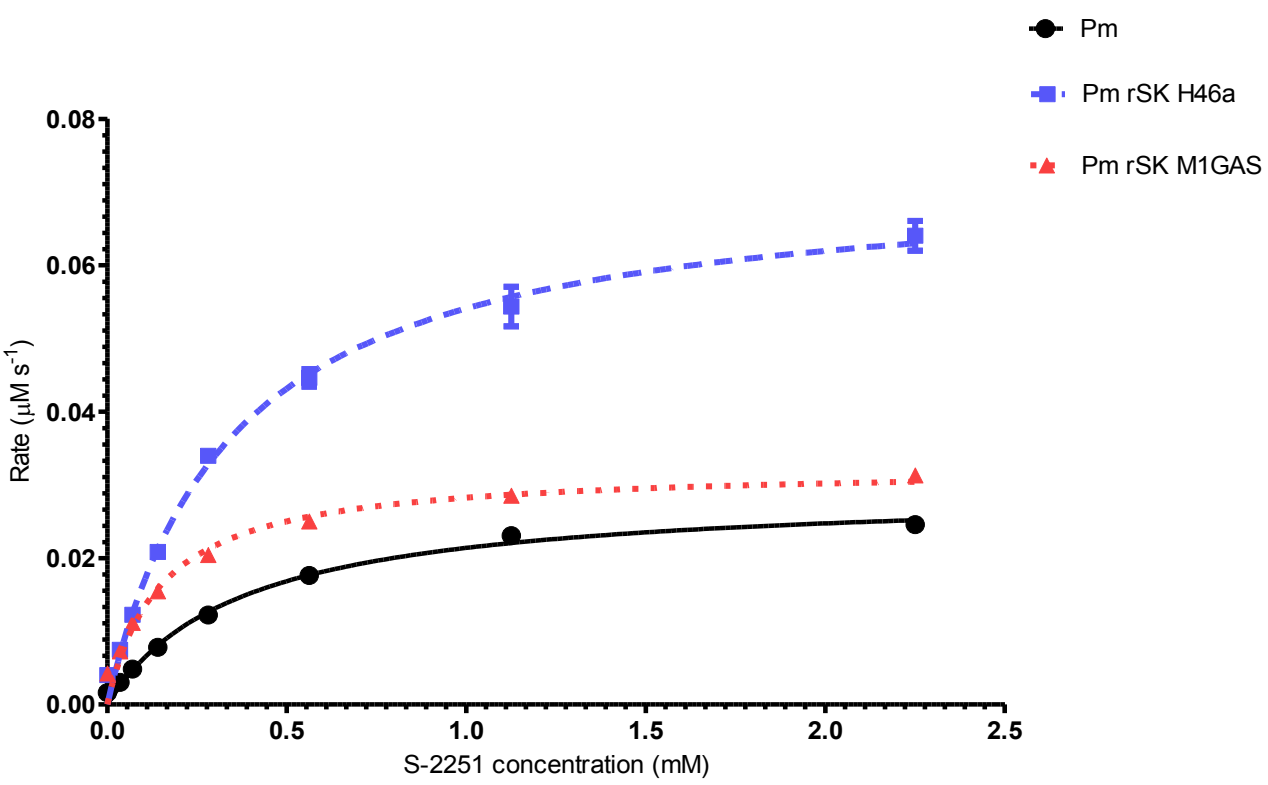

Figure 3.1 Representative fitting of amidolytic activity of plasmin in complex with rSK H46a and rSK M1GAS to Michaelis-Menten equation. Rates of amidolytic activity across a chromogenic substrate range were fitted to the Michaelis-Menten equation to determine values for the kinetic parameters V_{max} and K_M for plasmin alone and in complex with rSK H46a and rSK M1GAS and the N-terminal deletion mutants (not shown). Values shown are taken from one independent assay to represent typical profile.

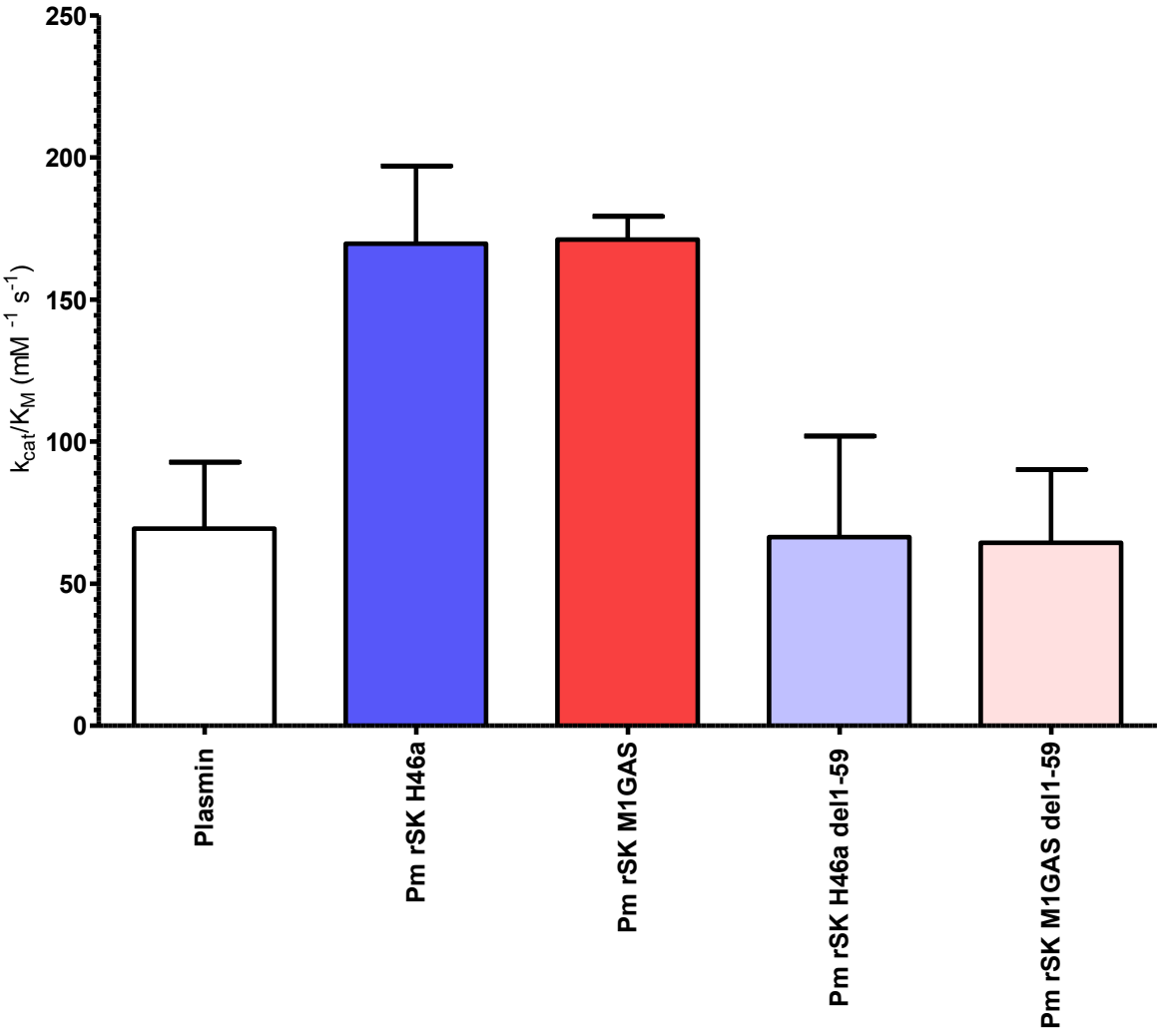

Figure 3.2 The effect of rSK H6a, rSK M1GAS and N-terminal deletion mutants on plasmin activity. Enzyme specificity constant (k_{cat}/K_M) was calculated to compare the activity of plasmin alone and in complex with rSK H46a, rSK M1GAS and the 1-59 deletion mutants of each. Error bars show standard deviation of 4 independent experiments.

Table 3.1 Effect of SK on plasmin activity. Kinetic parameters V_{max}, k_{cat}, K_M and k_{cat}/K_M (as calculated in GraphPad Prism) were determined for plasmin alone against S-2251, and in complex with the rSK H46a, rSK M1GAS and N-terminal truncated variants (del1-59). ± denotes SEM based on 4 independent assays. *represents significantly different values ($P < 0.05$) based on student t test against activity of plasmin alone.

	V_{max} (μM s^{-1})	k_{cat} (s^{-1})	K_M (mM)	k_{cat} / K_M (mM^{-1} s^{-1})
Plasmin (Pm)	0.03 ± 0.003	25.5 ± 1.9	0.39 ± 0.01	65.2 ± 5.5
Pm rSK H46a	0.08 ± 0.005*	60.4 ± 3.8*	0.36 ± 0.01	169.6 ± 6.4*
Pm rSK M1GAS	0.04 ± 0.003	27.8 ± 2.4	0.21 ± 0.06*	146.9 ± 22.4*
Pm rSK H46a del 1-59	0.03 ± 0.003	25.0 ± 2.0	0.38 ± 0.02	66.4 ± 5.2
Pm rSK M1GAS del 1-59	0.03 ± 0.002	25.6 ± 1.6	0.40 ± 0.02	64.4 ± 5.8

3.3.2 Effect of rSK H46a and rSK MIGAS on plasmin activity in presence of fibrinogen

Plasmin activity in complex with rSK H46a and rSK M1GAS was investigated in the presence of fibrinogen to determine the effect of fibrinogen binding on plasmin amidolytic activity in complex with the two SK variants. All assays were carried out at physiological fibrinogen concentrations (3 mg/ml). Analysis of data is complicated by the action of fibrinogen as a competitive inhibitor of plasmin action on S-2251 and further effects of fibrinogen on complexes of rSK H46a or rSK M1GAS with plasmin need to be isolated. The mechanisms underpinning fibrinogen interactions with plasmin and rSK complexes were not explored in detail (K_I values or type of inhibition were not determined). The effects of fibrinogen are summarised by the k_{cat}, K_M and k_{cat}/K_M values for hydrolysis of S-2251 and these are presented in Figure 3.4, which can be compared with Table 3.1 showing kinetic parameters without fibrinogen. As expected, as a competitive inhibitor, fibrinogen blocks the plasmin active site and increases K_M for S-2251 (from 0.37 to 1.6 mM), but there is also a small decrease in k_{cat} to 14.5 from 25.5 s^{-1}. Overall the effect of fibrinogen is to reduce k_{cat}/K_M to 17.9 $M^{-1}s^{-1}$, 13% of the value without fibrinogen. Interestingly, fibrinogen has a much weaker effect on plasmin in complex with rSK H46a and rSK M1GAS, as judged by k_{cat} and K_M values. Figure 3.4 clearly shows stimulation of the k_{cat} of the plasmin rSK M1GAS complex, which increases from 26.7 to 64.7 s^{-1} and is thus achieves equivalent activity to plasmin rSK H46a, which itself is unaffected by fibrinogen.

A)

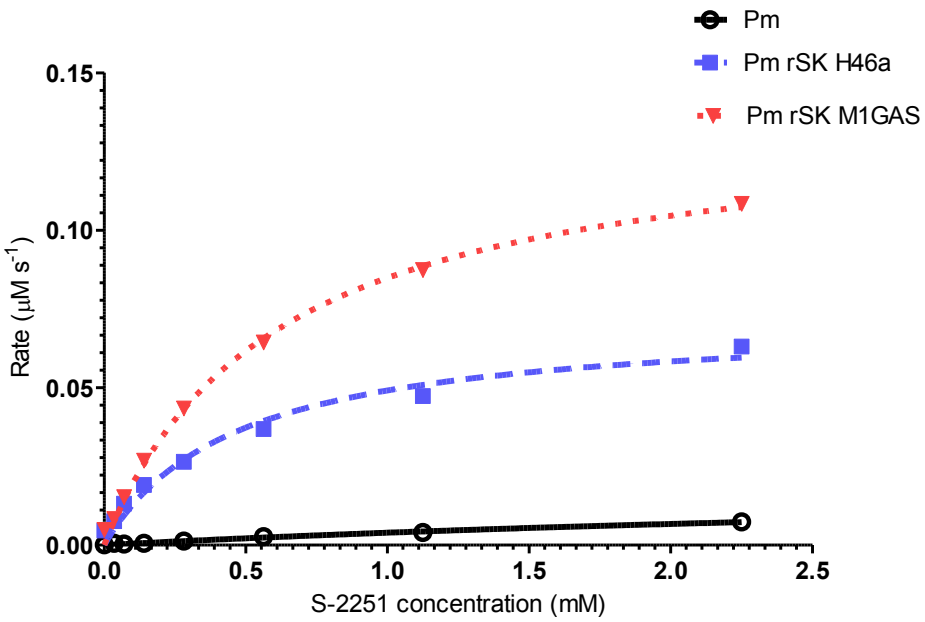

B)

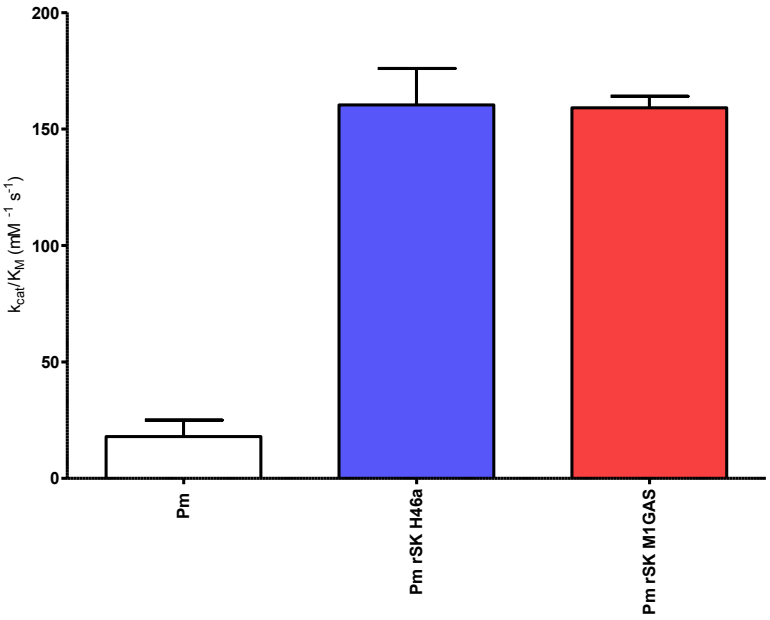

Figure 3.3 The effect of rSK H46a and rSK M1GAS on plasmin activity in the presence of fibrinogen. A) Rates were fitted to the Michaelis-Menten equation to determine values for the kinetic parameters V_{max} and K_M for plasmin alone and in complex with rSK H46a and rSK M1GAS. Error bars show standard deviation of 3 replicates. B) Enzyme specificity constant (k_{cat}/K_M) was calculated to compare the activity of plasmin alone and in complex with rSK H46a, rSK M1GAS. Error bars show standard deviation of 3 independent assays.

Table 3.2 Kinetic parameters V_{max}, k_{cat}, K_M and k_{cat}/K_M were determined for plasmin alone against S-2251, and in complex with the rSK H46a, rSK M1GAS in the presence of fibrinogen. ± denotes SEM of 3 independent assays. * represents significantly different values ($P < 0.05$) based on student t test against activity of plasmin alone.

	V_{max} (μM s^{-1})	k_{cat} (s^{-1})	K_M (mM)	k_{cat} / K_M (mM^{-1} s^{-1})
Plasmin (Pm) + fibrinogen	0.01 ± 0.009	14.5 ± 4.2	1.6 ± 1.03	17.9 ± 7.1
Pm rSK H46a + fibrinogen	0.09 ± 0.003*	70.3 ± 5.7*	0.4 ± 0.01*	160.4 ± 15.7*
Pm rSK M1GAS + fibrinogen	0.09 ± 0.004*	64.7 ± 12.6*	0.4 ± 0.07*	159.1 ± 5.0*

3.3.3 Effect of rSK H46a and rSK M1GAS on fibrinolysis with plasmin

The relative effect of plasmin alone and in complex with rSK H46a and rSK M1GAS on fibrin clot lysis was investigated. For plasmin alone it was difficult to obtain reproducible clot lysis curves and no linear dose response was seen as demonstrated in Figure 3.5. It was therefore not possible to assign specific activity to the two rSK variants in complex with plasmin relative to plasmin alone against a fibrin substrate.

When plasmin was in complex with rSK H46a and rSK M1GAS the reproducibility and linearity of the clot lysis curves improved (Figure 3.5), and it was possible to generate a dose response curve for each (Figure 3.6). Interestingly, the two complexes were found to be non-parallel. At low plasmin concentrations (3.1 nM) there was no observed difference between the activities of the plasmin rSK H46a complex compared to the plasmin rSK M1GAS complex (Figure 3.7). At higher concentrations (25 nM) however the plasmin rSK H46a complex was more effective producing faster clot lysis rates, up to nearly 3-fold faster than the plasmin rSK M1GAS complex (Figure 3.7).

All of the assay systems used thus far to investigate SK activation of plasminogen and effect on plasmin activity have utilised optical density as a read-out when determining activity. However, determining plasmin activity in fibrinolysis using absorbance is only one approach and may be complicated by absorbance changes caused be fibrin rearrangements, which can also increase during early stages of fibrin degradation (Meh et al., 2001). To investigate the activity of plasmin SK complexes further, the fibrinolysis properties were measured using a physical fibrinolysis assay based on the current European Pharmacopoeial method for assigning potencies to therapeutic tPA (e.g. see (Sands et al., 2002, Sands et al., 2004). In this instance, clots are formed by the addition of thrombin to fibrinogen in the presence of plasmin and the SK variant. Fibrinolysis proceeds and time to complete lysis was recorded as the time the clot structure could no longer support the bead and therefore reaches the bottom of the tube. In this system, the activity of plasmin alone was seen to be more reproducible and at low concentrations (7 nM) the plasmin SK complexes were more effective producing faster

clot lysis rates compared to plasmin alone. At higher concentrations (28 nM) there was no significant difference in lysis times between the two SK variants (Figure 3.7).

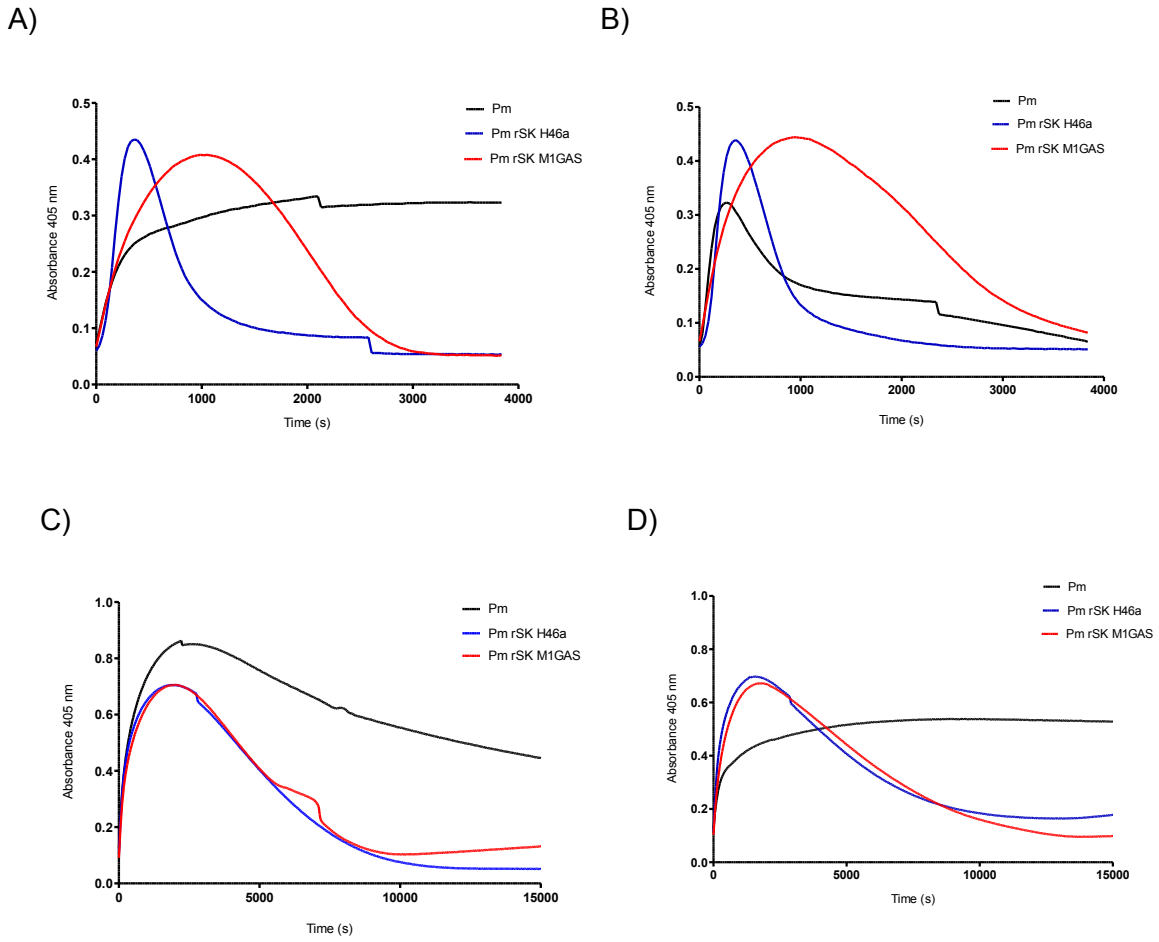

Figure 3.4 Representative clotting and lysis curves showing effect of rSK H46a and rSK M1GAS on plasmin activity in fibrinolysis assay. Fibrinolysis was investigated by measuring absorbance at 405 nm in the presence of plasmin alone, and plasmin in complex with rSK H46a and rSK M1GAS. Typical lysis profiles of plasmin alone and in complex with rSK H46a and rSK M1GAS from replicates on a single 96-well plate at 25 nM (Figures A and B) or 3 nM (Figures C and D) plasmin. Whilst rSK H46a and rSK M1GAS showed good reproducibility at both concentrations of plasmin, fibrinolysis by plasmin alone was inconsistent between replicate wells.

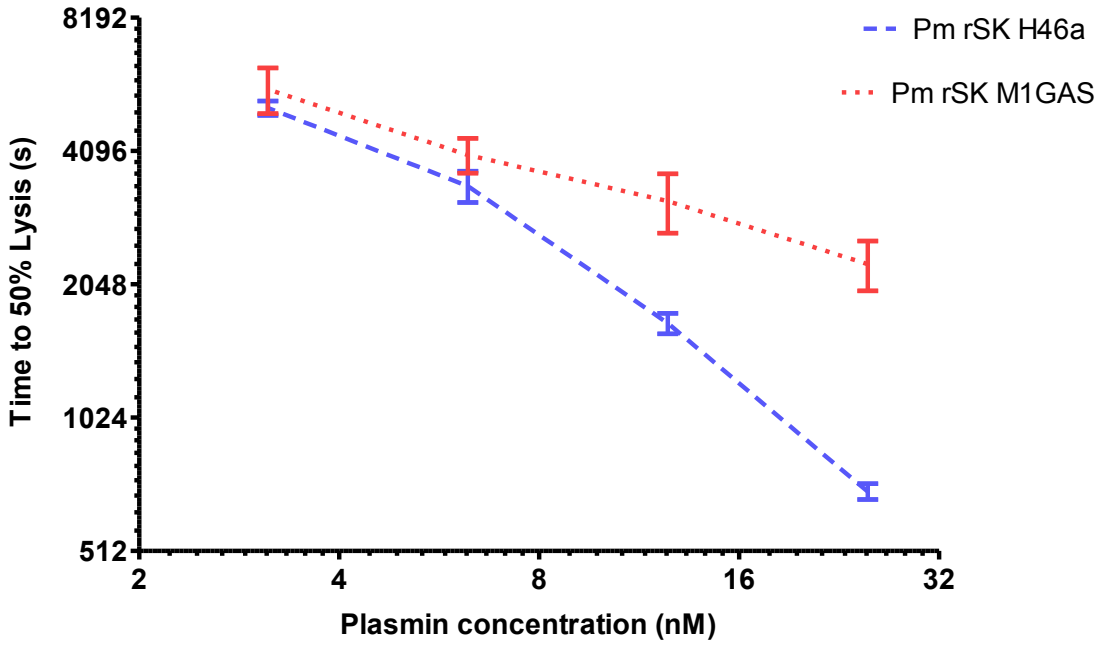

Figure 3.5 The effect of rSK H46a and rSK M1GAS on plasmin activity in fibrinolysis assay as determined by absorbance at 405 nM. Time to 50% lysis was determined over a range of plasmin concentrations (3-25 nM) to determine the effect of rSK H46a and rSK M1GAS on plasmin activity and fibrinolysis. Fibrinolysis facilitated by plasmin alone was not reproducible or linear in response, so is not included here. Error bars denote SEM of 4 replicates.

A)

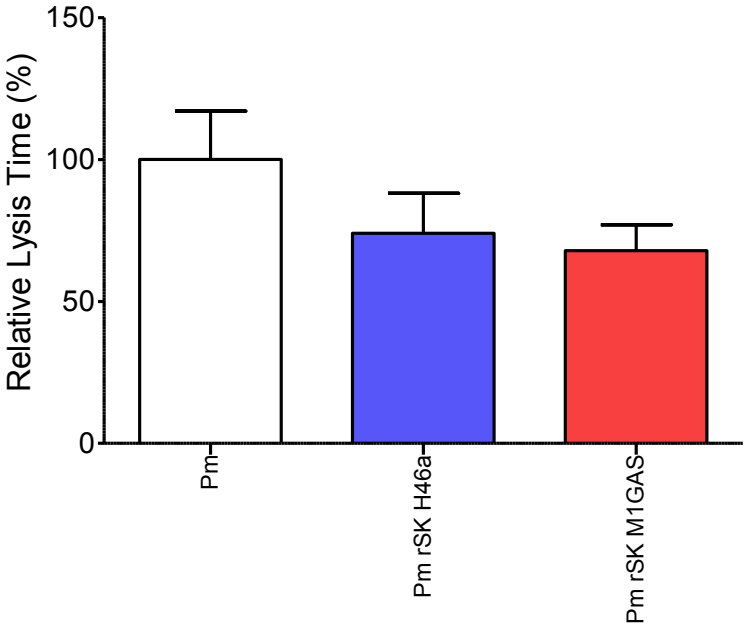

B)

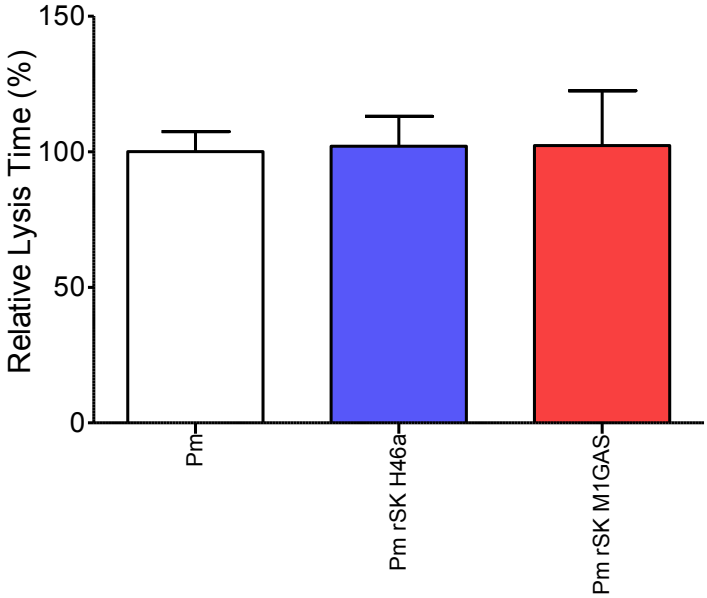

Figure 3.6 The effect of rSK H46a and rSK M1GAS on plasmin activity in a physical fibrinolysis assay. Time to lysis was measured at two plasmin concentrations (7 and 28 nM, panels A and B, respectively) to determine the effect rSK H46a and rSK M1GAS have on plasmin activity and fibrinolysis. Lysis times relative to plasmin alone were calculated to allow comparison between variants. Error bars show standard deviation of 4 independent experiments.

3.3.4 Microplasmin activity in complex with rSK H46a and rSK M1GAS

Microplasmin consists of the catalytic domain and the linker region of plasmin only. As such it lacks the binding sites present in the kringle domains that associate with SK and/or fibrin(ogen). Studying the interaction of microplasmin with SK variants and comparing their activities in complex with plasmin is useful when studying the mechanism of SK bound plasmin as a way to understand the contribution of plasmin kringles and their interactions with SK and fibrin(ogen) to the relative differences in activity between rSK H46a and rSK M1GAS.

Kinetic parameters were first determined for microplasmin activity in solution, alone and in complex with rSK H46a and rSK M1GAS. As demonstrated in Figure 3.8 and Table 3.2, there is no significant difference between the activity of microplasmin alone and in complex with rSK H46a and rSK M1GAS. From these data alone it is unclear whether there is effective plasmin complex formation with rSK H46a and rSK M1GAS, although the existence of a published crystal structure (Wang et al., 1998), suggests this is likely. However, the addition of fibrinogen alters the K_M of plasmin more dramatically than that of the complexes as a result of the competition between the chromogenic substrate and fibrinogen for the plasmin active site. This demonstrates that the effect of fibrinogen on (micro)plasmin is independent of kringle binding. It also shows that both SK variants interact with the catalytic domain and ameliorate (micro)plasmin inhibition by fibrinogen. Interestingly, rates for microplasmin are faster than full-length plasmin in all cases.

The activity of microplasmin (k_{cat} / K_M) shows little attenuation in complex with rSK H46a (258.0 mM^{-1} s^{-1}in solution vs. 208.1 mM^{-1} s^{-1}). Greater inhibition is seen with rSK M1GAS (326.6 mM^{-1} s^{-1} vs. 181.1 mM^{-1} s^{-1}) bringing it closer to the activity seen with the plasmin rSK M1GAS complex. This suggests the differences in microplasmin binding of rSK H46a and rSK M1GAS is facilitated by different sites in the catalytic domain of plasmin, with rSK M1GAS to a greater extent.

Overall, microplasmin is less affected by fibrinogen than full-length plasmin. This is expected as the lack of kringles domains removes the majority of fibrinogen binding sites.

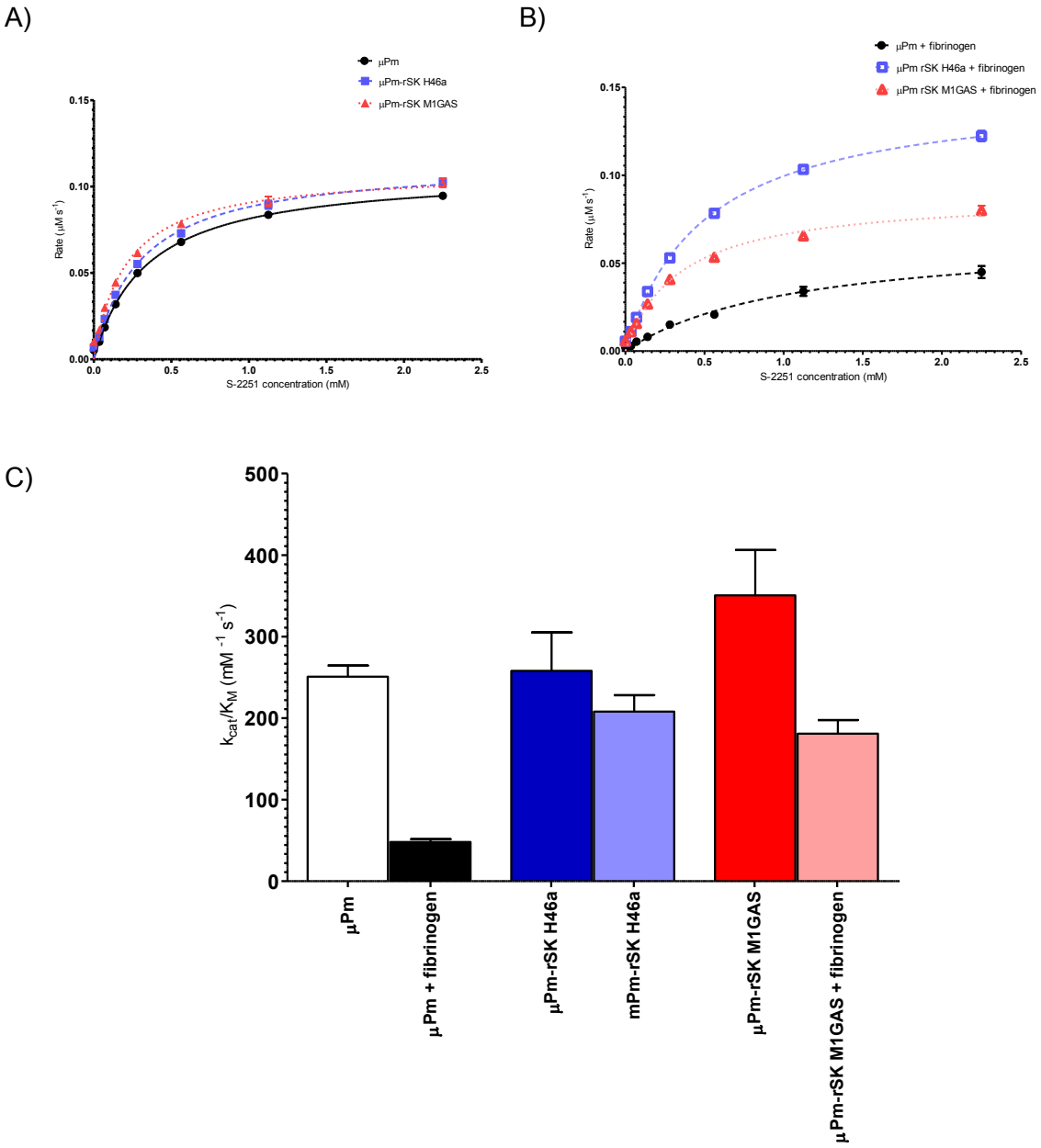

Figure 3.7 The effect of rSK H46a and rSK M1GAS on microplasmin activity. Rates were fitted to the Michaelis-Menten equation to determine values for the kinetic parameters V_{max} and K_M for microplasmin alone and in complex with rSK H46a and rSK M1GAS in solution (A) and in the presence of fibrinogen (B). Error bars show standard deviation of 3 replicates. C) Enzyme specificity constant (k_{cat}/K_M) was calculated to compare the activity of microplasmin alone and in complex with rSK H46a and rSK M1GAS in solution and the presence of 3 mg/mL fibrinogen. Error bars show standard deviation of 3 independent experiments.

Table 3.3 Effect of rSK H46a and rSK M1GAS on microplasmin activity. Kinetic parameters V_{max}, k_{cat}, K_M and k_{cat}/K_M were determined for microplasmin alone against S-2251, and in complex with the rSK H46a, rSK M1GAS. ± denotes SEM of 3 independent experiments. * represents significantly different values ($P < 0.05$) based on student t test against activity of microplasmin alone.

	V_{max} (μM s^{-1})	k_{cat} (s^{-1})	K_M (mM)	k_{cat} / K_M (mM^{-1} s^{-1})
Microplasmin (μPm)	0.10 ± 0.006	76.8 ± 4.3	0.3 ± 0.02	250.9 ± 7.9
μPm + fibrinogen	0.07 ± 0.005	52.5 ± 3.7	1.1 ± 0.02	48.2 ± 2.4
μPm rSK H46a	0.11 ± 0.010	79.5 ± 7.5	0.3 ± 0.01	258.0 ± 27.2
μPm rSK H46a + fibrinogen	0.15 ± 0.006*	114.5 ± 4.2*	0.6 ± 0.06*	208.1 ± 14.1*
μPm rSK M1GAS	0.10 ± 0.006	77.1 ± 4.8	0.3 ± 0.03	326.6 ± 32.1
μPm rSK M1GAS + fibrinogen	0.09 ± 0.001	65.5 ± 0.4	0.4 ± 0.02*	181.1 ± 11.8*

*The table below contains selected data from Tables 3.1 and 3.2, represented again here to allow ease of comparison between microplasmin and plasmin.

	V_{max} (μM s^{-1})	k_{cat} (s^{-1})	K_M (mM)	k_{cat} / K_M (mM^{-1} s^{-1})
Plasmin (Pm)	0.03 ± 0.003	25.5 ± 1.9	0.39 ± 0.01	65.2 ± 5.5
Pm + fibrinogen	0.01 ± 0.009	14.5 ± 4.2	1.60 ± 1.03	17.9 ± 7.1
Pm rSK H46a	0.08 ± 0.005*	60.4 ± 3.8*	0.36 ± 0.0y1	169.6 ± 6.4*
Pm rSK H46a + fibrinogen	0.09 ± 0.003*	70.3 ± 5.7*	0.40 ± 0.01*	160.4 ± 15.7*
Pm rSK M1GAS	0.04 ± 0.003	27.8 ± 2.4	0.21 ± 0.06*	146.9 ± 22.4*
Pm rSK M1GAS + fibrinogen	0.09 ± 0.004*	64.7 ± 12.6*	0.40 ± 0.07*	159.1 ± 5.0*

3.4 Discussion

Although in solution the kinetics of plasmin with an amidolytic substrate seem to follow simple kinetics, in the presence of fibrinogen or fibrin the system is much harder to study. As a first approximation, adding fibrinogen to plasmin and S-2251 would result in competitive inhibition and an increased K_M, which is observed in the case of plasmin and microplasmin. However, inhibition is more complicated and there may also be changes in k_{cat}, indicating a mixed type of inhibition (see Tables 3.1, 3.2 and 3.3). Further complexities are added when plasmin or microplasmin are in complex with SK, but there is a tendency for SK to shield the active site from competition with fibrinogen, and this is the case for both rSK H46a and rSK M1GAS. In this way there may be an evolutionary advantage to shifting the specificity of plasmin away from fibrinogen and towards other substrates, including plasminogen, or in this case, S-2251. An unexpected feature of the results presented above is the increased activity of microplasmin compared with plasmin, but this may indicate the purpose of the kringle domain in plasmin are to limit unwanted proteolysis and focus activity towards fibrin or other substrates that bind plasmin through lysine binding sites.

Another observation was the difficulty obtaining results when studying plasmin on its native substrate fibrin. Results were non-linear over dose ranges on plasmin and rather irreproducible. However, recent published work may explain these findings. It is presumed that initial binding of plasmin to fibrin and proteolytic cleavage generates C-terminal lysines which attract further plasmin molecule, binding *via* kringle domains, to produce a clustering effect, which has been expressed at a macroscale level as fractal kinetic behaviour leading to increasing apparent K_M during fibrinolysis (Varju et al., 2015). At higher plasmin concentrations, clustering may be less pronounced as plasmin spread along fibrin strands. Thus non-linear dose response ranges of plasmin on a fibrin substrate may be expected. Interestingly, this behaviour is largely supressed when plasmin is in complex with SK, suggesting SK significantly affects the interactions of plasmin kringles with C-terminal lysines during fibrinolysis. Further support for these ideas may come from the recently developed

WHO 4th IS Plasmin was prepared (Thelwell et al, 2015, in press). It was noted that none of the four standards for plasmin have used fibrin as a substrate, presumably because fibrin is a difficult substrate to study when measuring plasmin activity.

Chapter 4: Modelling the mechanism of M1GAS SK

4.1 Introduction

Understanding of streptokinase activation of plasminogen has almost exclusively focused on the Group C (GCS) S. *equisimilis* H46a SK variant which is used as a thrombolytic to treat myocardial infarction. This strain of SK demonstrates no, or limited, binding and stimulation by fibrinogen, see chapter 2, e.g. Figure 2.8 for example (Chibber et al., 1985, Takada et al., 1980) and presents the simplest mechanism of plasminogen to study. However, other strains of SK across many streptococcal species, including the Group A (GAS) S. *pyogenes* M1 strain, display interactions with receptor bound fibrinogen and plasminogen and are typically associated with pathogenicity. Understanding the details of the mechanism of plasmin generation by SK variants from Streptococcal species associated with disease may provide insights into combating pathogenicity and treating infections (Sun, 2011). Such studies will require inclusion of fibrinogen as a potential regulator of SK activity.

The mechanism of action of SK as a plasminogen or plasmin binding protein, and plasminogen activator, has been outlined in chapters 2 and 3 and has been understood for some time (Gonzalez-Gronow et al., 1978). More recently, Bock and co-workers have undertaken detailed studies on the various steps in the plasminogen activation process and developed the “trigger and bullet” model (Boxrud and Bock, 2004, Boxrud et al., 2004, Nolan et al., 2013). In this pathway, SK first binds plasminogen, generating an active site capable of converting free plasminogen to plasmin, providing the “trigger” step. The plasmin thus formed has a higher affinity for SK than plasminogen and displaces it. The plasmin M1GAS SK complex, the “bullet”, displays improved kinetics as a plasminogen activator, and this complex is responsible for subsequent plasmin generation. As with most studies, the trigger and bullet mechanism was developed using an H46a SK variant with little or no binding capability for fibrinogen or fibrin. It is of interest to explore the kinetics of plasminogen activation of a M1GAS SK, which does bind to fibrin and fibrinogen to better understand how plasminogen

activation is regulated. Developing a model to explain the kinetic results of SK stimulated by fibrinogen is the subject of this chapter.

4.2 Experimental procedures

M1GAS SK activity at 1.6 and 0.4 nM was simulated across a range of fibrinogen and plasminogen concentrations to replicate experimental data as closely as possible, and generate a matrix of kinetic data like that generated in a microtitre plate. The specified range of fibrinogen was 53 nM to 30.3 μM, n=11 (log scale); and for plasminogen the range was 25 nM to 1.6 μM, n=11, (linear scale). All simulations were performed using Gepasi, a computer program for simulating biochemical reactions (Mendes, 1993, Mendes, 1997). To facilitate comparison, 3D surfaces and contoured heat maps were fitted to the data using the Akima package in R (Akima, 1978). Curve fitting to the Michaelis-Menten equation of the data was accomplished using R and the Trellis package (Sarkar, 2008).

The reactions involved in the pathways, present in the laboratory assays and used to simulate M1GAS SK activation of plasminogen are listed in Table 4.1 and represented in the model in Figure 4.2. Reaction 1 and 2 depict plasmin cleavage of the chromogenic substrate, S-2251, and pNA generation which are not shown in the model in Figure 4.2. The interaction between plasmin and fibrinogen, which will act as a competitive substrate for plasmin cleavage of S-2251, is included in reaction 11. This model looks exclusively at initial rates so no reactions for the destruction of fibrinogen following plasmin generation are included. Simulations were typically followed for 600 s collecting 600, 1200 or 2400 time points. No significant differences were observed between various sampling rates.

To begin modelling, values for the kinetic constants were either based on those determined in laboratory assays under the appropriate conditions, or taken from published values (see results). Kinetic parameters in the model were then adjusted manually to find optimal agreement between the data generated in laboratory assays and the simulation. Simulated data were treated in the same way as data from kinetic assays such that tables of time versus absorbance were generated and imported into R so rates of plasmin generation could be calculated from plots of absorbance versus time squared (see section 2.2.4A) up to a maximum absorbance chosen to limit substrate depletion to <20%. A single R script was used

to determine rates of plasmin generation (pM s^{-1}) from kinetic data and simulated data of rates of S-2251 hydrolysis and plot results (Colin Longstaff, personal communication, see Appendix 2).

Table 4.1 Reactions required for Gepasi modelling.

Reaction number	Reaction	Note
1	E+S=ES	The substrate S-2251 (S) forms a complex with the enzyme plasmin (E)
2	ES-> E+P	S2251 (S) is converted into pNA (P) by plasmin; thus releasing the enzyme (E)
3	B+G=BG	M1GAS SK (B) binds to plasminogen (G) to form a plasminogen activator complex (BG)
4	BG+G=BGG	The plasminogen activator complex (BG) binds a further plasminogen molecule (G)
5	BGG-> BG+E	Plasminogen (G) is converted to its active enzyme form, plasmin (E) and released from the activator complex (BG).
6	G+F=GF	Plasminogen(G) binds to fibrinogen (F)
7	F+BG=FBG	The activator complex (BG) binds to fibrinogen (F)
8	GF+BG=GFBG	The activator complex (BG) binds to plasminogen bound to fibrinogen (GF) to form a trimolecular complex (GFBG)
9	G+FBG=GFBG	Free plasminogen (G) binds the activator complex bound to fibrinogen (FGB) to form a trimolecular complex (GFBG)
10	GFBG->E+FBG	Plasminogen (G) is converted to plasmin (E) and released from the trimolecular complex (GFBG). The activator complex remains bound to fibrinogen (FBG).
11	E+F=EF	Plasmin (E) binds to fibrinogen (F)
12	B+E=BE	M1GAS SK (B) binds to plasmin (E) to form a plasminogen activator complex (BE).
13	F+BE=FBE	The plasminogen activator complex (BE) binds to fibrinogen (F)
14	G+FBE=GFBE	Free plasminogen (G) binds the activator complex bound to fibrinogen (FBE) to form a trimolecular complex (GFBE)
15	GF+BE=GFBE	The activator complex (BE) binds to plasminogen bound to fibrinogen (GF) to form a trimolecular complex (GFBE)
16	GFBE->E+FBE	Plasminogen (G) is converted to plasmin (E) and released from the trimolecular complex (GFBE). The activator complex remains bound to fibrinogen (FBE).
17	BE+G=BEG	The activator complex (BE) binds plasminogen (G) in solution
18	BEG->BE+E	The plasminogen (G) is converted to plasmin (E) and released by the activator complex (BE).

Table 4.2 Initial concentrations of metabolites included in modelling reactions.

Metabolite	Initial Concentration
S	0.24 mM
G	0.025, 0.183, 0.34, 0.50, 0.655, 0.813, 0.970, 1.13, 1.29, 1.44, 1.60 µM
B	0.4 or 1.6 nM
F	0.052, 0.098, 0.186, 0.351, 0.651, 1.26, 2.37, 4.49, 8.48, 16.0, 30.3 µM
E, ES, P, BG, BE, FBG, FBE, GFBG, GFBE, BEG, BGG, EF, GF	0

4.3 Results

Figure 4.1 presents a comparison between laboratory and simulated data for M1GAS SK activity across a fibrinogen/plasminogen concentration matrix, for which there is good agreement. M1GAS SK activation of plasminogen was simulated in Gepasi using the model in Figure 4.2. To facilitate comparison the data has been presented in Figure 4.1 as fitted surfaces (panels A and B), and as a contoured heat map, (panels C and D), which show results for kinetic data (panels A and C) and simulations (B and D) with 1.6 nM SK. Panel E is a representation of the merged surfaces in panels A and C to illustrate the overlap of results. Panel F is a summary plot of apparent k_{cat}/K_M values from individual curve fits over a range of plasminogen concentrations, at each fibrinogen concentration. In this case, good agreement is seen for kinetic data using 1.6 nM and 0.4 nM SK data (presented as points) and the results from simulated data which are presented as a curve, where 1.6 nM and 0.4 nM SK are overlapping.

Curve fitting to the Michaelis-Menten equation using these data is presented in Figures 4.3, 4.4, 4.5, and 4.6, corresponding to kinetic data for 1.6 nM, kinetic data SK, 0.4 nM, simulated data for 1.6 nM SK and simulated data for 0.4 nM SK, respectively. The fitted parameters for k_{cat} and K_M from these curves and calculated values of k_{cat}/K_M are presented in Table 4.4 and 4.5 for kinetic data and simulated data, respectively. It was necessary to estimate and fix the K_M for simulated data based on the fits to the kinetic data in order to complete batch fitting on the simulated data. Visual inspection of kinetic data and simulated data (Figure 4.1) largely demonstrates excellent agreement and provides evidence to validate the model. However, it is the case that some parameters could be changed slightly with compensation in other parameters to also provide a good fit. Nevertheless, modifications to the parameters shown in Table 4.3 would be restricted to a narrow range. It was not found possible to simplify the model presented in Figure 4.2 and still get the correct curves shapes shown in Figure 4.1 (A-D), suggesting that the “trigger and bullet” mechanism is the minimal useful mechanism. Close examination of the Michaelis-Menten equation curve fits presented in Figures 4.3 to 4.6

suggests derived values for K_M and V_{max} (hence k_{cat}) are robust, especially in the case of the results for the kinetic data. There are some systematic deviations present in the curve fits for the simulated data (Figures 4.5 and 4.6), which may be improved with further optimisation of the model. It should be noted that these curve fittings are an approximation of a more complex model since they assume idealised conditions of enzyme substrate interactions and adherence to a simple Michaelis-Menten model. Fibrinogen is a complicating feature of the system that is likely to affect plasminogen activation over the concentration ranges used, therefore a simple Michaelis-Menten model is not truly accurate. Thus the model illustrated in Figure 4.1 and Table 4.3 is a better approximation since it includes some additional interactions with fibrinogen. The simulated rate data do not include any noise, which is unavoidable in real kinetic data. It is therefore easier to identify systematic deviation in the simulated data, which may be masked in the curve fits of the actual kinetic data.

Association rate constants for all reactions with the exception of plasmin binding to M1GAS SK (reaction 12) are approximated to 10^7 $M^{-1}s^{-1}$ at 37 °C. Many interactions of biological interest have association rate constants in the range 10^5 to 10^8 M^{-1} s^{-1} (0.1-100 μM^{-1} s^{-1}) (Fersht, 1984) and it is common when fitting by numerical integration methods to begin with a fixed association rate constant and adjust K_D or K_M values by varying the dissociation rate constant e.g. (Kuzmic, 1996). The formation of the plasmin M1GAS SK complex was assigned a rate constant of 10^8 $M^{-1}s^{-1}$ to reflect higher affinity and faster association (Boxrud et al., 2000, Boxrud et al., 2001). Reported Biacore measurements at 25 °C determined association rate constants to be approximately 10^6 $M^{-1}s^{-1}$ for the SK-Pg* complex formation (Cook et al., 2012, Zhang et al., 2012), and for the SK-Pm* formation (Nolan et al., 2013).

The kinetic constants for plasmin binding and cleavage of the chromogenic substrate, S-2251 (reactions 1 and 2) were based on experiments described in chapter 3, whilst the binding of M1GAS SK to plasminogen (reaction 3) was best defined by a K_D of 40 nM which fits well with published results by (Cook et al., 2012) and (Nolan et al., 2013).

The binding of the SK-Pg* complex to a further plasminogen molecule (reaction 4) and the subsequent generation of plasmin (reaction 5) were given a k_{cat} of 0.04 and a K_M of 0.6 μM as derived from fitting of Michaelis-Menten curves without fibrinogen. This is approximately 7-fold lower than results published (Boxrud and Bock, 2004) for H46a SK which is expected since M1GAS SK has been shown to be less effective without fibrinogen (K_M was 0.27 μM and k_{cat} 0.31 for Lys-Pg in (Boxrud and Bock, 2004). In the model, when M1GAS SK complexes with plasmin, the K_M was reduced by half to 0.3 μM, but the k_{cat} was kept the same which is similar to the modest improvements in activity seen by (Boxrud et al., 2004).

Upper limits of published K_D values for fibrinogen binding to Lys-Pg are 8.3 μM (Lucas et al., 1983), with lower estimates of 0.23 μM also available (Stewart et al., 1998). The value assigned here of 6.0 μM sits within this range.

Reaction 8 represents the starting estimate from Michaelis-Menten fits at each fibrinogen concentration just as reaction 3 indicates the equivalent in solution. The work on plasmin in this thesis (chapter 3) suggests fibrinogen can affect K_M and k_{cat}, but Michaelis-Menten fits of the data here indicate that the V_{max} (and k_{cat}) are much more affected than the K_M.

A 18-fold k_{cat} increase from 0.1 s^{-1} to 1.8 s^{-1} for the generation of plasmin when the activator complex is in solution (reaction 5) or bound to fibrinogen (reaction 10) respectively accounts for most of the stimulation caused by fibrinogen in the assays systems. Some additional stimulation is seen with a small improvement in the K_M to 0.25 from 0.6 μM.

An initial estimate for the binding of plasmin to fibrinogen (reaction 11) was based on the value published in (Longstaff and Whitton, 2004) but that assumed a simple competitive inhibition. As seen in chapter 3, this is not the case. Therefore, this is unlikely to be the true value, so may be a source of error and deviation at high fibrinogen concentrations.

This binding of plasmin to SK (reaction 12) is tighter than the K_D for SK-Pg* (reaction 3) and is similar to previously published Biacore measurements. (Cook et al., 2012, Nolan et al., 2013, Boxrud et al., 2000). The difference between these two values appears to be important

for the degree of curvature as plasminogen varies in the model to match the shape of the curves for laboratory data seen in Figure 4.1.

The improvement between plasmin M1GAS SK complex and M1GAS SK-Pg* activity resulting from plasminogen binding is due to a decrease in K_M (from 0.6 μM for plasminogen, reaction 4, to 0.3 μM for plasmin, reaction 17, without fibrinogen, and 0.6 μM for plasminogen to 50 nM for plasmin with fibrinogen). There is no change in k_{cat}, remaining consistent at 1.8 s^{-1} for both the plasminogen and plasmin complexes (reactions 10 and 16). This is in good agreement with laboratory data in chapter 3.

Table 4.3 Kinetic constants determined for chemical reactions in Gepasi modelling.

Reaction number	Reaction	k_{on}[a] (μM^{-1} s^{-1})	k_{off} (s^{-1})	k_{cat} (s^{-1})	K_D or K_M (μM)
1	E+S=ES	10	3680		368
2	ES-> E+P			25.5	
3	B+G=BG	10	0.4		0.04
4	BG+G=BGG	10	6		0.6
5	BGG-> BG+E			0.1	
6	G+F=GF	10	60		6.0
7	F+BG=FBG	10	60		6.0
8	GF+BG=GFBG	10	2.5		0.25
9	G+FGB=GFBG	10	2.5		0.25
10	GFBG->E+FBG			1.8	
11	E+F=EF	10	5		5
12	B+E=BE	100	0.01		0.0001
13	F+BE=FBE	10	60		6.0
14	G+FBE=GFBE	10	0.5		0.05
15	GF+BE=GFBE	10	0.5		0.05
16	GFBE->E+FBE			1.8	
17	BE+G=BEG	10	3		0.3
18	BEG->BE+E	10		0.1	

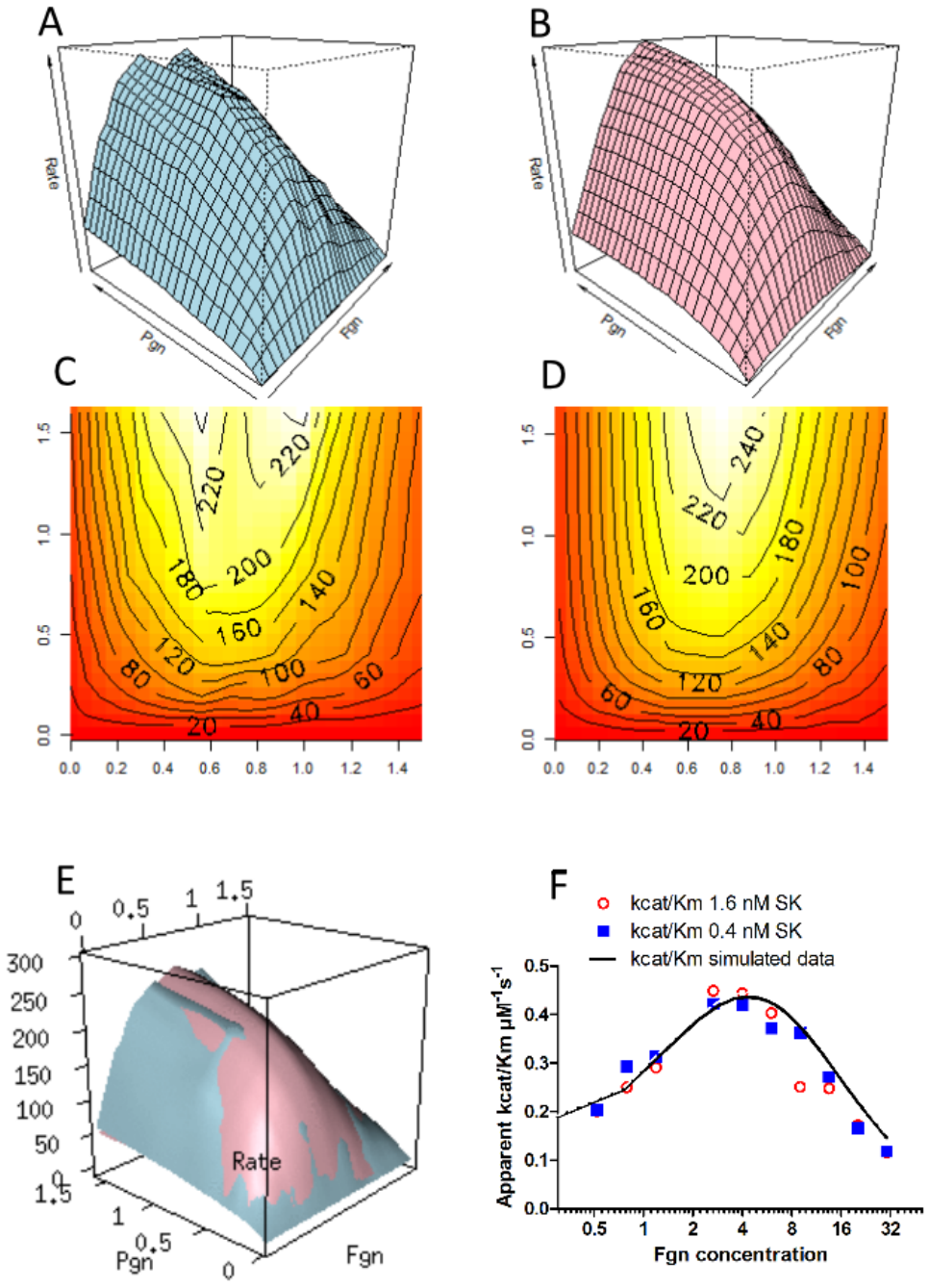

Figure 4.1 A comparison of lab-based and simulated M1GAS SK activation of plasminogen across a fibrinogen and plasminogen concentration matrix. Figures A) and C) illustrate data generated in the laboratory, whilst B) and D) show simulated data. E) is an overlay of the two to allow comparison, whilst F) compares lab values at two M1GAS SK concentrations with Gepasi simulated data for both. Axis in Figures A-D show plasminogen (Pgn) concentration in μM, fibrinogen (Fgn) concentration as $\log_{10}$ μM and rates of plasmin production in pM s^{-1}. In panel F fibrinogen concentration in μM is presented on a log scale.

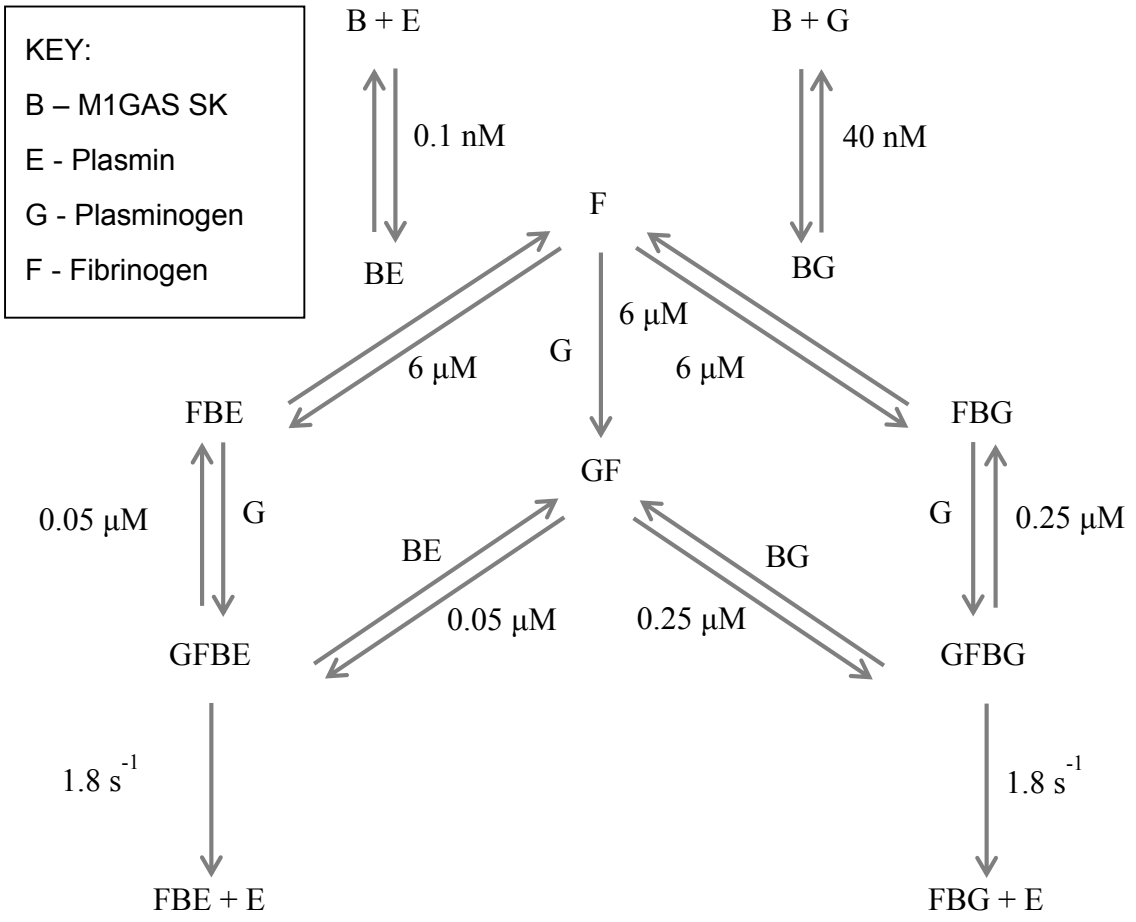

Figure 4.2 A kinetic model to describe plasminogen activation by M1GAS SK. For clarity, some reactions listed in Table 4.3 have been omitted. This are reactions 1 and 2 (E hydrolysis of S-2251), reactions 4 and 5 (E formation by BG without F binding) and reactions 17 and 18 (E formation by BE without F binding).

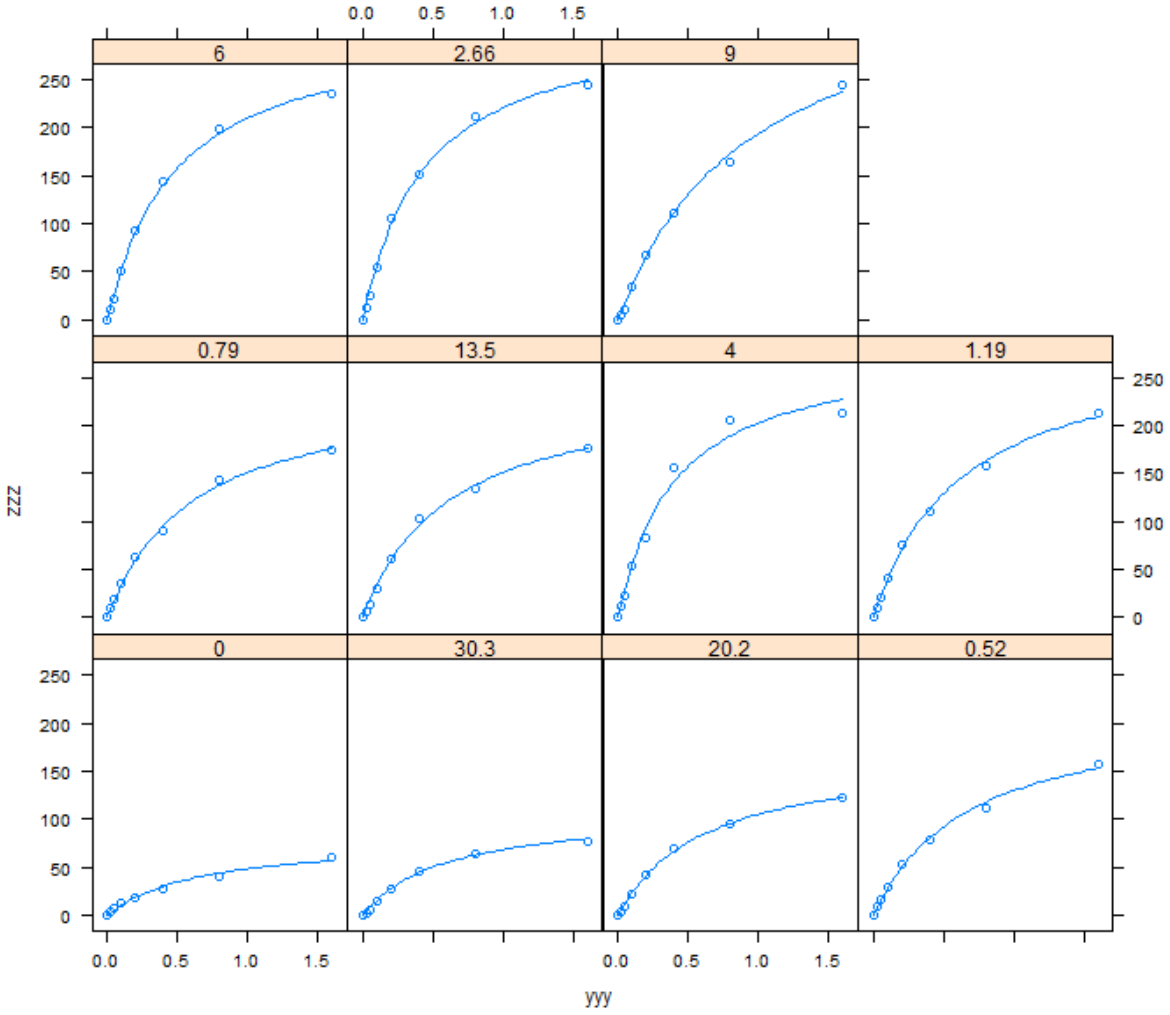

Figure 4.3 Michaelis-Menten curve fits of kinetic data for 1.6 nM M1GAS SK activity across a fibrinogen concentration range. The values in the boxes above the curves denote the fibrinogen concentration (μM) with the Michaelis-Menten fits ordered from lowest V_{max} (bottom left) to highest (top right). The y axis values are the plasminogen concentration (μM) and the z axis values denote rates of plasmin production in (pM s^{-1}).

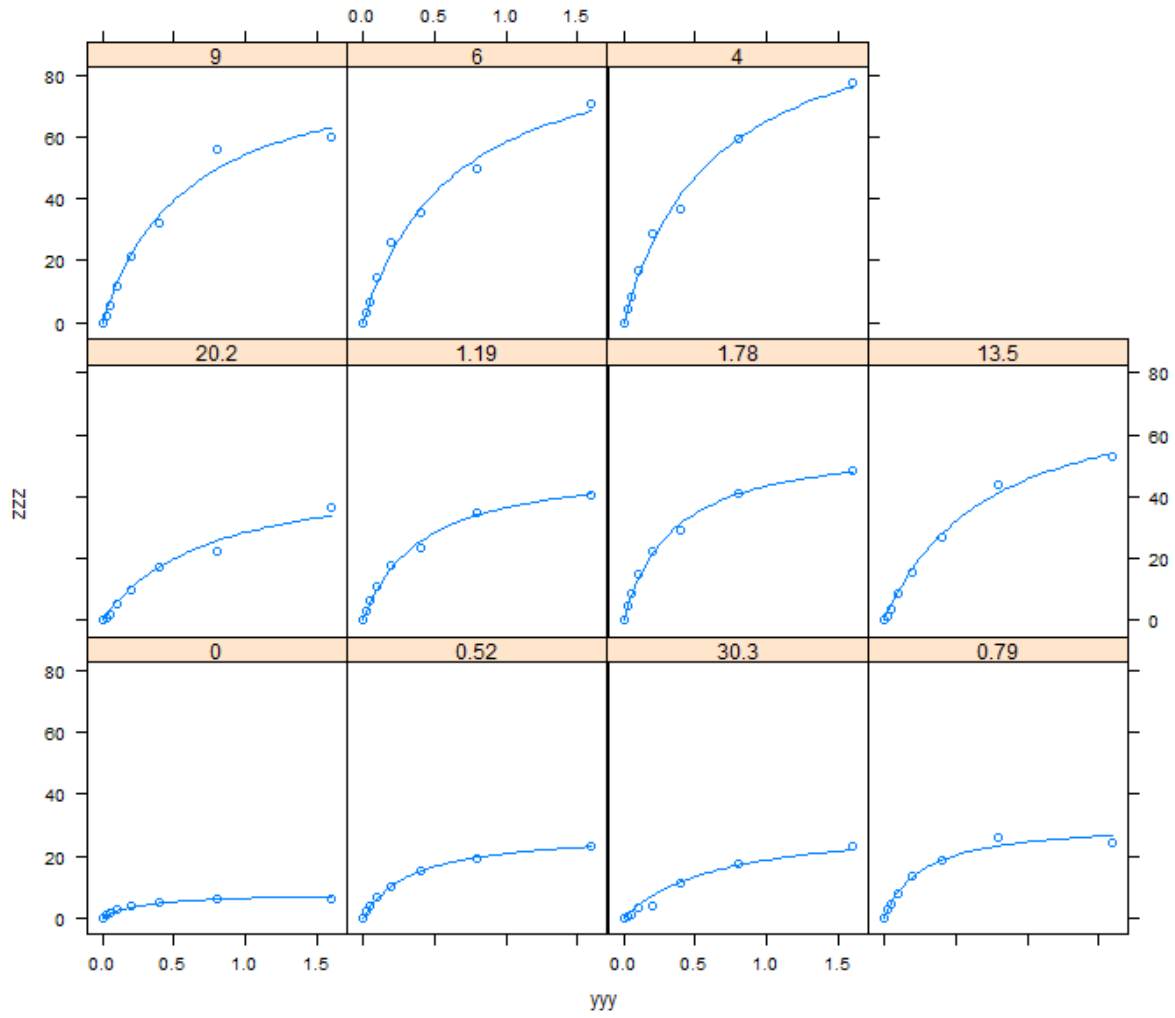

Figure 4.4 Michaelis-Menten curve fits of kinetic data for 0.4 nM M1GAS SK activity across a fibrinogen concentration range. The values in the boxes above the curves denote the fibrinogen concentration (μM) with the Michaelis-Menten fits ordered from lowest V_{max} (bottom left) to highest (top right). The y axis values are the plasminogen concentration (μM) and the z axis values denote rates of plasmin production in (pM s^{-1}).

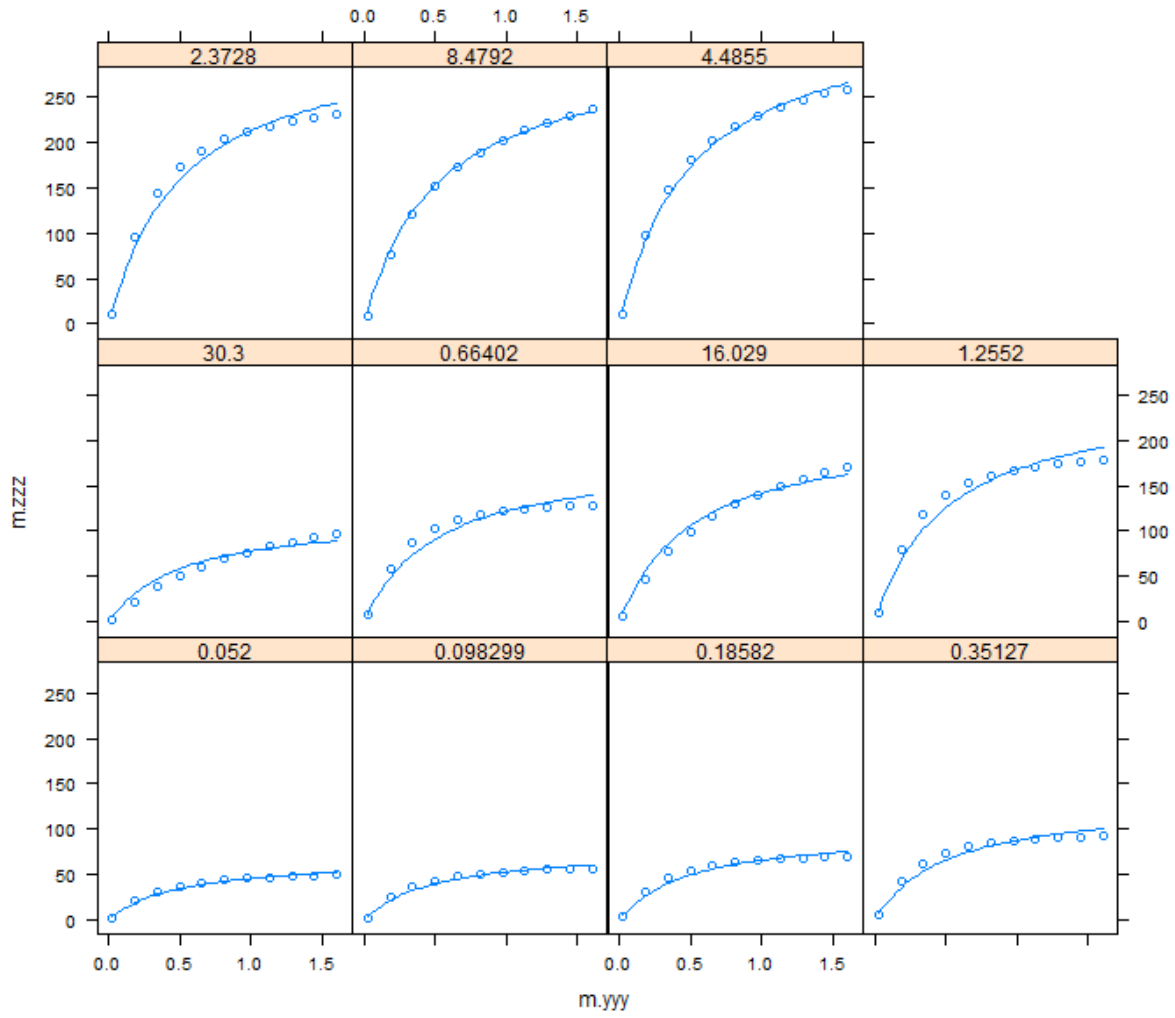

Figure 4.5 Michaelis-Menten curve fits of simulated data for 1.6 nM M1GAS SK activity across a fibrinogen concentration range. The values in the boxes above the curves denote the fibrinogen concentration (μM) with the Michaelis-Menten fits ordered from lowest V_{max} (bottom left) to highest (top right). The y axis values are the plasminogen concentration (μM) and the z axis values denote rates of plasmin production in (pM s^{-1}).

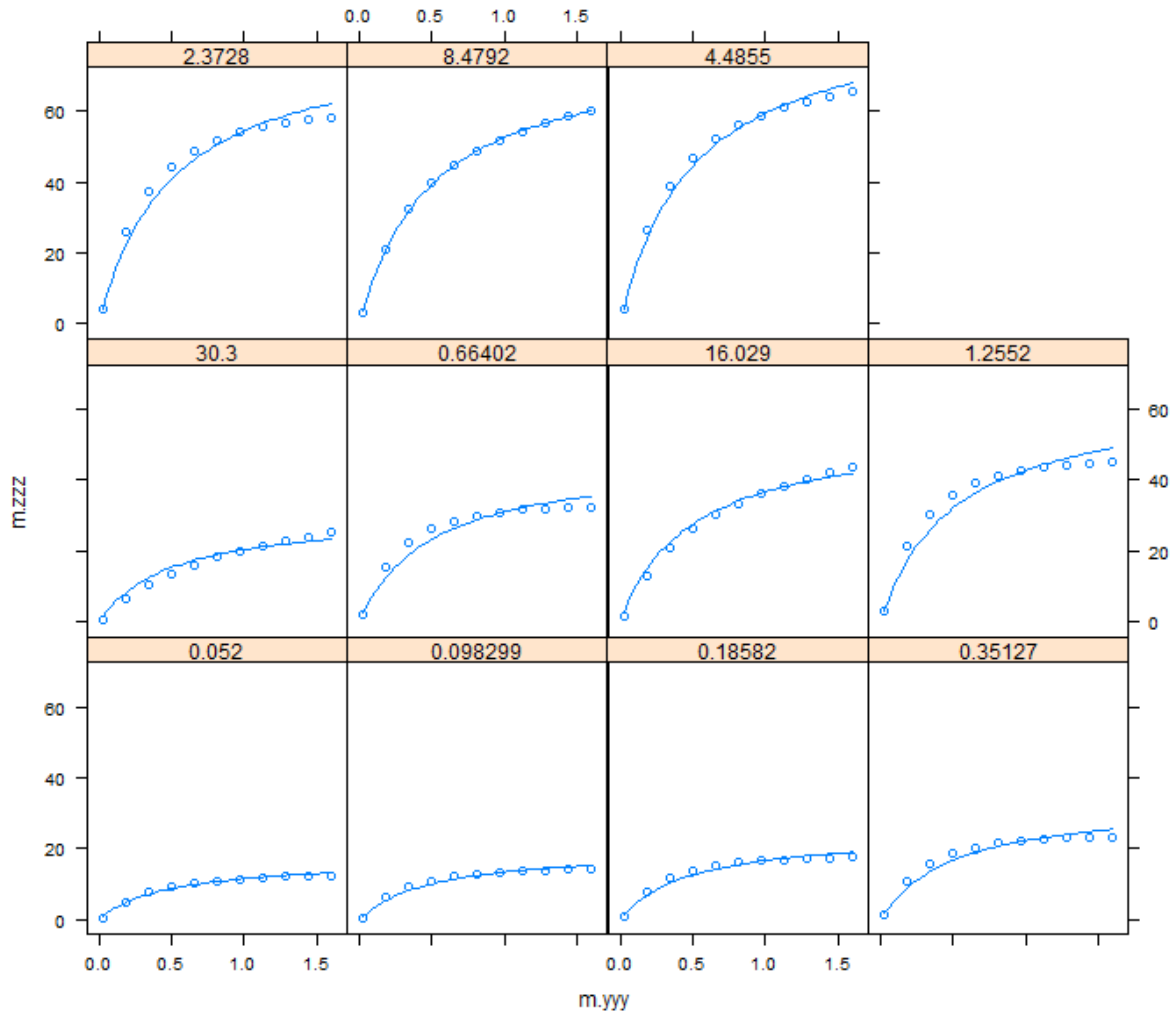

Figure 4.6 Michaelis-Menten curve fits of simulated data for 0.4 nM M1GAS SK activity across a fibrinogen concentration range. The values in the boxes above the curves denote the fibrinogen concentration (μM) with the Michaelis-Menten fits ordered from lowest V_{max} (bottom left) to highest (top right). The y axis values are the plasminogen concentration (μM) and the z axis values denote rates of plasmin production in (pM s^{-1}).

Table 4.4 Summary of Michaelis-Menten curve fitting results for kinetic data using 1.6 and 0.4 nM M1GAS SK.

	M1GAS SK concentration (nM)							
	1.6				0.4			
Fibrinogen concentration (μM)	V_{max} (pM s^{-1})	K_M (μM)	k_{cat} (s^{-1})	k_{cat}/K_M (μM^{-1} s^{-1})	V_{max} (pM s^{-1})	K_M (μM)	k_{cat} (s^{-1})	k_{cat}/K_M (μM^{-1} s^{-1})
0.00	79.4	0.65	0.05	0.08	8.3	0.29	0.02	0.07
0.52	217.9	0.68	0.14	0.20	28.1	0.35	0.07	0.20
0.79	242.1	0.61	0.15	0.25	31.1	0.27	0.08	0.29
1.19	291.6	0.63	0.18	0.29	51.3	0.41	0.13	0.31
2.66	318.7	0.44	0.20	0.45	58.4	0.35	0.15	0.42
4.00	283.8	0.40	0.18	0.44	106.1	0.63	0.27	0.42
6.00	311.9	0.48	0.20	0.40	95.7	0.64	0.24	0.37
9.00	375.7	0.94	0.24	0.25	86.4	0.59	0.22	0.36
13.50	244.0	0.62	0.15	0.25	78.4	0.73	0.20	0.27
20.20	170.1	0.62	0.11	0.17	49.6	0.75	0.12	0.17
30.30	108.9	0.59	0.07	0.12	31.2	0.66	0.08	0.12
Min	79.4	0.40	0.05	0.08	8.3	0.27	0.02	0.07
Max	375.7	0.94	0.24	0.45	106.1	0.75	0.27	0.42
Ratio	4.7	2.34	4.70	5.83	12.8	2.81	12.62	5.86
Average		0.60				0.51		

Table 4.5 Summary of Michaelis-Menten curve fitting results for simulated data assuming 1.6 and 0.4 nM M1GAS SK.

	M1GAS SK concentration (nM)							
	1.6				0.4			
Fibrinogen concentration (μM)	Vmax (pM s-1)	KM (μM)	kcat (s-1)	kcat/KM (μM-1 s-1)	Vmax (pM s-1)	KM (μM)	kcat (s-1)	kcat/KM (μM-1 s-1)
0.05	68.1	0.50	0.04	0.09	17.2	0.50	0.04	0.09
0.10	78.9	0.50	0.05	0.10	20.0	0.50	0.05	0.10
0.19	98.3	0.50	0.06	0.12	24.9	0.50	0.06	0.13
0.35	131.4	0.50	0.08	0.16	33.3	0.50	0.08	0.17
0.66	183.1	0.50	0.11	0.23	46.5	0.50	0.12	0.23
1.26	252.2	0.50	0.16	0.32	64.2	0.50	0.16	0.32
2.37	320.1	0.50	0.20	0.40	81.6	0.50	0.20	0.41
4.49	348.6	0.50	0.22	0.44	89.1	0.50	0.22	0.45
8.48	307.3	0.50	0.19	0.38	78.9	0.50	0.20	0.39
16.03	213.0	0.50	0.13	0.27	55.0	0.50	0.14	0.28
30.30	117.0	0.50	0.07	0.15	30.4	0.50	0.08	0.15
Min	68.1	0.50	0.04	0.09	17.2	0.50	0.04	0.09
Max	348.6	0.50	0.22	0.44	89.1	0.50	0.22	0.45
Ratio	5.1	1.00	5.07	5.13	5.2	1.00	5.19	5.19

5.4 Discussion

The starting point for this work was the 'trigger and bullet' model for H46a SK activation of plasminogen proposed in (Nolan et al., 2013, Boxrud and Bock, 2004). A key difference between H46a SK and M1GAS SK is the interaction of fibrinogen so the model was adapted to incorporate the fibrinogen binding and stimulation of M1GAS SK demonstrated throughout this work. This work used the basic model, laboratory data with ranges of plasminogen and fibrinogen and simulated results, to gain agreement between the kinetic data and the model to further our understanding of the mechanism of M1GAS SK.

There is a strong agreement between the model and laboratory data but there are some parameters which are not known for certain and could be different, for instance the K_D for plasmin and plasminogen with M1GAS SK. The values used in this model were taken from literature values (Cook et al., 2012, Zhang et al., 2012, Nolan et al., 2013) which have dealt primarily with group 2b strains. These share some characteristics with 2a SK variants of which S. *pyogenes* is a member (McArthur et al., 2008), however, future work into these interactions using Biacore could yield improves. Of further note, (Cook et al., 2012) binding studies were carried out at 25 °C, so the values will also differ slightly compared to at 37 °C, as used in this study.

With S. *pyogenes* and Cluster 2a Streptococci, there is M1 expression and fibrinogen binding but no PAM expression and subsequently no direct plasminogen binding (typical of cluster 2b Streptococci) (McArthur et al., 2008). Seemingly, the bacteria's interaction with fibrinogen is key to its mechanism of invasion, so it's unsurprising that the SK would display fibrinogen and fibrin specificity. Without a capacity for direct plasminogen binding, which is less crucial in the blood considering the abundance of plasminogen (1.5 – 2.0 μM), there is a shift towards binding fibrinogen, another key haemostatic protein, as a way of localising plasmin activity to the cell surface. Any benefits of surface plasmin binding through surface-bound fibrinogen over direct PAM-plasmin binding are unknown.

The model shows how fibrinogen stimulates M1GAS activity in solution by binding SK and plasminogen to form a trimolecular complex, as hypothesized previously (McArthur et al., 2008). Stimulation of activity of the M1GAS SK-Pg* complex by fibrinogen is achieved by improvements in K_M (0.6 to 0.25 μM) and k_{cat} (0.1 to 1.8 s^{-1}). Similarly for the plasmin M1GAS SK complex, K_M is improved (0.3 to 0.05 μM) and k_{cat} (0.1 to 1.8 s^{-1}), as shown in Table 4.1. These values also illustrate that most of the improvements seen when plasmin replaces plasminogen in the active complex with M1GAS are due to K_M, which achieves its lowest value of 0.05 μM for plasmin M1GAS SK in the presence of fibrinogen. Stimulation of kinetics is one way in which fibrinogen is deployed in regulating M1GAS activity and influencing pathogenesis (Cook et al., 2012), however accumulation of plasmin activity on the surface of the bacteria is also likely to be an important mechanism in promoting bacterial metastasis. Thus the cluster 2a bacteria have evolved to bind host fibrinogen molecules to their cell surface M1 receptor proteins to form the template for pericellular plasmin generation, as shown in Fig 1.3 (McArthur et al., 2008). A different mechanism has been adopted by Cluster 2b bacteria which have PAM receptors able to bind and concentrate plasminogen, which may be tailored to environments with lower circulating plasminogen, explaining why PAM-expression is associated with skin infections (Svensson et al., 2002).

The model outlined here only deals with the role of fibrinogen but fibrin is of great interest and seen to exhibit different binding and stimulatory effects on M1GAS SK, see chapter 2. As the fibrin concentrations cannot be varied in a manner similar to that employed for fibrinogen, and there are diffusion issues with assay systems, modelling this in the same way as attempted with fibrinogen is more complicated. The heterogeneous nature of fibrin means that studying plasminogen activation at a solid liquid interface and modelling fibrinolysis is challenging. However, recent progress has been made in modelling fibrinolysis with tPA and similar approaches may be possible using SK (Bannish et al., 2014b, Bannish et al., 2014a, Longstaff and Kolev, 2015).

Chapter 5 Producing a recombinant SCG

5.1 Introduction

There have been several studies with SCG positive and SCG deficient strains of S. *aureus* to demonstrate the contributions of this virulence factor to pathogenesis (Cheng et al., 2010, DeDent et al., 2012, Cheng et al., 2009, Panizzi et al., 2011). However, very little is known about the mechanism of prothrombin activation with regard to bacterial virulence at the molecular level. There is also no clear understanding of why S. *aureus* expresses both a plasminogen activator (SAK) to promote fibrinolysis and SCG, a prothrombin activator which facilitates fibrin formation.

The expression and purification of recombinant proteins is a useful tool for research. Bacterial systems, such as E. *coli*, typically give good protein yields and relative simplicity and ease of expression in comparison to other systems, such as mammalian (Baneyx and Mujacic, 2004, Malakhov et al., 2004, Thelwell and Longstaff, 2014). Work which served to demonstrate the potential of SCG as a ZAAP, and provide evidence for the "molecular sexuality" mechanism was carried out using recombinant truncated fragments of SCG. Native N-terminal sequences of S. *aureus* Tager strain SCG 1-325 as well as SCG 2-325, SCG 3-325 and SCG 147-325 were expressed in E. *coli* using a His-tag system and a factor Xa cleavage site after the initiating 'Met' residue (Friedrich et al 2003). The same group has also expressed Met-SCG 1-325 with a C-terminal His-tag (Panizzi et al 2006). Full-length GST-tagged SCG has been expressed in E. *coli*. A GST expression system was stated as being chosen since SCG seemed to undergo degradation during purification in a pET15b vector with a Strep tag (McAdow et al., 2012a). The GST tag system employed here used a PreScission (GE Healthcare) protease cleavage site, which does not allow purification of a recombinant protein with an intact, native N-terminal sequence, as removal of the tag leaves additional amino acids. This was not necessary for the work in (McAdow et al., 2012) as the focus was on the effect antibodies raised against SCG have on the ability for S. *aureus* to clot blood and

establish infection in a murine model, not the in vitro activity of the SCG protein. However, the N-terminal Ile^1 residue on SK is critical for plasminogen activation (Wang et al., 2000) and an integral part of ZAAP “molecular sexuality” (Wang et al., 1999). Therefore, the recombinant expression strategies employed in this work were chosen to express a SCG protein with a preserved native N-terminal sequence, in order to investigate its potential as a prothrombin activator in manners analogous to those detailed above for SK. Following on from successful expression of SK in E. *coli* in a SUMOstar expression system (Chapter 2), the decision was taken to utilise this for SCG expression. SUMOstar has also been optimised for expression of recombinant proteins in P. *pastoris* and the initial cloning strategy is common between the two systems. As such, both strategies were explored in parallel.

5.2 Experimental procedures

5.2.1 Materials, equipment and software

One Shot TOP10 chemically competent E. *coli* cells, Zero Blunt TOPO PCR cloning kit, pCR – Blunt II-TOPO vector, Ampicillin, Zeocin, Blue Juice loading buffer, pGAPZα vector (Invitrogen, Merelbeke, Belgium)

T7 Express LysY Competent high efficiency *E. coli* cells, Phusion High Fidelity DNA Polymerase Master Mix (New England BioLabs, Hertfordshire, UK).

pE SUMOstar expression kit, pY SUMOstar expression kit, SUMOstar protease (LifeSensors, Pennsylvania, USA).

QIAprep Spin Miniprep Kit, QIACUBE, QIAquick gel extraction kit, Empty columns (QIAGEN, Greater Manchester, UK)

Nuclease free water, NanoDrop 2000 UV-Vis spectrophotometer, Rapid DNA ligation kit, aLICator LIC cloning and expression kit 2 (Thermo Scientific, Massachusetts, USA)

All restriction digesion enzymes were FastDigest enzymes obtained from Thermo Scientific (Massachusetts, USA).

Gel Red (Biotium, California, USA)

rEK capture kit (Novagen, Wisconsin, USA)

E-Gel® CloneWell™ 0.8% SYBR Safe™ gel s, E-Gel® iBase™ and Safe Imager system (Life Technologies, Renfrewshire, UK)

Agarose,Glycerol, NiNTA Agarose (Sigma Aldrich, St Louis, Missouri, USA)

AKTApurifier (GE Healthcare, Buckinghamshire, UK)

S-2238 (H-D-Phe-Pip-Arg-pNA) (Chromogenix, Milan, Italy) – reconstituted in 15 ml H_2O, to give a 3 mM stock solution. Stored at 2-8 °C, stable for several months.

Fibrinogen (Calbiochem, Merck Millipore, Billerica, Massachusetts, USA) - reconstituted in Buffer B to give stock solution of 50 mg/ml, and flash frozen in liquid nitrogen in small aliquots and stored at -40 °C. All dilutions for reaction set ups were in buffer B also.

Prothrombin (Calbiochem, Merck Millipore, Billerica, Massachusetts, USA) - reconstituted in H_20 to 1 mg/ml and flash frozen in liquid nitrogen in small aliquots and stored at -40 °C. All dilutions for reactions were in buffer C.

5.2.2 Culture media and assay buffers

YPD, YPDS and Low salt LB media were made according to recipes in the Invitrogen manual for pGAPZα A, B and C (MAN0000043).

LB Media, made from LB media powder (Thermo Scientific, Massachusetts, USA)

SOC medium (Invitrogen, Merelbeke, Belgium). Stored at 2 – 8 °C.

TBE buffer, made from 10x TBE (Thermo Scientific, Massachusetts, USA)

Buffer A - 0.5 M Tris pH 8.4 at 37 °C. Stored at 2-8 °C for 6 months.

Buffer B – 10 mM Tris HCL 100 mM NaCl 0.01% Tween 20. Store at 2-8 °C for 1 week.

Buffer C – Buffer B + 1mg/mL Human Serum Albumin (HSA). Store at 2-8 °C for 3 days.

All laboratory chemicals used to make buffers were from Sigma Aldrich, St Louis, Missouri, USA.

5.2.3 Bacterial strains and culture

5.2.3A E. coli strains

Commercially available chemically competent Top10 *E. coli* cells were used for initial transformation after cloning and plasmid maintenance. Protein expression was carried out in T7 Express LysY Competent high efficiency *E. coli* cells (New England Biolabs, Hertfordshire, UK)

5.2.3B E. coli culture conditions

Unless otherwise stated, *E. coli* cultures were routinely grown at 37 °C on LB-agar plates or in LB liquid culture with constant shaking. Culture media was supplemented with selective antibiotics as appropriate to the transformed plasmid (ampicillin (50 µg/mL) or zeocin in low salt LB (25 µg/mL)). For long term storage, *E. coli* cultures were stored at -80 °C in 2 ml aliquots containing 15% (w/v) glycerol.

5.2.4 Yeast strains and culture

5.2.4A P. pastoris strains

Commercially available X-33 wild-type *Pichia pastoris* yeast strain (Thermo Scientific, Massachusetts, USA) were used for protein expression.

5.2.4B P. pastoris culture conditions

Successful transformants were plated on YPDS agar plates containing 100-1000 µg/mL zeocin and incubated statically at 30 °C for 2-3 days. Zeocin resistant colonies were grown on YPD plates containing 100 µg/mL zeocin to confirm presence of desired insert. Overnight colonies of P. *pastoris* necessary for electroporation and recombinant protein expression colonies of P. *pastoris* were grown in YPD media at 30 °C with shaking (300 rpm). Expression colonies were incubated for up to 72 hours.

5.2.5 General methods for DNA manipulation

5.2.5A Primer design and PCR amplification of staphylocoagulase from S. aureus Newman strain genomic DNA

Primers were designed for the full-length mature peptide, based upon the staphylocoagulase sequence identified in (Baba et al., 2008) (accession code AP009351). Annealing

temperatures and secondary structures were verified using Thermo Scientific Multiple Primer Analyzer and Sigma Genosys DNA Calculator, available free online.

All primers used in this study were synthesised by LifeTechnologies Invitrogen Custom DNA Oligo service to include any necessary sequences and restriction sites as detailed by the manufacturers guidance for the relevant expression vectors (Table 2.2).

A PCR reaction was carried out using Phusion High Fidelity DNA Polymerase Master Mix according to manufacturer's instructions. Briefly, 160 ng Newman strain S. *aureus* genomic DNA (kindly provided by Angelika Grundling at Imperial College, London) was used as a template with 0.5 µM of the respective primers (Table 2.2) in a 50 µL reaction containing 3% DMSO. Initial denaturation was carried out at 98 °C for 3 min followed by 35 cycles (denaturation at 98 °C for 10 s, and annealing and extension for 1 min at 72 °C) and a final extension period at 72 °C for 10 min.

Agarose gel electrophoresis was used to confirm a single, discrete band of approximately 1900 bp in size consistent with the predicted product of 1822 bp.

5.2.5B TOPO cloning

Where appropriate, a Zero Blunt TOPO PCR cloning kit was used to capture the successful SCG PCR amplification. A TOPO cloning reaction containing 2 µL PCR reaction (Table 2.3) and 10 ng pCR – Blunt II-TOPO vector was incubated at room temperature for 5 min according to manufacturer's instructions. 5 µL of TOPO cloning reaction was added to one 50 µL vial of One Shot TOP10 chemically competent E. *coli* cells and incubated on ice for 30 min. The cells were heat shocked at 42 °C for 30 s, and returned to ice for 2 min before 250 µL SOC medium was added. The mixture was incubated for 60 min at 37 °C with shaking before 200 µL aliquots were plated on zeocin selective plates and incubated overnight at 37 °C.

5.2.5C Plasmid purification from E. coli

Plasmid constructs (Table 2.3) were isolated from 5 mL overnight cultures containing the selective antibiotic of transformed One Shot TOP10 cells using the QIAprep Spin Miniprep Kit manually or using the automated QIACUBE standard miniprep protocol according to manufacturer's instructions.

5.2.5D Restriction enzyme digestion

Restriction endonuclease digestion was used to confirm the presence of insert and to release inserts from construct ready for subcloning or cloning into expression vector. All restriction enzymes were FastDigest enzymes and digestion conditions set up according to manufacturer's recommendations.

Briefly, 500 ng DNA was incubated with 1 µL of each of the relevant restriction enzymes and 3 µL FastDigest reaction buffer in a 30 µl reaction for 15 min at 37 °C. 1 µg of the corresponding vector (Table 2.3) was digested with 2 µL of the appropriate restriction enzymes in a 30 µL reaction containing 3 µL FastDigest buffer for 15 min at 37°C according to manufacturer's instructions.

5.2.5E Agarose gel electrophoresis and gel extraction.

PCR products, restriction digests etc were visualised using agarose gel electrophoresis. Typically, E-Gel® CloneWell™ 0.8% SYBR Safe™ gel s and the E-Gel® iBase™ and Safe Imager system were used with DNA bands collected in nuclease free water via the collection wells. Alternatively, a 1% agarose gel was cast with 0.5x TBE buffer including Gel Red. DNA samples were loaded with Blue Juice loading buffer and visualised under UV light. Where necessary, required bands were isolated from the gel with a scalpel and purified using QIAquick gel extraction kit according to the manufacturer's instructions.

5.2.5F Determining DNA concentrations

In all instances, DNA concentrations were measured using a NanoDrop 2000 UV-Vis spectrophotometer.

5.2.5G DNA ligation and transformation of chemically competent E. coli

Ligation of the SCG insert and corresponding vector was performed using Rapid DNA ligation kit according to manufacturer's instructions. Typically 50 ng of digested vector was mixed with the required insert at a molar ratio of 1:3 in the presence of ligation buffer and Ligase for 5 min at 22 °C.

5 µL of ligation reaction was added to one 50 µL vial of One Shot TOP10 chemically competent E. *coli* cells and incubated on ice for 30 min. The cells were heat shocked at 42 °C for 30 s, and returned to ice for 2 min before 250 µl SOC medium was added. The mixture was incubated horizontally for 60 min at 37 °C with shaking before 200 µL aliquots were plated on LB agar plates containing 100 µg/mL ampicillin and incubated overnight at 37 °C.

5.2.5H Preparation and transformation of P. pastoris by electroporation.

A 50 mL conical flask containing 5 mL YPD media was inoculated with *P. pastoris* and incubated overnight at 30 °C with shaking. 500 µL of the overnight culture was used to inoculate a 500 mL culture held in a 2 L baffled flask which was grown overnight at 30 °C with shaking until an OD_{600} of 1.3 to 1.5 was achieved. The cells were centrifuged at 1500 xg for 5 min at 4 °C, and the pellet resuspended in 500 mL of sterile ice cold water (0 °C). Cells were centrifuged and resuspended a further 3 times, but in 250 mL sterile ice cold water and then 20 mL and 1 mL of 1M sorbitol, respectively. The final volume of cells were held on ice, and used immediately. 5 µg in 10 µL sterile water was mixed with 80 µL of the prepared cells in a 0.2 cm electroporation cuvette held on ice, for 5 min. Cells were pulsed on *P. pastoris* settings using a Bio-Rad Gene Pulser MXCell electroporation machine (Bio-Rad Laboratories INC, Hertfordshire, UK), and 1 mL of 1M sorbitol (ice cold) added immediately to the cuvette. The

cells were then transferred to sterile 15 mL tube and incubated at 30 °C, statically, for 1-2 hours. 10 – 200 µL were spread on YPD agar plates containing zeocin (100 µg/mL, 500 µg/mL or 1000 µg/mL) and incubated for up to 72 hours.

5.2.5I DNA sequencing

Purified plasmid DNA was sequenced by GATC Biotech (Constance, Germany) using sequencing primers (Table 5.4) designed according to specifications. The primers were designed to ensure sequencing of both strands. M13 primers, available in the lab, or aLICator sequencing primers provided in the aLICator expression kit, were included for sequencing of constructs. The results were aligned with source sequence and the sequence confirmed.

5.2.6 Cloning strategies for SCG constructs

5.2.6A Preparation of pE SUMOstar SCG and pY SUMOstar SCG

A PCR reaction containing primers A and B amplified SCG from S. *aureus* and a Zero Blunt TOPO PCR cloning kit captured the successful PCR product which was used to transform chemically competent *E. coli* as detailed above. TOPO-SCG constructs obtained via minipreps of overnight cultures of successful transformants were digested with BsmBI and XhoI to release the SCG insert. pE SUMOstar and pY SUMOstar were digested with BsmBI only. Ligation reactions containing the SCG insert and digested pE SUMOstar and pY SUMOstar vector were used to transform TOP10 cells. Successful pE SUMOstar constructs were purified from overnight cultures and used to transform T7 lysY cells ready for SCG expression.

5.2.6B Preparation of pGAP Z α SUMO SCG and transformation of P. pastoris

pY SUMOstar constructs were purified from overnight cultures of successful transformants. A restriction digest reaction with XhoI and XbaI was set up to obtain a SUMOstar SCG insert. XhoI and XbaI were also used to digest pGAPZ α vector isolated from E. *coli* glycerol stocks

provided by Craig Thelwell. A ligation reaction and transformation of chemically competent E. coli was performed and successful colonies used to make overnight cultures from which purified pGAPZ α SUMO SCG were obtained. Linearization of approx. 5 µg of construct was carried out via restriction digest with Avr II and used to transform competent P. *pastoris* cells by electroporation.

5.2.6C Preparation of aLICator SCG

A PCR reaction containing primers C and D amplified SCG from S. *aureus*, and confirmed by using the PCR product as a template to clone SCG with known primers. Overhangs were created on the successful purified PCR product by incubating 0.1 pmol PCR product with 1x LIC buffer, 1 µL of T4 DNA polymerase and nuclease free water in a 10 µL reaction according to manufacturer's instructions. The mixture was vortexed, centrifuged briefly, and incubated at room temp for 5 min before the reaction was stopped with the addition of 0.6 µL EDTA. 1 µL of the pLATE 51 vector was added to the mixture, vortexed and centrifuged briefly and held at room temp for 5 min to allow annealing to occur. The annealing mixture was used to transform chemically competent *E. coli* as detailed above. Successful transformants were purified from overnight cultures and used to transform T7 lysY cells ready for SCG expression. As part of the cloning strategy for using aLICator system with enterokinase cleavage, the SCG sequence checked to confirm that there were no enterokinase cleavage sites using REBASE, free online software from New England Biolabs.

Table 5.1 Description of the primers used for PCR amplification of SCG from genomic S. *aureus* DNA in this research.

Name	Description	Restriction sites	Corresponding vector	Sequence (5' to 3')
A	5' end from start of mature peptide	BsmBI	pE SUMOstar, pY SUMOstar	AACTACGTCTCAAGGTATAGTAACAAAGGATTATAGTGGGAAATCACAAGTTAATG
B	3' end to the stop codon	XhoI	pE SUMOstar, pY SUMOstar	AACTCGAGTTATTTTGTTACTCTAGGCCCATATGTCGCA
C	aLICator/EK	n/a	aLICator	GGTGATGATGATGACAAGATAGTAACAAAGGATTATAGTGGGAAATCACAAGTTAATG
D	aLICator/EK	n/a	aLICator	GGAGATGGGAAGTCATTATTTTGTTACTCTAGGCCCATATGTCGCA

Table 5.2 Description of the plasmids used in this research.

Plasmid Name	Source	Description or use	Antibiotic Resistance
pCR-Blunt II-TOPO	Invitrogen	PCR cloning vector	Kanamycin, Zeocin
pCR-Blunt II-TOPO SCG	Section 5.2.3-5.2.6	PCR cloning vector with SCG PCR product insert	Kanamycin, Zeocin
pE-SUMOstar	LifeSensors	Vector for T7 lac promoter based expression of SUMOstar fusion proteins in *E. coli*	Ampicillin
pE-SUMOstar SCG	Section 5.2.3-5.2.6	Vector construct for expression of N-terminal SUMOstar fusion of full-length SCG in *E. coli*	Ampicillin
pY-SUMOstar	LifeSensors	Vector for expression of SUMOstar fusion protein in *P. pastoris*	Zeocin
pY SUMOstar SCG	Section 5.2.3-5.2.6	Vector construct for expression of N-terminal SUMOstar fusion of full-length SCG in *P. pastoris*	Zeocin
pGAPZ α	Invitrogen	Vector for constitutive expression in *P. pastoris*	Zeocin
pGAPZ α SUMO SCG	Section 5.2.3-5.2.6	Vector construct for N-terminal SUMOstar fusion of full-length SCG in *P. pastoris* with constitutive expression	Zeocin
aLICator pLATE51	Thermo Scientific	Vector for expression of N-terminal 6xHis-tag proteins in *E. coli* with enterokinase recognition sites.	Ampicillin
aLICator pLATE51 SCG	Section 5.2.3-5.2.6	Vector construct for N-terminal 6xHis-tag full-length SCG in *E. coli* with enterokinase recognition site.	Ampicillin

Table 5.3 Sequencing primers used to confirm successful SCG vector constructs in this research.

Primer name	Primer sequence
Forward 1	GAGAGCACTGGATGATTTTC
Forward 2	GCCAGTAGTAAAAGAAGAG
Forward 3	GTGAATACAACGATGGAAC
Reverse 1	GCTTTATCTTCTTCTGCTGC
Reverse 2	GCTTTATCTTCTTCTGCTGC
Reverse 3	TTTGCATGTGTTGTTACG

5.2.7 Recombinant protein expression and purification

5.2.7A Expression of recombinant proteins in E. coli

Expression of recombinant SCG was attempted using the SUMOstar fusion tag system and the aLICator system according to the protocol used to express recombinant SK variants in section 2.2.2. However in this instance the binding buffer used for AKTA purification contained 20 mM imidazole.

5.2.7B Expression of recombinant proteins in P. pastoris

Expression of recombinant SCG was attempted using the SUMOstar fusion tag system for *P. pastoris.* 50 mL of YPD media was inoculated with an overnight culture from a successful transformant colony. Incubation was for up to 72 hours at 30 °C with shaking. 15 mL fractions of culture media was taken at 24, 48 and 72 hours and concentrated down to approx. 150 µL by 2x centrifugation in amicon tubes at 5000 x g for 20 min, at 4 °C. Concentrates were stored at -40 °C until analysis.

5.2.7C Cleavage of SUMOstar fusion tag with SUMOstar protease

Following dialysis overnight in 20 mM Tris-HCL, pH 8.0 containing 1.5 M NaCl), the SUMOstar fusion tag was cleaved using SUMOstar protease according to the manufacturer's protocol. Cleavage was attempted from 4 - 16 hours at 22 - 30°C in the presence of 2 - 5 mM DTT and was confirmed by SDS-PAGE. The SUMOstar tag and protease were bound to Ni-NTA agarose by mixing for 1 hour and the cleaved purified protein was recovered by filtration through an empty column.

5.2.7D Cleavage of His-tag with enterokinase

Protein eluates following AKTA purification were dialysed against 3 L cleavage buffer overnight. Cleavage of the N-terminal tag with enterokinase was attempted with 2-4 units at

room temperature over several time courses (4-16 hours) with and without the presence of DTT (0- 5 mM). rEK was removed with a capture kit according to manufacturer's instructions. The SCG prep was incubated with Ni-NTA agarose for 1 hour with mixing and ran through an empty column to bind and remove the cleaved HIS-tag.

5.2.8 SCG activity

5.2.8A SCG activity against S-2238, a chromogenic substrate for thrombin

A reaction containing 50 µL of the SCG prep following rEK cleavage and removal, prothrombin (final concentration 1.4 µM) and the chromogenic substrate for thrombin S-2238 (final concentration 0.24 mM), was carried out in Buffer A. Absorbance at 405 nm was measured on a SpectraMax M5 plate reader (Molecular Diagnostics) at 30 s intervals for 2 hours at 37 °C.

5.2.8B SCG activity against fibrinogen

A reaction containing 50 µL of the SCG prep following rEK cleavage and removel, prothrombin (final concentration 1.4 µM) and fibrinogen (final concentration 3 mg/mL) was set up in Buffer A. Absorbance at 405 nm was measured on a SpectraMax M5 plate reader (Molecular Diagnostics) at 30 s intervals for 2 hours at 37 °C.

5.3 Results

5.3.1 Expression and purification of SUMOstar fusion-tagged SCG

5.3.1A E. coli

Following on from the successful expression of SK variants (Chapter 2), the expression of SCG, another ZAAP, was attempted using the same SUMOstar fusion tag system. Successful cloning into the pE SUMOstar vector was verified by sequencing, and SDS-page gels demonstrated a band of an appropriate size (approx. 79 kDa) following the expression and purification strategy outlined in section 2.2.2 (Figure 5.1). As depicted in Figure 5.1 there are also several other bands, and at this stage it was not determined whether these were non-specific contaminants or possibly truncated SUMOstar SCG. Gel electrophoresis of the purified SCG with a native N-terminal sequence following attempts to cleave the SUMOstar tag, using the SUMOstar protease, could not detect any protein (not shown). This suggests that potentially SUMOstar SCG was not expressed. A band of the appropriate size (79 kDa) for uncleaved SCG was detected by gel electrophoresis of the protein bound to the Ni-NTA agarose used for purification of the SUMOstar tag and protease following cleavage attempts. This demonstrates that the protein was potentially expressed but cleavage conditions were not optimal (Figure 5.2).

SUMOstar protease activity has been shown to be protein specific. Cleavage of rSK H46a and rSK M1GAS in this project, which share 88.4% sequence homology, appeared to cleave at differing rates with rSK M1GAS cleavage taking approx. 4 hours, whilst rSK H46a required overnight incubation. To investigate whether the protein was expressed but insufficiently cleaved, increasing amounts of SUMOstar protease were trialled. DTT, which relaxes the protein structure by reducing disulphide bonds, was shown to be critical for SUMOstar protease cleavage of the SUMOstar tag for SK variants. As such, differing amounts of DTT were also attempted, as were a variety of cleavage times from 4 – 16 hours. SUMOstar

protease was also added in several stages to the prep, as there was some suggestion from optimisation of SK purification that the protease was inactivated after several hours.

The presence of multiple bands of a similar size all bound to the NiNTA-agarose, suggested perhaps the protein was being cleaved resulting in a series of truncated SUMOstar-tagged SCG proteins. To attempt to improve expression conditions, various strategies were employed. Alternative culture media, Magic Media and Terrific Broth, (both Thermo Scientific, Massachusetts, USA) were also used. Magic Media allows recombinant protein expression without the need for IPTG induction, whilst Terrific Broth is a rich media intended to improve cell density and growth. Induction was also attempted at 30 °C, as lower temperatures can reduce proteolytic cleavage during expression of sensitive proteins, and is recommended for Magic Media expression.

Incubation of the protein preps following SUMOstar protease cleavage attempts, with prothrombin and the thrombin chromogenic substrate, S-2238, could not detect any thrombin-like activity. This may be because the protein was not expressed, or because the SCG remained uncleaved and inactive as a SUMOstar fusion protein. Unfortunately, none of the conditions tried improved yields of purified protein, and it was not possible to detect a cleaved native N-terminal sequence full-length SCG using SDS-page.

Recombinant expression is specific to each individual protein, and it is very difficult to predict the optimal conditions for success. As such, the aLICator system for *E. coli*, an expression system which also enables preservation of the native N-terminal sequence in the final, purified protein was investigated alongside the SUMOstar strategies. This utilises a smaller, simpler N-terminal 6xHis tag for purification, and an alternative cleavage protease (enterokinase, rEK).

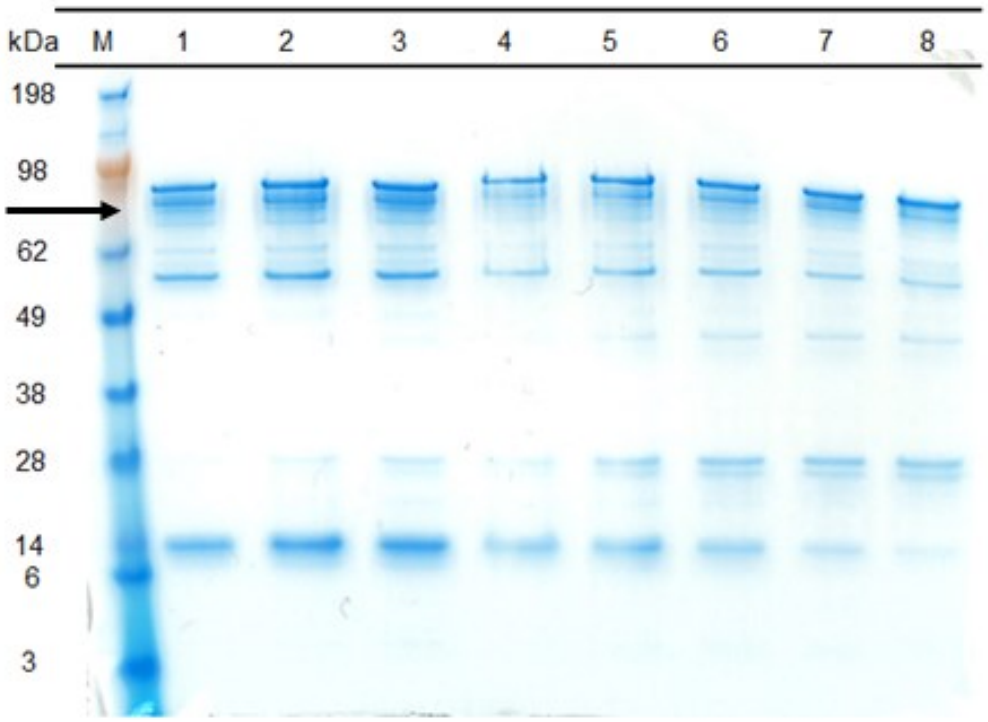

Figure 5.1 SDS-PAGE of SUMOstar SCG expression cultures following AKTA purification. SDS-page of 0.5 mL elution fractions (1-8) corresponding to a absorbance peak on the AKTApurifier chromatogram indicating protein detection. SCG expression cultures were run through a Ni-affinity column designed for purification of 6-His-tag bound recombinant proteins and eluted with an imidazole concentation gradient. The black arrow represents where a band of 79 kDa would run, representing the predicted weight of SUMOstar SCG.

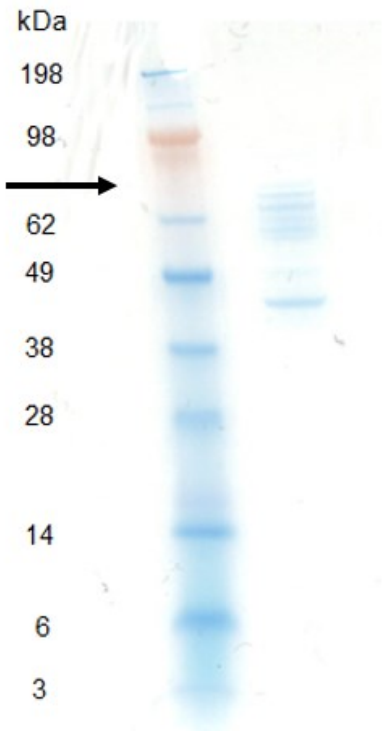

Figure 5.2 SDS-PAGE of proteins bound to Ni-NTA agarose following SUMOstar protease cleavage. Following Ni-affinity purification on an AKTApurifier, protein eluates were incubated with SUMOstar protease to allow cleavage of the SUMOstar tag from the SCG protein. The protein eluates were the incubated with Ni-NTA agarose and run through a blank sample to column to remove SUMOstar protease, cleaved SUMOstar tag and uncleaved SUMOstar-SCG protein. Proteins bound to the column were eluted with 300 mM imidazole and subjected to SDS-page. Black arrow indicates predicted size (79 kDa) of SUMOstar SCG protein indicating poor cleveage with SUMOstar protease.

5.3.1B P. pastoris

For SUMOstar tagged SCG expression in P. *pastoris*, successful cloning was also possible as determined by sequencing. An initial attempt at expression was conducted with 2 separate colonies, with a control (vector with no SCG) for comparison. Colony 1 was selected from a successful transformation plate containing 100 µg/mL zeocin. Colony 2 was selected from a successful transformation plate containing 500 µg/mL zeocin. Growth under higher antibiotic concentrations can be an indication that the plasmid DNA has integrated into multiple sites in the yeast genome during transformation, which can result in higher protein expression.

Aliquots of the cultures were collected at 24, 48 and 72 hours for analysis. As seen in Figure 5.3, gel electrophoresis of the culture media revealed an excess of proteins, so it was difficult to determine whether there was any difference between the control vector (no SCG) and the positive cultures. It was also difficult to conclude any differences in protein expression over the time course. As such, the culture supernatants were subjected to IMAC purification. Running the elution fractions through a gel revealed that there was no distinct band at 79 kDa, the expected size of the SUMOstar tagged SCG protein (Figure 5.4). Given that multiple strategies were pursued in parallel for this project, the optimisation of the expression of SUMOstar tagged SCG in P. *pastoris* was not continued beyond this point.

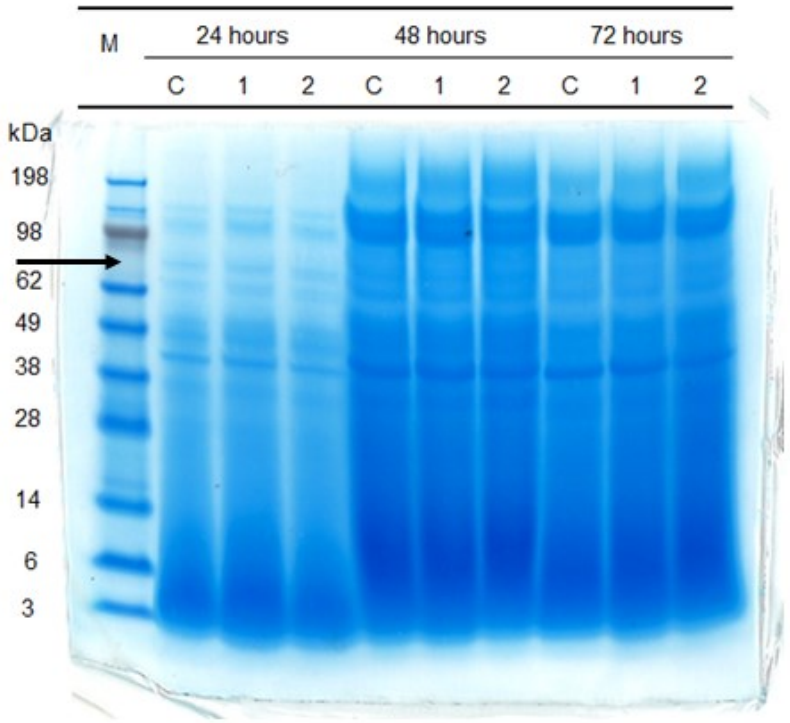

Figure 5.3 SDS-PAGE of SUMOstar SCG expression time course in *P. pastoris.* Culture samples were taken from a control vector only expression and two colonies which were successfully transformed with SUMOstar-SCG after 24, 48 and 72 hours expression at 30 °C. Black arrow indicates predicted band size of SUMOstar-SCG (79 kDa).

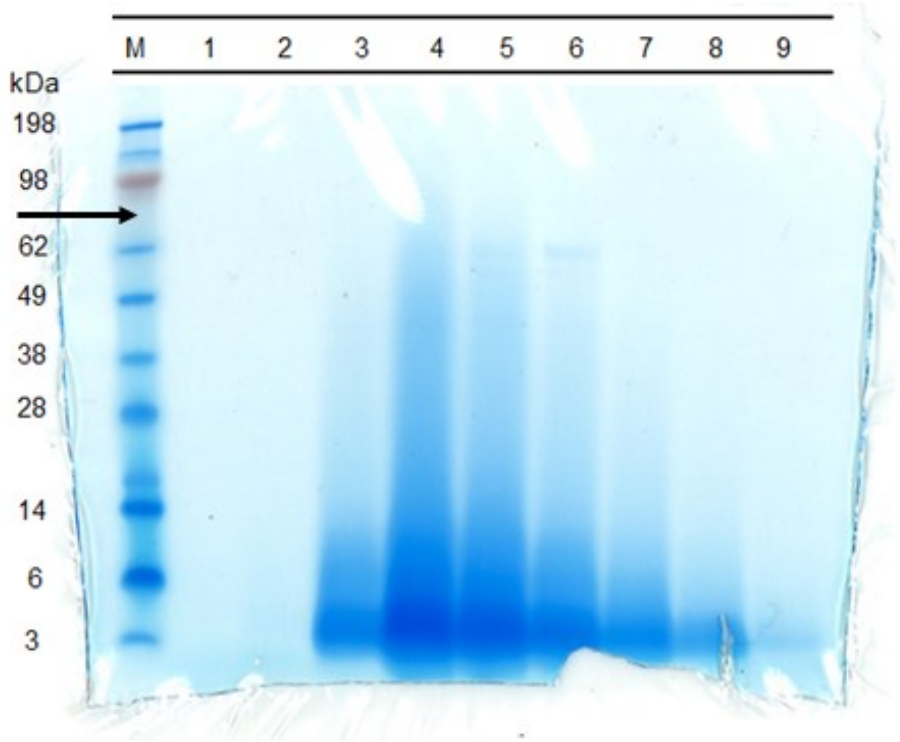

Figure 5.4 SDS-PAGE of SUMOstar SCG expression cultures from *P. pastoris* following AKTA purification using Ni-affinity. 0.5 ml elution fractions (1-9) corresponding to a peak on the AKTApurifier chromatogram indicating protein detection. Note the absences of a band at 79 kDa, the predicted weight of SUMOstar SCG, as indicated by the black arrow.

5.3.2 Optimising the expression and purification of recombinant SCG in E. *coli* using aLICator expression and rEK cleavage

As well as attempts to express SCG using a SUMOstar fusion tag in *E. coli* or *P. pastoris*, the aLICator system (Thermo Scientific) was explored as a potential alternative. This system allows purification *via* Ni-affinity chromatography utilising a 6xHis tag as with the SUMOstar systems, but cleavage of the N-terminal tag is achieved in this instance with enterokinase (rEK). This was a valuable approach to use alongside the SUMOstar systems given that the tag was much smaller, and therefore would offer different properties and restrictions to the fusion protein which may aid expression and correct protein folding. It may also alleviate the potential problem with truncations of SCG suspected in the E*. coli* expression of SUMOstar SCG. This is consistent with (McAdow et al., 2012) where a GST-fusion system was used to alleviate problems with protein degradation when a pET15b construct with a Strep tag was used.

Following IMAC purification on the AKTA purifier system, SDS page visualisation showed a strong band of the correct size for tagged SCG, 64 kDa (Figure 5.5). The samples were subjected to rEK cleavage; initially for 4 hours with DTT. The protease was removed and the cleavage preps were incubated with prothrombin and a chromogenic substrate for thrombin (S-2238), to determine whether any thrombin-like activity was detectable. As demonstrated in Figure 5.6., an increase in absorbance at 405 nm and therefore SCG activity could be detected in the presence of S-2238 and prothrombin, but not in control reactions (A) S-2238 alone, B) S-2238 + prothrombin only, C) S-2238 + SCG prep only D) uncleaved SCG prep).

Despite chromogenic activity, following 6xHis-tag cleavage and clean–up, visualisation of the purified SCG protein using SDS page was not possible; presumably due to low yield of cleaved protein (gel not shown).

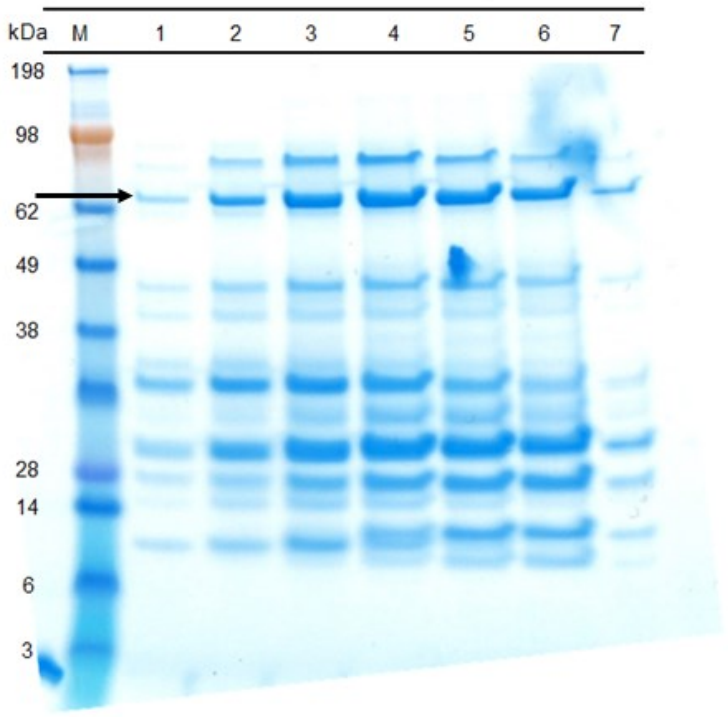

Figure 5.5 SDS-PAGE of aLICator SCG expression cultures following AKTA purification. 0.5 ml elution fractions (1-7) corresponding to a peak on the AKTApurifier chromatogram indicating protein detection. The band at 64 kDa corresponds to the predicted weight of aLICator SCG, indicated by the black arrow.

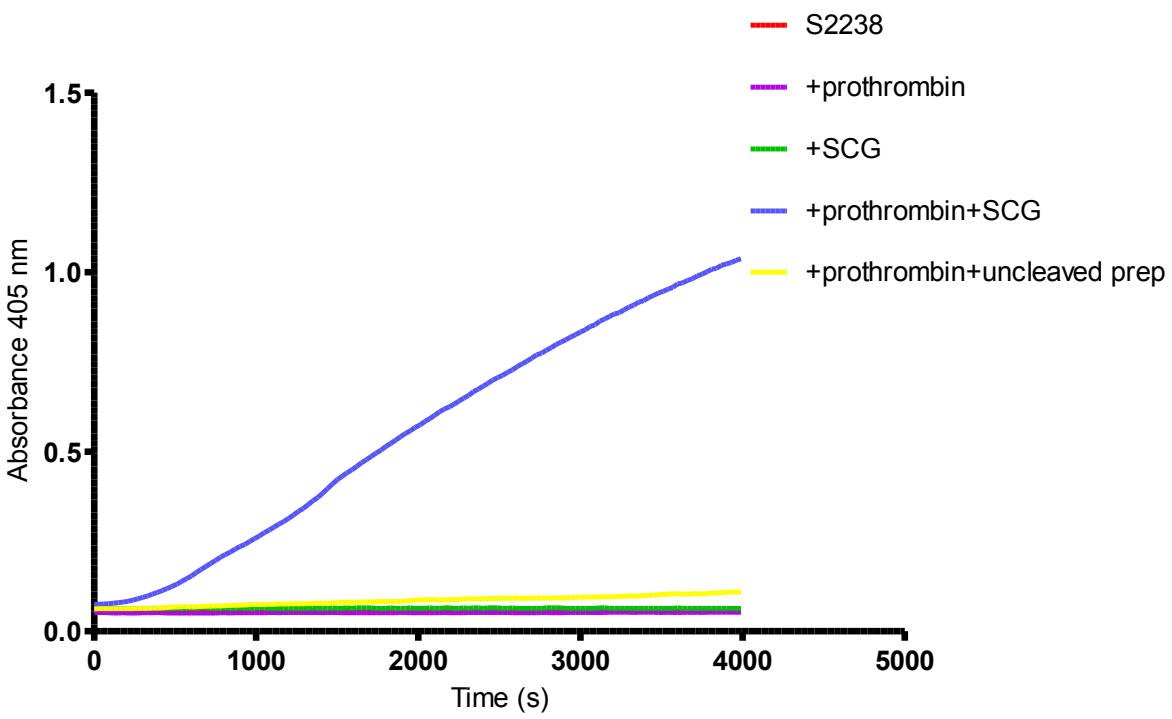

Figure 5.6 Chromogenic activity against S-2238 of an aLICator SCG protein prep following rEK cleavage. After tag cleavage with rEK, the aLICator SCG protein prep was incubated with prothrombin and S-2238, a chromogenic substrate for thrombin, and the absorbance of 405 nm measured to detect any SCG-like activity. S2238 was also incubated alone, with prothrombin, SCG, and prothrombin and the uncleaved prep as assay controls.

To attempt to optimise the 6xHis-tag cleavage and improve purified protein yields, a time course of rEK cleavage was employed. rEK was incubated with the SCG prep for 2, 4, 8 hours and overnight. Again, following removal of rEK, the samples were incubated with the chromogenic substrate S-2238 (Figure 5.7A) and also, in this instance, fibrinogen (Figure 5.7B). Here, around 4 hours was determined as optimal, with overnight resulting in a loss of activity. Once more though, SDS page analysis following clean-up did not reveal a band for the purified, cleaved SCG protein (gel not shown).

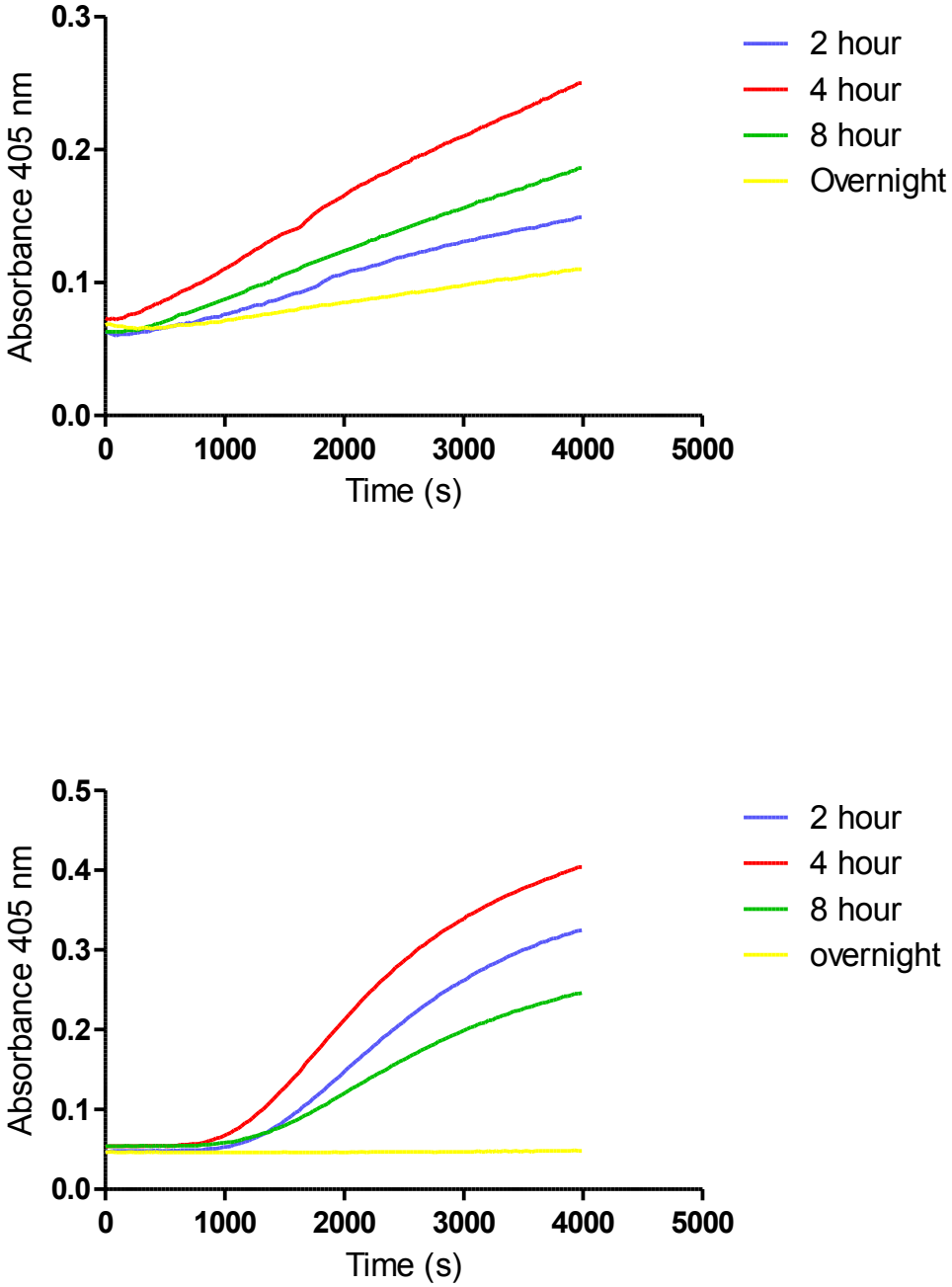

Figure 5.7 A time course of rEK cleavage of aLICator SCG as determined by activity against the chromogenic substrate S-2238 (top) and fibrinogen (bottom). To optimise the conditions of tag cleavage with rEK, a time course was set up. Samples were taken from the cleavage prep after 2, 4 and 8 hours as well as overnight, and the rEK removed. The prep was then incubated with prothrombin and S-2238 or fibrinogen to detect any thrombin-like activity.

5.4 Discussion

Despite several attempts, it was not possible to make a purified tag-free native N-terminal sequence SCG protein within the time frame of this project. The difficulties encountered with the expression strategies explored here could be attributed to cleavage of the N-terminal tags. The rSK variants H46a and M1GAS expressed using the SUMOstar system in this project share more than 88% sequence homology. Despite this, the efficiency of SUMOstar cleavage varied quite considerably. The SUMOstar tag appears to be susceptible to subtle differences in protein interactions, therefore it is perhaps not surprising that despite the system proving very successful for the expression of SK, it is seemingly not suitable for other ZAAP proteins, which share much less homology. There is a possibility that smaller, truncated SUMOstar-SCG proteins may have been produced in the *E.coli* system, suggested by multiple bands around the predicted size for SUMOstar-tagged SCG. Appropriate stains could be employed to determine whether the bands on the gel contained the 6xHis-tag and therefore are SUMO-SCG or a truncation.

Though optimising the conditions was attempted to a certain extent, more could be done with attention to timing, temperature and the ratio of protease to protein. Attempts to cleave the aLICator 6xHis-tag showed loss of SCG activity when the protein was subjected to overnight incubation with rEK. This suggests non-specific cleavage of the protein, even though the sequence was checked for rEK recognition sites, and therefore alternative restriction endonucleases may need to be explored.

The aLICator system was useful as the precut vector and rEK combination allowed the first codon of SCG to sit adjacent to the recognition sequence for rEK, which is also the point at which the protease cleaves. The unique SUMOstar protease also allows precise cleavage between the start of the protein of interest and the purification tag without leaving additional amino acids. Alongside the decision to attempt expression of SCG with the aLICator/rEK system following difficulties with the SUMOstar system, other vectors with alternative tags and cleavage approaches were considered. There are a large number of expression systems

which utilise N-terminal tags in addition to the SUMOstar and aLICator options explored in this work. However, the necessity to preserve the N-terminal Ile[1] residue in this instance, severely limits vector options. Many vectors utilise restriction sites to allow insertion of the gene of interest into the expression vector adjacent to the recognition sequence for protease cleavage, but this often leaves additional amino acids. Many proteases typically employed in recombinant protein expression cleave within the recognition sequence also leaving additional amino acid residues attached to the final protein product. Such examples include thrombin, FXa and PreScission (GE Healthcare). Given that that this work intended to understand SCG interaction with the haemostatic system, specifically prothrombin and thrombin to promote fibrin formation, the use of coagulation factors in the expression and purification process were avoided. Commercial capture and removal kits for FXa and thrombin are available, but complete capture can never be guaranteed, so these options were considered less rigorously than others.

C-terminal tags can be a useful alternative to N-terminal tags in many instances, but require the addition of an N-terminal methionine (Met) residue, or 'start' codon for protein translation. Cleavage of N-terminal 'Met' by bacterial enzymes in post- translational modifications is known to be inefficient and dependent on expression conditions such as temperature (Thelwell and Longstaff, 2014), therefore C-terminal tags are not a viable option for the expression of SCG with a native N-terminal sequence. Insufficient processing of N-terminal 'Met' residues would also be an issue with native, untagged SCG expression. The absence of a tag may or may not improve the expression of SCG. It also complicates the purification process, with reliance on techniques such as ion exchange chromatography, size exclusion chromatography, or potentially the more tailored, immobilised prothrombin, which would all require extensive optimisation.

A GST tag was used by (McAdow et al., 2012) to overcome SCG degradation during expression with alternatives including a pET15b/Strep tag system. Whilst the *E. coli* cells, used in this work are protease deficient, use of a GST tag or alternative expression strains could be

explored. There does not seem to be a GST tag vector system which allows conservation of the N-terminal sequence but mutagenesis could allow removal of extra bases to enable this as a viable option.

Chapter 6: Discussion

6.1 Streptokinase and thrombolytics

GCS S. *equisimilis* H46a SK has been used as a thrombolytic since 1980, and remains the most extensively used thombolytic worldwide (Armstrong and Collen, 2001). Scientific understanding of the mechanism is extensive but there has been no consideration for the properties of SK from other Streptococcal strains, such as GAS, until very recently. Even so, this new interest has been focused on the understanding of Streptococcal virulence, and there has also been little appreciation for the implications alternative SK variants could have for the therapeutic and its use in the treatment of myocardial infarction. This is the only mechanistic study to date comparing the mechanistic activity of GCS H46a SK with that of GAS SK from S. *pyogenes*, a cluster 2a M1 serotype strain. The work herein has demonstrated that MIGAS SK is stimulated by fibrinogen (Figure 2.5 and 2.7 and 2.8 as examples), and to an even greater extent fibrin (e.g. Figure 2.5 and Table 2.2). Furthermore, M1GAS SK displays characteristic similarities to the fibrin-specific physiological plasminogen activator, tPA, suggesting a similar template mechanism of action (Figure 2.6 and Figure 2.19). This discovery directly disputes one of the historically defining features of SK activation of plasminogen; a lack of fibrin specificity (Boyle and Lottenberg, 1997). This notion was based on studies which investigated H46a SK, used in the therapeutic for treatment of myocardial infarction, which displays no increase in activity in the presence of fibrinogen or fibrin, verified in Figure 2.5. Given the contrasting mechanisms of plasminogen activation demonstrated here between a single GCS and GAS SK, it is very likely there are many more SK variants with distinct mechanisms among Streptococci.

The fibrin-independent mechanism of H46a SK has contributed significantly to the historical direction of thrombolytic design (Armstrong and Collen, 2001). It was the pursuit of fibrin specificity, lacking in H46a SK and uPA, the first generation thrombolytics, and the associated bleeding complications that often ensued, that drove the development of the second

generation alternatives including Alteplase (recombinant tPA) (Verstraete, 2000). It is possible that had M1GAS SK been chosen in place of H46a SK originally, the course of thrombolytic development may be significantly different. Second generation thrombolytics exhibited fibrin binding domains and as such were perceived to offer more fibrin targeted plasminogen activation (Verstraete, 2000). The GUSTO trial, an international randomised trial to compare demonstrated improvements compared to SK for incidences of haemorrhagic stroke and mortality with Alteplase (Investigators, 1993), and Alteplase largely replaced the use of SK in developed nations. However, in reality second generation thrombolytics were not as successful as initially hoped, with bleeding complications such as intracranial haemorrhage still a serious concern (Armstrong and Collen, 2001). The short half life of tPA, and less than optimal fibrin specificity encouraged the development of thrombolytic design further. Fibrin targeted activity remained the apparent best option for thrombolytic enhancement and as such also governed some of the rationale behind third generation therapeutics (Verstraete, 2000). One such example includes tenectaplase, a recombinant deletion mutant tPA with increased fibrin specificity, PAI-1 resistance and plasma half life (Armstrong and Collen, 2001). However, despite significant effort, fibrin specificity in laboratory assays, never transferred well to *in vivo* results and severe bleeding complications such as intracranial haemorrhage remain a genuine concern even with the third generation therapeutics (Dundar et al., 2003).

There is an increasing incidence of cardiovascular disease in the developing world, and limited options for treatment (Feigin and Krishnamurthi, 2011). Due to the expense, tPA based thrombolytics not viable treatment options. SK is a cheaper and easily produced alternative that can be made in large quantities recombinantly with relatively inexpensive equipment (Thelwell, 2010, Thelwell and Longstaff, 2014, Butcher et al., 2013). Several trials have determined no benefit for the use of SK in the treatment of ischaemic stroke, but there remains support for further investigations into its use in ischaemic stroke to allow a cost-effective alternative for the developing world (Butcher et al., 2013, Feigin, 2007, Feigin and Krishnamurthi, 2011). SK variants, such as the fibrin-stimulated M1GAS SK in this project,

may offer more benefit than the current H46a SK, which exhibits no fibrin specificity, and could be explored as potential therapeutics. Furthermore, should a suitable alternative be identified, the nature of recombinant protein technology would enable movement to production of the new SK variant with minimal cost and effort.

Typically fibrin specificity can be thought of as the stimulation of plasminogen activators in the presence of fibrinogen or fibrin compared to in solution. However, it has also been proposed that perhaps a more accurate assessment of fibrin specificity would be to compare the stimulation of plasminogen activators by fibrin in comparison to fibrinogen, as this may determine more accurately the likelihood of systemic activation *in vivo* (Bringmann et al., 1995). Desmoteplase, by this definition exhibits good fibrin specificity, with significantly more activity in the presence of fibrin than fibrinogen (Bringmann et al., 1995). In this instance, M1GAS SK, and the fibrinogen stimulation it displays here (Figures 2.5 and 2.7 as examples), would not be a particularly good alternative for use as a fibrin targeted thrombolytic, as it would not be deemed truly fibrin specific. This does not discount the possibility that there may be many superior alternatives in the SK family with enhanced or 'true' fibrin specificity according to this definition. Perhaps exploring the mechanisms of other SK variants may provide some answers for rationale thrombolytic design to enhance targeted plasminogen activation, improve fibrin specificity and reduce unwanted bleeding complications.

Treatment for myocardial infarction has largely moved beyond plasminogen activators with PCI being more commonly used in developed countries (Armstrong et al., 2003). However, the only approved treatment available for stroke is Alteplase (Longstaff and Kolev, 2015). Despite this, there is significant concern about the safety of Alteplase, and there is a need for safer alternatives. Recently an expert working group investigation from the Medicines and Healthcare products Regulatory Agency (MHRA) was initiated to assess efficacy and safety of the drug, given the increasing evidence from clinical trials (Independent expert review concludes alteplase is safe and effective for use within existing treatment guidelines, 2015).

6.2 Streptokinase and bacterial virulence

Beginning to piece together the complexities of mechanistic differences between SK sheds new understanding on Streptococcal virulence. The SK from S. *pyogenes,* an M1 type Group A Streptococcal (GAS) strain displays a distinct plasminogen activation potential disparate from that of the SK S. *equisimilis,* a Group C streptococcal (GCS) strain, in the purified assay systems in this work. The key difference between rSK M1GAS and rSK H46a identified in this work is fibrin specificity, whereby rSK M1GAS demonstrates fibrin and fibrinogen localised activation. This is consistent with the expression of the fibrinogen receptor M1 on the bacterial cell surface (McArthur et al., 2008). Studies have demonstrated that M1, in particular its association with fibrinogen, has an important interplay with the haemostatic and innate immune systems. (Herwald et al., 2004) demonstrated that M1 binding with fibrinogen caused vascular leakage while work by (Macheboeuf et al., 2011) proposed an intricate association of M1 and fibrinogen molecules and demonstrated how it causes neutrophil activation. This compliments work that demonstates M1 binding of fibrinogen is involved in phagocytotic resistance (Anderson et al., 2014). It is also known that bacterial entrapment in fibrin clots by the human host is in part a result of FXIIIa cross-linking of the M1 protein to fibrin strands (Loof et al., 2011, Loof et al., 2012). Whilst this project has demonstrated that neither M1GAS SK nor H46a SK are affected directly by FXIIIa (see Figure 2.15), the interaction between fibrinogen, M1 and SK remains to be explored. Particularly, it would be interesting to determine the activation of plasminogen by rSK M1GAS in the presence of M1-bound fibrinogen to establish if that further modifies the mechanism, perhaps as binding of fibrin does compared to fibrinogen most apparent in Figures 2.5 and 2.13.

M1 is one of several fibrinogen binding M proteins. It has been demonstrated that different serotypes of fibrinogen-binding M proteins bind *via* unique sequences to promote Streptococcal survival in blood (Ringdahl et al., 2000, Sun, 2006). Understanding how other M protein fibrinogen binding mechanisms influence SK activity could shed further light on the

Streptococcal survival observed here, and may help to understand why M1 is considered the M protein most associated with invasive infection (Steer et al., 2009).

This work has focused on understanding the kinetics of rSK H46a and rSK M1GAS interaction with plasminogen and plasmin for the promotion of fibrinolysis, and proposed a kinetic model based on laboratory and simulated data with fibrinogen to make assumptions for the mechanism in the presence of fibrin (Figure 4.2). This is an extension to compliment previous published work by Bock *et al*, who proposed the "trigger and bullet" hypothesis for H46a SK activation of plasminogen (Boxrud et al., 2001, Boxrud and Bock, 2004, Boxrud et al., 2004, Nolan et al., 2013).

Both GCS and GAS are capable of producing the same breadth of infections in humans but it is GAS that are more commonly isolated in invasive infections (Ekelund et al., 2005, Cole et al., 2011). It seems possible that the differences in fibrin specificity between the GCS and GAS SK demonstrated in this thesis could at least in part explain the differences in pathogenicity; forming part of the necessary steps for establishing invasive disease. Specifically, it is possible to perceive that fibrin(ogen) specificity demonstrated by rSK M1GAS here would be greatly advantageous in escaping the fibrin clot in order to establish systemic infection.

Plasminogen is abundant in the blood, and aside from plasminogen activators, GAS bacteria employ the use of several plasminogen binding receptors to promote their survival in the human host. Cluster 2b GAS express the cell surface molecule PAM which is shown to increase pericellular plasmin generation and bacterial virulence (Ringdahl et al., 1998, Sun et al., 2004), while cluster 1 GAS display the antiphagocytic GAPDH and SEN plasminogen binding receptors (Sun, 2006). Cluster 1 bacteria, typically isolated in pharyngeal infections, demonstrate higher solution SK activity than PAM expressing cluster 2b bacteria, the isolate commonly associated with skin infections. Work by (Zhang et al., 2012, Zhang et al., 2013) have begun to link these functional differences with structural differences, particularly in the β domain to better understand the distinct tissue tropism and virulence of GAS strains.

The findings in this work with regard to the mechanism of plasminogen activation by SK from pathogenic M1GAS bacteria complement an extensive body of research with regard to GAS and the importance of plasminogen in establishing infection. Work with transgenic mice with human plasminogen has demonstrated that SK is critical for GAS infection (Sun et al., 2004).

The use of plasminogen is apparent throughout bacterial virulence. As mentioned before it is a key feature in Y. *pestis*, responsible for the bubonic plaque (Degen et al., 2007). Furthermore*, Borrelia burgdorferi*, responsible for Lyme disease, express the plasminogen binding receptor lipoprotein A on its cell surface, which enhances plasmin generation by physiological plasminogen activators uPA and tPA (Fuchs et al., 1994). A plasminogen knockout mouse model determined that host plasminogen was necessary for B. *burgdorferi* dissemination within the tick vector, and contributed to the establishment of disease within the host (Coleman et al., 1997).

This work has focused on understanding the kinetics of rSK H46a and rSK M1GAS interaction with plasminogen and plasmin for the promotion of fibrinolysis, determining that rSK M1GAS is fibrin(ogen)-targeted. However, plasmin is a broad specificity protease, and its other substrates include the extracellular matrix, matrix metalloproteases and complement proteins (Lambris et al., 2008). Little attention has been paid to how SK binding of plasminogen and plasmin, to promote plasmin generation and alter protease function, could affect the activation of these substrates as well as the role this could play on bacterial virulence. An important part of innate mammalian immunity against invading pathogens is the complement cascade. As such, many bacteria have evolved means by which to evade this defence system, which has been comprehensively reviewed by (Lambris et al., 2008). In particular, S. *aureus* has been shown to promote the degradation of C3b and IgG through SAK plasmin generation (Lahteenmaki et al., 2001). It would be interesting to further our understanding of the role of SK in bacterial virulence by investigating the influence it has on the proteolysis of plasmin substrates, and if again a difference is seen for GAS and GCS variants, such as the fibrin stimulation seen by GAS SK in this work.

Understanding the mechanisms of bacterial virulence factors and their interaction with the human coagulation and fibrinolysis systems can enhance understanding of pathogenesis and identify potential new targets for antimicrobial action. The development of new antimicrobial technologies is an increasing pressing need, as demonstrated by incentives such as the Longitude prize which offers £10 million in funding for better diagnostic tests to ensure more effective use of antimicrobial agents (*Longitude Prize Open*, 2015). Microbial resistance to current antibiotics is increasing, and it is predicted that 10 million people could die every year by 2050, from infections caused by resistant microbial strains if no significant developments are made (O'Neill, 2014). Studies such as this, which provide detailed molecular understanding of the interplay between bacterial virulence factors and host proteins, could provide rationale for antimicrobial therapies. This work has demonstrated the fibrin specificity of the plasminogen activation by SK from S. *pyogenes*, commonly isolated from invasive infections (Ekelund et al., 2005, Steer et al., 2009). Interupting this interaction with fibrinogen, critical for M1GAS SK activity, could be a possible way of reducing the invasive potential of S. *pyogenes* to treat infection.

It is important to be aware that *in vitro* data from purified assay systems does not always correlate well with the effect in living organisms. This is evident with the lack of success seen with the fibrin-targeted activity of second and third generation thrombolytics *in vivo,* despite laboratory assays demonstrating fibrin specificity for tPA, recombinant mutants and desmoteplase (Verstraete, 2000). Therefore there is always a possibility that the mechanism of M1GAS SK identified in this project could simply be an artefact in a far more elaborate story.

6.3 Staphylocoagulase

Though generation of a full-length native N-terminal sequence SCG protein was not feasible within the timeframe of this project, the need to further understand the mechanism of SCG activation of prothrombin is still a valuable aim. S. *aureus* expresses the plasminogen activator SAK, which serves to breakdown fibrin and the prothrombin activator SCG, which promotes

fibrin formation. There is currently no clear understanding why one bacterial strain would gain advantage from employing two seemingly opposing mechanisms.

SCG is present in several Staphylococcal strains, which display a degree of genetic diversity and evolutionary disparity as described for SK. M1GAS SK and H46a SK share over 88.4 % sequence homology, yet this work has shown they display remarkably different mechanisms at the molecular level. It would interesting to investigate whether SCG variants offer mechanistic variations too. The benefit of plasminogen activators is apparent if the need is to escape the confines of a fibrin clot, in order to avoid neutrophils and their defence mechansisms such as neutrophil extracellular trap's (NET's), and establish invasive disease (Varju et al., 2015). Whereas, if the aim is to remain inconspicuous whilst travelling throughout the host with the intent to establish systemic infection, an invisibility shield of host fibrinogen/fibrin would prove valuable. One hypothesis regarding the role of staphylothrombin in pathogen invasion is as a protective coat to avoid detection by the host immune system (McAdow et al., 2012). As such, the need to effectively bind and cleave fibrinogen within close vicinity of the cell surface with a prothrombin activator, SCG, is understandable. It is also known that fibrinogen and SCG are critical component of abscess formation (Cheng et al., 2009, Cheng et al., 2010, Cheng et al., 2011). This work has revealed that the fibrinogen network and SCG is generally at the host interface, further suggesting it is a protective feature. However, at a certain point, the breakdown of the abscess is essential to further promote infection, so it is possible that SAK plays a role here, breaking down the staphylothrombin product.

6.4 Future work

6.3.1 Streptokinase

The model made in this work to explain the mechanism of M1GAS SK was derived in part from laboratory data, and in part from values taken from the literature. These numbers are unlikely to be completely representative of the assay conditions employed here, or the

specifics of the SK from S. *pyogenes*. Improvements could therefore be made to this work by conducting further experiments such as determining true binding kinetics with Biacore technologies, such as work carried out by (Cole et al., 2011). As mentioned earlier, this work looks at the simpler binding of fibrinogen and uses this understanding to make assumptions about fibrin interactions. Recently, work with tPA and fibrin has been carried out and similar efforts could be made with SK variants (Bannish et al., 2014b, Bannish et al., 2014a). Soluble fibrin analogues such as chloramine T or cyanogen bromide treated fibrinogen could also be used in purified assay systems such as in this study to further probe the difference in fibrin and fibrinogen stimuolation of M1GAS SK activation of plasminogen (Stief et al., 2001).

Alongside the expression attempts for SCG, initial cloning work was done to produce fluorescent rSK M1GAS. This work was not completed within the time frame of the project, but the aim was to generate yellow fluorescent protein (YFP) recombinant M1GAS SK and use confocal microscopy to visualise the interaction and distribution of SK within fibrin clots, in a manner similar to work with tPA (Longstaff et al., 2011).

The decision to investigate the mechanism of M1GAS SK from cluster 2a in this project was made because it is generally considered to be the most significant streptococcal variant with regard to human invasive disease (Cole et al., 2011, Ekelund et al., 2005). There is however a lot of merit in studying SK from other clusters or even more variants within cluster 2a. This may bring to light other interesting mechanistic variations, and provide rationale for improvements to thrombolytic therapies and antimicrobial technologies.

6.3.2 Staphylocoagulase

Successful expression of a full-length native N-terminal sequence SCG would need to occur to enable any mechanistic exploration. Should recombinant systems not allow this, an increasingly affordable option is to have the peptide construct synthesized, and would have been investigated if time had allowed. Kinetic studies similar those employed for the investigation of SK in this project could be used for SCG activation of prothrombin. Comparing

staphylothrombin fibrin formation with physiological fibrin formation initiated by thrombin may shed some understanding on the structure of the bacterial fibrin product.

Of further interest would be the fibrinolysis of the staphylothrombin product by both physiological plasminogen activators, tPA and uPA, as well as bacterial plasminogen activators, SK and SAK. It could be that the fibrin is more suited to SAK and SK mechanisms, and resistant to physiological hydrolysis, but there have been no studies specifically comparing the fibrinolysis mechanisms of each plasminogen activator. It would also be valuable to compare fibrin formation by SCG to that of snake enzymes, which exhibit thrombin-like activity. Examples include batroxabin and ancrod isolated from pit vipers. These snake enzymes make an easily digestible fibrin product, by unique cleavage of fibrinogen to promote fibrin formation, in order to deplete the host of fibrinogen and induce bleeding (Swenson and Markland, 2005, Markland, 1998).

References

Akima, H. 1978. A Method of Bivariate Interpolation and Smooth Surface Fitting for Irregularly Distributed Data Points. ACM Transactions on Mathematical Software (TOMS).

Anderson, E. L., Cole, J. N., Olson, J., Ryba, B., Ghosh, P. and Nizet, V. (2014) 'The Fibrinogen-binding M1 Protein Reduces Pharyngeal Cell Adherence and Colonization Phenotypes of M1T1 Group A Streptococcus', *Journal of Biological Chemistry,* 289(6), pp. 3539-3546.

Armstrong, P. W. and Collen, D. (2001) 'Fibrinolysis for acute myocardial infarction - Current status and new horizons for pharmacological reperfusion, Part 1', *Circulation,* 103(23), pp. 2862-2866.

Armstrong, P. W., Collen, D. and Antman, E. (2003) 'Fibrinolysis for acute myocardial infarction - The future is here and now', *Circulation,* 107(20), pp. 2533-2537.

Baba, T., Bae, T., Schneewind, O., Takeuchi, F. and Hiramatsu, K. (2008) 'Genome sequence of Staphylococcus aureus strain newman and comparative analysis of staphylococcal genomes: Polymorphism and evolution of two major pathogenicity islands', *Journal of Bacteriology,* 190(1), pp. 300-310.

Baneyx, F. and Mujacic, M. (2004) 'Recombinant protein folding and misfolding in Escherichia coli', *Nature Biotechnology,* 22(11), pp. 1399-1408.

Bannish, B. E., Keener, J. P. and Fogelson, A. L. (2014a) 'Modelling fibrinolysis: a 3D stochastic multiscale model', *Mathematical Medicine and Biology-a Journal of the Ima,* 31(1), pp. 17-44.

Bannish, B. E., Keener, J. P., Woodbury, M., Weisel, J. W. and Fogelson, A. L. (2014b) 'Modelling fibrinolysis: 1D continuum models', *Mathematical Medicine and Biology-a Journal of the Ima,* 31(1), pp. 45-64.

Bean, R. R., Verhamme, I. M. and Bock, P. E. (2005) 'Role of the streptokinase alpha-domain in the interactions of streptokinase with plasminogen and plasmin', *Journal of Biological Chemistry,* 280(9), pp. 7504-7510.

Bergmann, S. and Hammerschmidt, S. (2008) 'Fibrinolysis and Host Response in Bacterial Infections', *Progress and Challenges in Transfusion Medicine, Hemostasis and Hemotherapy: State of the Art 2008*, pp. 71-88.

Bhattacharya, S., Ploplis, V. A. and Castellino, F. J. (2012) 'Bacterial Plasminogen Receptors Utilize Host Plasminogen System for Effective Invasion and Dissemination', *Journal of Biomedicine and Biotechnology,* 2012, pp. 482096.

Bisno, A. L., Brito, M. O. and Collins, C. M. (2003) 'Molecular basis of group A streptococcal virulence', *Lancet Infectious Diseases,* 3(4), pp. 191-200.

Bode, W. and Huber, R. (1976) 'Induction of the bovine trypsinogen-trypsin transition by peptides sequentially similar to the N-terminus of trypsin.', *FEBS Lett,* 68(2), pp. 231-6.

Boxrud, P. D. and Bock, P. E. (2000) 'Streptokinase binds preferentially to the extended conformation of plasminogen through lysine binding site and catalytic domain interactions', *Biochemistry,* 39(45), pp. 13974-13981.

Boxrud, P. D. and Bock, P. E. (2004) 'Coupling of conformational and proteolytic activation in the kinetic mechanism of plasminogen activation by streptokinase', *Journal of Biological Chemistry,* 279(35), pp. 36642-36649.

Boxrud, P. D., Fay, W. P. and Bock, P. E. (2000) 'Streptokinase binds to human plasmin with high affinity, perturbs the plasmin active site, and induces expression of a substrate recognition exosite for plasminogen', *Journal of Biological Chemistry,* 275(19), pp. 14579-14589.

Boxrud, P. D., Verhamme, I. M. and Bock, P. E. (2004) 'Resolution of conformational activation in the kinetic mechanism of plasminogen activation by streptokinase', *Journal of Biological Chemistry,* 279(35), pp. 36633-36641.

Boxrud, P. D., Verhamme, I. M. A., Fay, W. P. and Bock, P. E. (2001) 'Streptokinase triggers conformational activation of plasminogen through specific interactions of the amino-terminal sequence and stabilizes the active zymogen conformation', *Journal of Biological Chemistry,* 276(28), pp. 26084-26089.

Boyle, M. D. P. and Lottenberg, R. (1997) 'Plasminogen activation by invasive human pathogens', *Thrombosis and Haemostasis,* 77(1), pp. 1-10.

Bringmann, P., Gruber, D., Liese, A., Toschi, L., Kratzschmar, J., Schleuning, W. D. and Donner, P. (1995a) 'Structural features mediating fibrin selectivity of vampire bat pasminogen activators', *Journal of Biological Chemistry,* 270(43), pp. 25596-25603.

Bugge, T. H., Flick, M. J., Danton, M. J. S., Daugherty, C. C., Romer, J., Dano, K., Carmeliet, P., Collen, D. and Degen, J. L. (1996) 'Urokinase-type plasminogen activator is effective in fibrin clearance in the absence of its receptor or tissue-type plasminogen activator', *Proceedings of the National Academy of Sciences of the United States of America,* 93(12), pp. 5899-5904.

Butcher, K., Shuaib, A., Saver, J., Donnan, G., Davis, S. M., Norrving, B., Wong, K. S. L., Abd-Allah, F., Bhatia, R. and Khan, A. (2013) 'Thrombolysis in the developing world: is there a role for streptokinase?', *International Journal of Stroke,* 8(7), pp. 560-565.

Cesarman-Maus, G. and Hajjar, K. A. (2005) 'Molecular mechanisms of fibrinolysis', *British Journal of Haematology,* 129(3), pp. 307-321.

Chapin, J. C. and Hajjar, K. A. (2015) 'Fibrinolysis and the control of blood coagulation', *Blood Reviews,* 29(1), pp. 17-24.

Cheng, A. G., DeDent, A. C., Schneewind, O. and Missiakas, D. (2011) 'A play in four acts: Staphylococcus aureus abscess formation', *Trends in Microbiology,* 19(5), pp. 225-232.

Cheng, A. G., Kim, H. K., Burts, M. L., Krausz, T., Schneewind, O. and Missiakas, D. M. (2009) 'Genetic requirements for Staphylococcus aureus abscess formation and persistence in host tissues', *Faseb Journal,* 23(10), pp. 3393-3404.

Cheng, A. G., McAdow, M., Kim, H. K., Bae, T., Missiakas, D. M. and Schneewind, O. (2010) 'Contribution of Coagulases towards Staphylococcus aureus Disease and Protective Immunity', *Plos Pathogens,* 6(8).

Chibber, B. A. K., Morris, J. P. and Castellino, F. J. (1985) 'Effects of human-fibrinogen and its celavage products on activation of human-plasminogen by streptokinase', *Biochemistry,* 24(14), pp. 3429-3434.

Clemetson, K. J. (2012) 'Platelets and Primary Haemostasis', *Thrombosis Research,* 129(3), pp. 220-224.

Cole, J. N., Barnett, T. C., Nizet, V. and Walker, M. J. (2011) 'Molecular insight into invasive group A streptococcal disease', *Nature Reviews Microbiology,* 9(10), pp. 724-736.

Cole, J. N., McArthur, J. D., McKay, F. C., Sanderson-Smith, M. L., Cork, A. J., Ranson, M., Rohde, M., Itzek, A., Sun, H. M., Ginsburg, D., Kotb, M., Nizet, V., Chhatwal, G. S. and Walker, M. J. (2006) 'Trigger for group A streptococcal M1T1 invasive disease', *Faseb Journal,* 20(10), pp. 1745-+.

Coleman, J. L., Gebbia, J. A., Piesman, J., Degen, J. L., Bugge, T. H. and Benach, J. L. (1997) 'Plasminogen is required for efficient dissemination of B-burgdorferi in ticks and for enhancement of spirochetemia in mice', *Cell,* 89(7), pp. 1111-1119.

Collen, D. and Lijnen, H. R. (1991) 'Basic and clinical aspects of fibrinolysis and thrombolysis', *Blood,* 78(12), pp. 3114-3124.

Collen, D. and Lijnen, H. R. (2005) 'Thrombolytic agents', *Thrombosis and Haemostasis,* 93(4), pp. 627-630.

Cook, S. M., Skora, A., Gillen, C. M., Walker, M. J. and McArthur, J. D. (2012) 'Streptokinase variants from Streptococcus pyogenes isolates display altered plasminogen activation characteristics - implications for pathogenesis', *Mol Microbiol,* 86(5), pp. 1052-62.

D'Costa, S. S. and Boyle, M. D. P. (2000) 'Interaction of group A streptococci with human plasmin(ogen) under physiological conditions', *Methods-a Companion to Methods in Enzymology,* 21(2), pp. 165-177.

Davie, E. W. (2003) 'JBC Centennial 1905-2005 - 100 years of biochemistry and molecular biology - A brief historical review of the waterfall/cascade of blood coagulation', *Journal of Biological Chemistry,* 278(51), pp. 50819-50832.

Davie, E. W. and Ratnoff, O. D. 1964. Waterfall Sequence for Intrinsic Blood Clotting. Science.

DeDent, A., Kim, H. K., Missiakas, D. and Schneewind, O. (2012) 'Exploring Staphylococcus aureus pathways to disease for vaccine development', *Seminars in Immunopathology,* 34(2), pp. 317-333.

Degen, J. L., Bugge, T. H. and Goguen, J. D. (2007) 'Fibrin and fibrinolysis in infection and host defense', *Journal of Thrombosis and Haemostasis,* 5, pp. 24-31.

Dundar, Y., Hill, R., Dickson, R. and Walley, T. (2003) 'Comparative efficacy of thrombolytics in acute myocardial infarction: a systematic review', *Qjm-an International Journal of Medicine,* 96(2), pp. 103-113.

Duval, C., Allan, P., Connell, S. D. A., Ridger, V. C., Philippou, H. and Ariens, R. A. S. (2014) 'Roles of fibrin alpha- and gamma-chain specific cross-linking by FXIIIa in fibrin structure and function', *Thrombosis and Haemostasis,* 111(5), pp. 842-850.

Ekelund, K., Skinhoj, P., Madsen, J. and Konradsen, H. B. (2005) 'Invasive group A, B, C and G streptococcal infections in Denmark 1999-2002: epidemiological and clinical aspects', *Clinical Microbiology and Infection,* 11(7), pp. 569-576.

Europe, C. o. (2008a) *Chapter 5.3 Statistical analysis of results of biological assays and tests. European Pharmacopoeia* 7th edn. Strasbourg, France: EDQM.

Europe, C. o. (2008b) *Streptokinase bulk solution. European Pharmacopoeia* Strasbourg, France: EDQM.

Feigin, V. L. (2007) 'Stroke in developing countries: can the epidemic be stopped and outcomes improved?', *Lancet Neurology,* 6(2), pp. 94-97.

Feigin, V. L. and Krishnamurthi, R. (2011) 'Stroke Prevention in the Developing World', *Stroke,* 42(12), pp. 3655-3658.

Fersht, A. (1984) *Enzyme Structure and Mechanism.* 2nd edn. New York: W.H.Freeman & Co Ltd2nd.

Fraser, S. R., Booth, N. A. and Mutch, N. J. (2011) 'The antifibrinolytic function of factor XIII is exclusively expressed through alpha(2)-antiplasmin cross-linking', *Blood,* 117(23), pp. 6371-6374.

Friedrich, R., Panizzi, P., Fuentes-Prior, P., Richter, K., Verhamme, I., Anderson, P. J., Kawabata, S. I., Huber, R., Bode, W. and Bock, P. E. (2003) 'Staphylocoagulase is a

prototype for the mechanism of cofactor-induced zymogen activation', *Nature,* 425(6957), pp. 535-539.

Friedrich, R., Panizzi, P., Kawabata, S. I., Bode, W., Bock, P. E. and Fuentes-Prior, P. (2006) 'Structural basis for reduced staphylocoagulase-mediated bovine prothrombin activation', *Journal of Biological Chemistry,* 281(2), pp. 1188-1195.

Fuchs, H., Wallich, R., Simon, M. M. and Kramer, M. D. (1994) 'The outer surface protein-A of the spirochete *Borrelia burgdorferi* is a plasmin(ogen) receptor', *Proceedings of the National Academy of Sciences of the United States of America,* 91(26), pp. 12594-12598.

Gladysheva, I. P., Turner, R. B., Sazonova, I. Y., Liu, L. and Reed, G. L. (2003) 'Coevolutionary patterns in plasminogen activation', *Proceedings of the National Academy of Sciences of the United States of America,* 100(16), pp. 9168-9172.

Gonzalez-Gronow, M., Siefring, G. E. and Castellino, F. J. (1978) 'Mechanism of activation of human plasminogen by activator complex, streptokinase.plasmin', *Journal of Biological Chemistry,* 253(4), pp. 1090-1094.

Guggenberger, C., Wolz, C., Morrissey, J. A. and Heesemann, J. (2012) 'Two Distinct Coagulase-Dependent Barriers Protect Staphylococcus aureus from Neutrophils in a Three Dimensional in vitro Infection Model', *Plos Pathogens,* 8(1).

Hendrix, H., Lindhout, T., Mertens, K., Engels, W. and Hemker, H. C. (1983) 'Activation of human-thrombin by stoichiometric levels of staphylocoagulase', *Journal of Biological Chemistry,* 258(6), pp. 3637-3644.

Henschen, A., Lottspeich, F., Kehl, M. and Southan, C. (1983) 'Covalent structure of fibrinogen', *Annals of the New York Academy of Sciences,* 408(JUN), pp. 28-43.

Herwald, H., Cramer, H., Morgelin, M., Russell, W., Sollenberg, U., Norrby-Teglund, A., Flodgaard, H., Lindbom, L. and Bjorck, L. (2004) 'M protein, a classical bacterial virulence determinant, forms complexes with fibrinogen that induce vascular leakage', *Cell,* 116(3), pp. 367-379.

Herwald, H., Morgelin, M., Dahlback, B. and Bjorck, L. (2003) 'Interactions between surface proteins of Streptococcus pyogenes and coagulation factors modulate clotting of human plasma', *Journal of Thrombosis and Haemostasis,* 1(2), pp. 284-291.

Hethershaw, E. L., La Corte, A. L. C., Duval, C., Ali, M., Grant, P. J., Ariens, R. A. S. and Philippou, H. (2014) 'The effect of blood coagulation factor XIII on fibrin clot structure and fibrinolysis', *Journal of Thrombosis and Haemostasis,* 12(2), pp. 197-205.

Hijikata-Okunomiya, A. and Kataoka, N. (2003) 'Argatroban inhibits staphylothrombin', *Journal of Thrombosis and Haemostasis,* 1(9), pp. 2060-2061.

Horrevoets, A. J. G., Smilde, A. E., Fredenburgh, J. C., Pannekoek, H. and Nesheim, M. E. (1995) 'The activation-resistant conformation of recombinant human plasminogen is stabilized by basic residues in the amino-terminal hinge region', *Journal of Biological Chemistry,* 270(26), pp. 15770-15776.

Huang, T. T., Malke, H. and Ferretti, J. J. (1989) 'Heterogeneity of the streptokinase gene in group-A streptococci', *Infection and Immunity,* 57(2), pp. 502-506.

Independent expert review concludes alteplase is safe and effective for use within existing treatment guidelines. 2015. Medicine and Healthcare products Regulatory Agency.

Investigators, T. G. (1993) 'An international randomized trial comparing four thrombolytic strategies for acute myocardial infarction. The GUSTO investigators', *The New England journal of medicine,* 329(10), pp. 673-82.

Johansson, L., Thulin, P., Low, D. E. and Norrby-Teglund, A. (2010) 'Getting under the Skin: The Immunopathogenesis of Streptococcus pyogenes Deep Tissue Infections', *Clinical Infectious Diseases,* 51(1), pp. 58-65.

Kawabata, S. I., Morita, T., Miyata, T., Kaida, S., Igarashi, H. and Iwanaga, S. (1986) 'Difference in enzymatic-properties between staphylohrombin and free alpha-thrombin', *Annals of the New York Academy of Sciences,* 485, pp. 27-40.

Khil, J., Im, M., Heath, A., Ringdahl, U., Mundada, L., Engleberg, N. C. and Fay, W. P. (2003) 'Plasminogen enhances virulence of group A streptococci by streptokinase-dependent and streptokinase-independent mechanisms', *Journal of Infectious Diseases,* 188(4), pp. 497-505.

Kunamneni, A., Abdelghani, T. T. A. and Ellaiah, P. (2007) 'Streptokinase - the drug of choice for thrombolytic therapy', *Journal of Thrombosis and Thrombolysis,* 23(1), pp. 9-23.

Kuzmic, P. (1996) 'Program DYNAFIT for the analysis of enzyme kinetic data: Application to HIV proteinase', *Analytical Biochemistry,* 237(2), pp. 260-273.

Lahteenmaki, K., Kuusela, P. and Korhonen, T. K. (2001) 'Bacterial plasminogen activators and receptors', *Fems Microbiology Reviews,* 25(5), pp. 531-552.

Lambris, J. D., Ricklin, D. and Geisbrecht, B. V. (2008) 'Complement evasion by human pathogens', *Nature Reviews Microbiology,* 6(2), pp. 132-142.

Law, Ruby H. P., Caradoc-Davies, T., Cowieson, N., Horvath, Anita J., Quek, Adam J., Encarnacao, Joanna A., Steer, D., Cowan, A., Zhang, Q., Lu, Bernadine G. C., Pike, Robert N., Smith, A. I., Coughlin, Paul B. and Whisstock, James C. 'The X-ray Crystal Structure of Full-Length Human Plasminogen', *Cell Reports,* 1(3), pp. 185-190.

Longitude Prize Open (2015). Available at: https://longitudeprize.org/.

Longstaff, C. and Gaffney, P. J. (1991) 'Serpin-serine protease binding kinetics: .alpha.2-antiplasmin as a model inhibitor', *Biochemistry,* 30(4), pp. 979-986.

Longstaff, C. and Kolev, K. (2015) 'Basic mechanisms and regulation of fibrinolysis', *Journal of Thrombosis and Haemostasis,* 13, pp. S98-S105.

Longstaff, C., Merton, R. E. and Sinniger, V. (1995) 'A comparison of cultured-cells with other promoters of tissue-plasminogen activator kinetics', *Fibrinolysis,* 9(3), pp. 178-187.

Longstaff, C. and Thelwell, C. (2005) 'Understanding the enzymology of fibrinolysis and improving thrombolytic therapy', *Febs Letters,* 579(15), pp. 3303-3309.

Longstaff, C., Thelwell, C., Williams, S. C., Silva, M., Szabo, L. and Kolev, K. (2011) 'The interplay between tissue plasminogen activator domains and fibrin structures in the regulation of fibrinolysis: kinetic and microscopic studies', *Blood,* 117(2), pp. 661-668.

Longstaff, C. and Whitton, C. M. (2004) 'A proposed reference method for plasminogen activators that enables calculation of enzyme activities in S1 units', *Journal of Thrombosis and Haemostasis,* 2(8), pp. 1416-1421.

Loof, T. G., Deicke, C. and Medina, E. (2014) 'The role of coagulation/fibrinolysis during Streptococcus pyogenes infection', *Frontiers in Cellular and Infection Microbiology,* 4, pp. 8.

Loof, T. G., Morgelin, M., Johansson, L., Oehmcke, S., Olin, A. I., Dickneite, G., Norrby-Teglund, A., Theopold, U. and Herwald, H. (2011) 'Coagulation, an ancestral serine protease cascade, exerts a novel function in early immune defense', *Blood,* 118(9), pp. 2589-2598.

Loof, T. G., Morgelin, M., Johansson, L., Rohde, M., Dickneite, G., Norrby-Teglund, A., Chhatwal, G. S. and Herwald, H. (2012) 'Coagulation factor XIII crosslinks surface

proteins of Streptococcus pyogenes to the fibrin network - an early host defense mechanism', *International Journal of Medical Microbiology,* 302, pp. 38-38.

Lucas, M. A., Fretto, L. J. and McKee, P. A. (1983) 'The binding of human plasminogen to fibrin and fibrinogen', *J Biol Chem,* 258(7), pp. 4249-56.

Macheboeuf, P., Buffalo, C., Fu, C. Y., Zinkernagel, A. S., Cole, J. N., Johnson, J. E., Nizet, V. and Ghosh, P. (2011) 'Streptococcal M1 protein constructs a pathological host fibrinogen network', *Nature,* 472(7341), pp. 64-U89.

Malakhov, M. P., Mattern, M. R., Malakhova, O. A., Drinker, M., Weeks, S. D. and Butt, T. R. (2004) 'SUMO fusions and SUMO-specific protease for efficient expression and purification of proteins', *Journal of Structural and Functional Genomics,* 5(1-2), pp. 75-86.

Marder, V. J. (2012) *Hemostasis and Thrombosi: Basic Principles and Clinical Practice.* 6th edn. Philadelphia, USA: Lippincott Williams and Wilkins.

Markland, F. S. (1998) 'Snake venoms and the hemostatic system', *Toxicon,* 36(12), pp. 1749-1800.

McAdow, M., DeDent, A. C., Emolo, C., Cheng, A. G., Kreiswirth, B. N., Missiakas, D. M. and Schneewind, O. (2012a) 'Coagulases as Determinants of Protective Immune Responses against Staphylococcus aureus', *Infection and Immunity,* 80(10), pp. 3389-3398.

McAdow, M., Kim, H. K., DeDent, A. C., Hendrickx, A. P. A., Schneewind, O. and Missiakas, D. M. (2011) 'Preventing Staphylococcus aureus Sepsis through the Inhibition of Its Agglutination in Blood', *Plos Pathogens,* 7(10).

McAdow, M., Missiakas, D. M. and Schneewind, O. (2012b) 'Staphylococcus aureus Secretes Coagulase and von Willebrand Factor Binding Protein to Modify the Coagulation Cascade and Establish Host Infections', *Journal of Innate Immunity,* 4(2), pp. 141-148.

McArthur, J. D., McKay, F. C., Ramachandran, V., Shyam, P., Cork, A. J., Sanderson-Smith, M. L., Cole, J. N., Ringdahl, U., Sjobring, U., Ranson, M. and Walker, M. J. (2008) 'Allelic variants of streptokinase from Streptococcus pyogenes display functional differences in plasminogen activation', *Faseb Journal,* 22(9), pp. 3146-3153.

McKay, F. C., McArthur, J. D., Sanderson-Smith, M. L., Gardam, S., Currie, B. J., Sriprakash, K. S., Fagan, P. K., Towers, R. J., Batzloff, M. R., Chhatwal, G. S., Ranson, M. and Walker, M. J. (2004a) 'Plasminogen binding by group A streptococcal isolates from a region of hyperendemicity for streptococcal skin infection and a high incidence of invasive infection', *Infection and Immunity,* 72(1), pp. 364-370.

McKay, J., Mensah, G. A., Mendis, S. and Greelund, K. 2004b. The atlas of heart disease and stroke. Geneva: World Health Organization.

Medcalf, R. L. (2012) 'Desmoteplase: discovery, insights and opportunities for ischaemic stroke', *British Journal of Pharmacology,* 165(1), pp. 75-89.

Medved, L. and Nieuwenhuizen, W. (2003) 'Molecular mechanisms of initiation of fibrinolysis by fibrin', *Thrombosis and Haemostasis,* 89(3), pp. 409-419.

Meh, D. A., Mosesson, M. W., DiOrio, J. P., Siebenlist, K. R., Hernandez, I., Amrani, D. L. and Stojanovich, L. (2001) 'Disintegration and reorganization of fibrin networks during tissue-type plasminogen activator-induced clot lysis', *Blood Coagulation & Fibrinolysis,* 12(8), pp. 627-637.

Mendes, P. (1993) 'GEPASI – A software package for modelling the dynamics, steady-states and control of biochemical and other systems', *Computer Applications in the Biosciences,* 9(5), pp. 563-571.

Mendes, P. (1997) 'Biochemistry by numbers: simulation of biochemical pathways with Gepasi 3', *Trends in Biochemical Sciences,* 22(9), pp. 361-363.

Nieuwenhuizen, W. (2001) 'Fibrin-mediated plasminogen activation', *Fibrinogen,* 936, pp. 237-246.

Nieuwenhuizen, W., Voskuilen, M., Vermond, A., Hoegeedenobel, B. and Traas, D. W. (1988) 'The influence of fibrin(ogen) fragments on the kinetic-parameters of the tissue-type plasminogen-activator-mediated activation of different forms of plasminogen', *European Journal of Biochemistry,* 174(1), pp. 163-169.

Nolan, M., Bouldin, S. D. and Bock, P. E. (2013) 'Full Time Course Kinetics of the Streptokinase-Plasminogen Activation Pathway', *Journal of Biological Chemistry,* 288(41), pp. 29482-29493.

O'Neill, J. 2014. Antimicrobial Resistance: Tackling a crisis for the health and wealth of nations. AMR.

Pahlman, L. I., Morgelin, M., Kasetty, G., Olin, A. I., Schmidtchen, A. and Herwald, H. (2013) 'Antimicrobial activity of fibrinogen and fibrinogen-derived peptides - a novel link between coagulation and innate immunity', *Thrombosis and Haemostasis,* 109(5), pp. 930-939.

Panizzi, P., Friedrich, R., Fuentes-Prior, P., Bode, W. and Bock, P. E. (2004) 'The staphylocoagulase family of zymogen activator and adhesion proteins', *Cellular and Molecular Life Sciences,* 61(22), pp. 2793-2798.

Panizzi, P., Friedrich, R., Prior, P. F., Richter, K., Bock, P. E. and Bode, W. (2006) 'Fibrinogen substrate recognition by Staphylocoagulase center dot(pro) thrombin complexes', *Journal of Biological Chemistry,* 281(2), pp. 1179-1187.

Panizzi, P., Nahrendorf, M., Figueiredo, J. L., Panizzi, J., Marinelli, B., Iwamoto, Y., Keliher, E., Maddur, A. A., Waterman, P., Kroh, H. K., Leuschner, F., Aikawa, E., Swirski, F. K., Pittet, M. J., Hackeng, T. M., Fuentes-Prior, P., Schneewind, O., Bock, P. E. and Weissleder, R. (2011) 'In vivo detection of Staphylococcus aureus endocarditis by targeting pathogen-specific prothrombin activation', *Nature Medicine,* 17(9), pp. 1142-U153.

Parry, M. A. A., Zhang, X. C. and Bode, W. (2000) 'Molecular mechanisms of plasminogen activation: bacterial cofactors provide clues', *Trends in Biochemical Sciences,* 25(2), pp. 53-59.

Pisano, J. J., Finlayson, J. S. and Peyton, M. P. 1968. Cross-link in Fibrin Polymerized by Factor XIII: ε-(γ -Glutamyl)lysine. Science.

Reed, G. L., Houng, A. K., Liu, L., Parhami-Seren, B., Matsueda, L. H., Wang, S. G. and Hedstrom, L. (1999) 'A catalytic switch and the conversion of streptokinase to a fibrin-targeted plasminogen activator', *Proceedings of the National Academy of Sciences of the United States of America,* 96(16), pp. 8879-8883.

Ringdahl, U., Svensson, H. G., Kotarsky, H., Gustafsson, M., Weineisen, M. and Sjobring, U. (2000) 'A role for the fibrinogen-binding regions of streptococcal M proteins in phagocytosis resistance', *Molecular Microbiology,* 37(6), pp. 1318-1326.

Ringdahl, U., Svensson, M., Wistedt, A. C., Renne, T., Kellner, R., Muller-Esterl, W. and Sjobring, U. (1998) 'Molecular co-operation between protein PAM and streptokinase for plasmin acquisition by Streptococcus pyogenes', *Journal of Biological Chemistry,* 273(11), pp. 6424-6430.

Sands, D., Whitton, C. M. and Longstaff, C. (2004) 'International collaborative study to establish the 3rd International Standard for Streptokinase', *Journal of Thrombosis and Haemostasis,* 2(8), pp. 1411-1415.

Sands, D., Whitton, C. M., Merton, R. E. and Longstaff, C. (2002) 'A collaborative study to establish the 3(rd) international standard for tissue plasminogen activator', *Thrombosis and Haemostasis,* 88(2), pp. 294-297.

Sarkar, D. (2008) *Lattice Multivariate Data Visualization with R. Use R!* New York: Springer-Verlag.

Sazonova, I. Y., Robinson, B. R., Gladysheva, I. P., Castellino, F. J. and Reed, G. L. (2004) 'alpha domain deletion converts streptokinase into a fibrin-dependent plasminogen activator through mechanisms akin to staphylokinase and tissue plasminogen activator', *Journal of Biological Chemistry,* 279(24), pp. 24994-25001.

Schneider, M. and Nesheim, M. (2004) 'A study of the protection of plasmin from antiplasmin inhibition within an intact fibrin clot during the course of clot lysis', *Journal of Biological Chemistry,* 279(14), pp. 13333-13339.

Shannon, O., Rydengard, V., Schmidtchen, A., Morgelin, M., Alm, P., Sorensen, O. E. and Bjorck, L. (2010) 'Histidine-rich glycoprotein promotes bacterial entrapment in clots and decreases mortality in a mouse model of sepsis', *Blood,* 116(13), pp. 2365-2372.

Silva, M., Thelwell, C., Williams, S. C. and Longstaff, C. (2012) 'Regulation of fibrinolysis by C-terminal lysines operates through plasminogen and plasmin but not tissue-type plasminogen activator', *Journal of Thrombosis and Haemostasis,* 10(11), pp. 2354-2360.

Steer, A. C., Law, I., Matatolu, L., Beall, B. W. and Carapetis, J. R. (2009) 'Global emm type distribution of group A streptococci: systematic review and implications for vaccine development', *Lancet Infectious Diseases,* 9(10), pp. 611-616.

Stewart, R. J., Fredenburgh, J. C. and Weitz, J. I. (1998) 'Characterization of the interactions of plasminogen and tissue and vampire bat plasminogen activators with fibrinogen, fibrin, and the complex of D-dimer noncovalently linked to fragment E', *J Biol Chem,* 273(29), pp. 18292-9.

Stief, T. W., Kretschmer, V., Kosche, B., Doss, M. O. and Renz, H. (2001) 'Thrombin converts singlet oxygen (O-1(2))-oxidized fibrinogen into a soluble t-PA cofactor - A new method for preparing a stimulator for functional t-PA assays', *Annals of Hematology,* 80(4), pp. 189-194.

Sun, H. (2011) 'Exploration of the host haemostatic system by group A streptococcus: implications in searching for novel antimicrobial therapies', *Journal of Thrombosis and Haemostasis,* 9, pp. 189-194.

Sun, H. M. (2006) 'The interaction between pathogens and the host coagulation system', *Physiology,* 21, pp. 281-288.

Sun, H. M., Ringdahl, U., Homeister, J. W., Fay, W. P., Engleberg, N. C., Yang, A. Y., Rozek, L. S., Wang, X. X., Sjobring, U. and Ginsburg, D. (2004) 'Plasminogen is a critical host pathogenicity factor for group A streptococcal infection', *Science,* 305(5688), pp. 1283-1286.

Sun, H. M., Xu, Y. X., Sitkiewicz, I., Ma, Y. B., Wang, X. X., Yestrepsky, B. D., Huang, Y. P., Lapadatescu, M. C., Larsen, M. J., Larsen, S. D., Musser, J. M. and Ginsburg, D. (2012) 'Inhibitor of streptokinase gene expression improves survival after group A streptococcus infection in mice', *Proceedings of the National Academy of Sciences of the United States of America,* 109(9), pp. 3469-3474.

Svensson, M. D., Sjobring, U., Luo, F. and Bessen, D. E. (2002) 'Roles of the plasminogen activator streptokinase and the plasminogen-associated M protein in an experimental model for streptococcal impetigo', *Microbiology-Sgm,* 148, pp. 3933-3945.

Swenson, S. and Markland, F. S. (2005) 'Snake venom fibrin(ogen)olytic enzymes', *Toxicon,* 45(8), pp. 1021-1039.

Takada, A., Mochizuki, K. and Takada, Y. (1980) 'Effects of SK-potentiator and fibrinogen on SK-plasminogen complex in the presence of tranexamic acid', *Thrombosis Research,* 19(6), pp. 767-773.

Takada, Y. and Takada, A. (1989a) 'Evidence for the formation of a trimolecular complex between streptokinase, plasminogen and fibrinogen', *Thrombosis Research,* 53(4), pp. 409-415.

Takada, Y. and Takada, A. (1989b) 'The conversion of streptokinase-plasminogen complex to SK-plasmin complex in the presence of fibrin or fibrinogen', *Thrombosis Research,* 54(2), pp. 133-139.

Thelwell, C. (2010) 'Global health risk associated with the use of recombinant streptokinase as a biosimilar for thrombolytic therapy', *Journal of Thrombosis and Haemostasis,* 8, pp. 30-30.

Thelwell, C. and Longstaff, C. (2007) 'The regulation by fibrinogen and fibrin of tissue plasminogen activator kinetics and inhibition by plasminogen activator inhibitor 1', *Journal of Thrombosis and Haemostasis,* 5(4), pp. 804-811.

Thelwell, C. and Longstaff, C. (2014) 'Biosimilars: the process is the product. The example of recombinant streptokinase', *Journal of Thrombosis and Haemostasis,* 12(8), pp. 1229-1233.

Undas, A. and Ariens, R. A. S. (2011) 'Fibrin Clot Structure and Function A Role in the Pathophysiology of Arterial and Venous Thromboembolic Diseases', *Arteriosclerosis Thrombosis and Vascular Biology,* 31(12), pp. E88-E99.

Vanassche, T., Hoylaerts, M. and Verhamme, P. (2013a) 'Staphylothrombin-mediated fibrin facilitates s. aureus-platelet interactions', *Journal of Thrombosis and Haemostasis,* 11, pp. 22-22.

Vanassche, T., Kauskot, A., Verhaegen, J., Peetermans, W. E., van Ryn, J., Schneewind, O., Hoylaerts, M. F. and Verhamme, P. (2012) 'Fibrin formation by staphylothrombin facilitates Staphylococcus aureus-induced platelet aggregation', *Thrombosis and Haemostasis,* 107(6), pp. 1107-1121.

Vanassche, T., Peetermans, M., Van Aelst, L. N. L., Peetermans, W. E., Verhaegen, J., Missiakas, D. M., Schneewind, O., Hoylaerts, M. F. and Verhamme, P. (2013b) 'The Role of Staphylothrombin-Mediated Fibrin Deposition in Catheter-Related Staphylococcus aureus Infections', *Journal of Infectious Diseases,* 208(1), pp. 92-100.

Vanassche, T., Verhaegen, J., Peetermans, W. E., Hoylaerts, M. F. and Verhamme, P. (2010) 'Dabigatran Inhibits Staphylococcus aureus Coagulase Activity', *Journal of Clinical Microbiology,* 48(11), pp. 4248-4250.

Vanassche, T., Verhaegen, J., Peetermans, W. E., Van Ryn, J., Cheng, A., Schneewind, O., Hoylaerts, M. F. and Verhamme, P. (2011) 'Inhibition of staphylothrombin by dabigatran reduces Staphylococcus aureus virulence', *Journal of Thrombosis and Haemostasis,* 9(12), pp. 2436-2446.

Varju, I., Longstaff, C., Szabo, L., Farkas, A. Z., Varga-Szabo, V. J., Tanka-Salamon, A., Machovich, R. and Kolev, K. (2015) 'DNA, histones and neutrophil extracellular traps exert anti-fibrinolytic effects in a plasma environment', *Thrombosis and Haemostasis,* 113(6), pp. 1289-1299.

Verhamme, I. M. and Bock, P. E. (2008) 'Rapid-reaction kinetic characterization of the pathway of streptokinase-plasmin catalytic complex formation', *Journal of Biological Chemistry,* 283(38), pp. 26137-26147.

Verstraete, M. (2000) 'Third-generation thrombolytic drugs', *American Journal of Medicine,* 109(1), pp. 52-58.

Walker, M. J., McArthur, J. D., McKay, F. and Ranson, M. (2005) 'Is plasminogen deployed as a Streptococcus pyogenes virulence factor?', *Trends in Microbiology,* 13(7), pp. 308-313.

Wang, S. G., Reed, G. L. and Hedstrom, L. (1999) 'Deletion of Ile1 changes the mechanism of streptokinase: Evidence for the molecular sexuality hypothesis', *Biochemistry,* 38(16), pp. 5232-5240.

Wang, S. G., Reed, G. L. and Hedstrom, L. (2000) 'Zymogen activation in the streptokinase-plasminogen complex - Ile1 is required for the formation of a functional active site', *European Journal of Biochemistry,* 267(13), pp. 3994-4001.

Wang, X. Q., Lin, X. L., Loy, J. A., Tang, J. and Zhang, X. J. C. (1998) 'Crystal structure of the catalytic domain of human plasmin complexed with streptokinase', *Science,* 281(5383), pp. 1662-1665.

Wang, Z., Wilhelmsson, C., Hyrsl, P., Loof, T. G., Dobes, P., Klupp, M., Loseva, O., Morgelin, M., Ikle, J., Cripps, R. M., Herwald, H. and Theopold, U. (2010) 'Pathogen Entrapment by Transglutaminase-A Conserved Early Innate Immune Mechanism', *Plos Pathogens,* 6(2).

Xue, Y., Bodin, C. and Olsson, K. (2012) 'Crystal structure of the native plasminogen reveals an activation-resistant compact conformation', *Journal of Thrombosis and Haemostasis,* 10(7), pp. 1385-1396.

Yang, Z., Mochalkin, I. and Doolittle, R. F. 2000. A model of fibrin formation based on crystal structures of fibrinogen and fibrin fragments complexed with synthetic peptides. Proceedings of the National Academy of Sciences.

Zhang, Y., Liang, Z., Hsueh, H. T., Ploplis, V. A. and Castellino, F. J. (2012) 'Characterization of streptokinases from group A Streptococci reveals a strong functional relationship that supports the coinheritance of plasminogen-binding M protein and cluster 2b streptokinase', *J Biol Chem,* 287(50), pp. 42093-103.

Zhang, Y. L., Liang, Z., Glinton, K., Ploplis, V. A. and Castellino, F. J. (2013) 'Functional differences between Streptococcus pyogenes cluster 1 and cluster 2b streptokinases are determined by their beta-domains', *Febs Letters,* 587(9), pp. 1304-1309.

Appendix

Appendix 1: R script to produce clot lysis profiles and parameters for analysis of fibrinolysis assays in Chapters 2 and 3.

Kindly provided by Colin Longstaff, personal communication.

```
#Plate reader data is saved as .txt in Excel, here in C:\Tempdata\2013 folder, with a chosen name

#Results are written to C:\Tempdata\2013\Results folder


rm(list=ls())                                   #wipes all variables in memory


##                                              ADJUST SETTINGS IN SECTIONS 1-4 FOR YOUR DATA

##                                              ADDING A # MEANS THE LINE IS IGNORED

##                                              DELETING A # MEANS THE LINE WILL BE READ


##1.  SELECT TARGET FILE

target<- "C://Tempdata/sianclots.txt"  # A nice set of sample data

#target<- "C://Tempdata//2013//June10Actilyse1.txt" # insert the name of the file saved in target directory

plate1<- read.table(target, header=TRUE)
```

```
##OR Alternative file selection mechanism (seems not to work with 64 bit Windows!)

#library (RODBC)

#newtarget<- odbcConnectExcel(file.choose())

#plate1<-sqlFetch(newtarget,"Sheet1")

#odbcClose(newtarget)


attach(plate1)

Names<-as.vector(names(plate1))



##2.  FILL IN THESE PARAMETERS TO DESCRIBE THE DATA SHEET

nabsCols=2                                  #number of columns
before absorbance readings

absCols=96                                  #number of columns of
absorbance readings-best stick to 96 if possible

tint=30                                     #interval between
readings in s

delay=0                                     #optional delay to first
reading

RowNum=8                                    #For a normal plate will be
8 but can be changed to generate a different layout of results
```

##3. PLOTTING SETTINGS

y0=0.065 #adjust this to make a sensible absorbance for 100% lysis for whole plate

xtrim=0.5 #make "trim" a fraction to truncate the xscale on the plotted graphs (does not affect results)

ytrim=1.2 #make "trim" a fraction to truncate the yscale on the plotted graphs (does not affect results)

#J=1 #choose this if you want labels from the Headers included in wells in your plot, e.g. A1=1200 etc.

J=0 #choose this if you just want the answer printed in the wells. e.g. 1200

##4. SELELCT THE RESULTS YOU WANT PRINTED ON THE PLOT AND IN THE CLIPBOARD

ALL THE OPTIONS ARE STORED IN FILES IN TEMPDATA\RESULTS (OR OTHER DIRECTORY AS SPECIFIED)

#z<-1 #choose for max Abs

#z<-2 #time to max Abs

#z<-3

lyspoint=50

#time to selected % lysis

```
#z<-4

#time to selected %lysis from peak

#z<-5

#time to complete lysis

z<-6

#sum of abs, like area under curve to full lysis


##The program goes to work!


absCol1<-nabsCols+1

dataCols<-absCols+nabsCols


vect1<-absCol1:dataCols

vect2<-absCol1:dataCols

vect3<-absCol1:dataCols

vect4<-absCol1:dataCols

vect5<-absCol1:dataCols

vect6<-absCol1:dataCols

vectz<-absCol1:dataCols
```

Appendix 2: R script to produce surface contour and heat maps for kinetic and simulated data in Chapter 4

Kindly provided by Colin Longstaff, personal communication.

```
##Data are generated by gepasi

##Read from a text file containing OD values plus other columns

##Time is generated not read from the file


rm(list=ls())  #wipes all variables in memory


#setwd("Y:/Sian/Models")

#setwd("T:/Sian/Models")

setwd("C:/May 5")


##REAL DATA OCT 3

##FILL IN THESE PARAMETERS

nabsCols=1                  #number of columns before absorbance readings

absCols=88                  #number of columns of absorbance readings

tint=30                     #interval between readings

delta=0.1                   #delta in absorbance to calculate rate

absRows=absCols             #number of rows in results = 8 for plate, 96 for whole plate
```

```
Bfact=3.56e4              #conversion factor for abs to pM/s


xx3=c(30.3, 20.2, 13.5, 9.0, 6.0, 4.0, 2.66, 1.19, 0.79, 0.52, 0)

#Lxx<-log10(xx)

yy3=c(1.6, 0.8, 0.4, 0.2, 0.1, 0.05, 0.025, 0)

xxx3<-rep(xx3,length(yy3))

yyy3<-rep(yy3, each=length(xx3))

Lxxx3<-(log10(xxx3 + 1))


absCol1<-nabsCols+1

dataCols<-absCols+nabsCols

vect3<-absCol1:dataCols



targetO3<- "Data/OCT3.txt"

plate13<- read.table(targetO3, header=TRUE)



pointsnum<-length(plate13[,1])-1

tend=pointsnum*tint


Time<- seq(0,tend, by=tint)
```

```
tsq<-Time^2


par(mfrow=c(8,11))

par(mar=c(0.2,0.2,0.2,0.2))


x0<- 0

xend<- tend^2          #can be changed to a number make plots better

y0<- 0

yend<-delta

cropx=.006             #crop the plotted x axis

cropy=1                #crop the plotted y axis


for(i in absCol1:dataCols){

  yi<- plate13[,i]

  yic<- plate13[,i]-plate13[1,i]

  Yi<-yic[yic<delta]

  Tsq<-tsq[1:length(Yi)]

  regrCol<-lm(Yi~Tsq)

  #plot(Tsq,Yi,       col="red",       pch=20,xaxt="n",       yaxt="n",       xlim=c(x0,cropx*xend),
ylim=c(y0,cropy*yend))

  ##It is possible to change the plotting paramters here, x or y axis length etc

  #abline(regrCol)

  Res<-summary(regrCol)
```

```
  ODans<-Res$coef[2]
  ans<-signif(1e12*ODans/Bfact, digits=4)
  #legend(x0,yend,bty="n", ans)
  #text(cropx*tend^2/2, cropy*yend*0.9, ans)
  vect3[i-nabsCols]<-ans

}
mat3<- matrix(vect3, byrow=TRUE, nrow=absRows)
platemat3<-matrix(vect3, byrow=TRUE, nrow=8)
write.table(mat3, "clipboard", sep="\t", col.names=F, row.names=F)
write.table(platemat3, "C:/Tempdata/plateRes3.txt", sep="\t", col.names=F, row.names=F)
#print(paste(names(plate13[i]),"=", signif(Res$coef[2]*1e9, digits=4)))
#Results are in plateRes3.txt and in clipboard for pasting into ExcelTimeplate
#print(round(platemat3, digits=3))



nabsCols=1                  #number of columns before absorbance readings
absCols=88                      #number of columns of absorbance readings
tint=30                     #interval between readings
#delta=0.2                      #delta in absorbance to calculate rate
absRows=absCols                 #number of rows in results = 8 for plate, 96 for whole
plate
Bfact=3.56e4                #conversion factor for abs to pM/s
```

```
xx4=c(30.3, 20.2, 13.5, 9.0, 6.0, 4.0, 1.77, 1.19, 0.79, 0.52, 0)

yy4=c(1.6, 0.8, 0.4, 0.2, 0.1, 0.05, 0.025, 0)

xxx4<-rep(xx4,length(yy4))

yyy4<-rep(yy4, each=length(xx4))

Lxxx4<-(log10(xxx4 + 1))


absCol1<-nabsCols+1

dataCols<-absCols+nabsCols

vect4<-absCol1:dataCols



targetO4<- "Data/OCT4.txt"

plate14<- read.table(targetO4, header=TRUE)



pointsnum<-length(plate14[,1])-1

tend=pointsnum*tint


Time<- seq(0,tend, by=tint)

tsq<-Time^2
```

```
par(mfrow=c(8,11))

par(mar=c(0.2,0.2,0.2,0.2))


x0<- 0

xend<- tend^2          #can be changed to a number make plots better

y0<- 0

yend<-delta

cropx=.01              #crop the plotted x axis

cropy=1                #crop the plotted y axis


for(i in absCol1:dataCols){

  yi<- plate14[,i]

  yic<- plate14[,i]-plate14[1,i]

  Yi<-yic[yic<delta]

  Tsq<-tsq[1:length(Yi)]

  regrCol<-lm(Yi~Tsq)

  #plot(Tsq,Yi,      col="red",      pch=20,xaxt="n",      yaxt="n",      xlim=c(x0,cropx*xend),
ylim=c(y0,cropy*yend))

  ##It is possible to change the plotting paramters here, x or y axis length etc

  #abline(regrCol)

  Res<-summary(regrCol)

  ODans<-Res$coef[2]

  ans<-signif(1e12*ODans/Bfact, digits=4)
```

```
  #legend(x0,yend,bty="n", ans)
  #text(cropx*tend^2/2, cropy*yend*0.9, ans)
  vect4[i-nabsCols]<-ans

}
mat4<- matrix(vect4, byrow=TRUE, nrow=absRows)
platemat4<-matrix(vect4, byrow=TRUE, nrow=8)
write.table(mat4, "clipboard", sep="\t", col.names=F, row.names=F)
write.table(platemat4, "C:/Tempdata/plateRes4.txt", sep="\t", col.names=F, row.names=F)
#print(paste(names(plate14[i]),"=", signif(Res$coef[2]*1e9, digits=4)))
#Results are in plateRes4.txt and in clipboard for pasting into ExcelTimeplate
#print(round(platemat4, digits=3))
#print(round(platemat3, digits=3))

#######SIMULATED DATA

simtint=0.5                 #interval between readings
#delta=.2                   #delta in absorbance to calculate rate
NumSets<-11                 #take from gepasi set up
NumTempl<-NumSets^2
FirstRead<-1
EndTime<-600                #take from gepasi setup
```

```
NumGroups<-NumSets*EndTime/simtint

vect3s<-1:NumTempl

#Bfact=3.56e4          #conversion factor for OD/s2 to pM/s


#targetSO3<- "Sept 11 Pyo 1600 K.txt"

targetSO3<- "May 5 Pyo 1600 K.txt"


plate03s<- read.table(targetSO3, header=TRUE)

plate13S<-na.omit(plate03s)

#attach(plate13S)



#OD<-X.OD              ##simple name change

Time<-seq(0,EndTime,simtint)

tsq<-Time^2


tstart<-which(plate13S$OD==0)

tlast<-tstart+EndTime

Var13<-plate13S[,1]

Var23<-plate13S[,2]

vectempl3<-Var13[c(tstart)]

vectempl13<-vectempl3[1:NumSets]
```

```
vectempl23<-Var23[seq(NumGroups, length(Var13), NumGroups)]

write.table(vectempl13, "C:/Tempdata/Var13.txt", col.names=F, row.names=F)

write.table(vectempl23, "C:/Tempdata/Var23.txt", col.names=F, row.names=F)

SimF3<-rep(vectempl13,length(vectempl23))

SimG3<-rep(vectempl23, each=length(vectempl23))

SimFF3<-SimF3*1e6

SimGG3<-SimG3*1e6

LSimFF3<-(log10(SimFF3+1))


##Graphing

par(mfrow=c(11,11))

par(mar=c(0.2,0.2,0.2,0.2))


x0<- 0

xend<- EndTime^2     #can be changed to a number make plots better

y0<- 0

yend<-max(plate13S$OD)

cropx=1                  #crop the plotted x axis

cropy=.1                 #crop the plotted y axis


for(i in 1:NumTempl){

  yi<- plate13S$OD[tstart[i]:tlast[i]]
```

```
  Yi<-yi[yi<delta]
  Tsq<-tsq[1:length(Yi)]
  regrCol<-lm(Yi~Tsq)
  #plot(Tsq,Yi, col="red", pch=20,xaxt="n", yaxt="n", xlim=c(x0,cropx*xend), ylim=c(y0,cropy*yend))
  ##It is possible to change the plotting paramters here, x or y axis length etc
  #abline(regrCol)
  Res<-summary(regrCol)
  ODans<-Res$coef[2]
  ans<-signif(1e12*ODans/Bfact, digits=4)
  #text(cropx*xend/2, cropy*yend*0.9, ans)
  vect3s[i]<-ans
}
mat3s<- matrix(vect3s, byrow=TRUE, nrow=NumSets)
write.table(t(mat3s), "clipboard", sep="\t", col.names=F, row.names=F) # large datasets Clipboard overflows
write.table(mat3s, "C:/Tempdata/m.plateRes3.txt", sep="\t", col.names=F, row.names=F)
#detach(plate13S)
#Results are in m.plateRes3.txt and in clipboard for pasting
#print(round(mat3s, digits=3))
```

#######SIMULATED DATA 2

```
simtint=0.5                          #interval between readings

#delta=.1                    #delta in absorbance to calculate rate

NumSets<-11                  #take from gepasi set up

NumTempl<-NumSets^2

FirstRead<-1

EndTime<-600                 #take from gepasi setup

NumGroups<-NumSets*EndTime/simtint

vect4s<-1:NumTempl


targetSO4<- "May 5 Pyo 400 K.txt"


plate04<- read.table(targetSO4, header=TRUE)

plate14S<-na.omit(plate04)

#names(plate14)


#OD<-X.OD            ##simple name change

Time<-seq(0,EndTime,simtint)

tsq<-Time^2

##Make vectors for other variables

##Note, these are not numbers that can be read

##See accompanying file to generate real vectors from gepasi inputs
```

```
tstart<-which(plate14S$OD==0)

tlast<-tstart+EndTime

#vectempl<-X.F.i[seq(600, length(X.F.i), 600)]                    #alternative route

Var14<-plate14S[,1]

Var24<-plate14S[,2]

vectempl4<-Var14[c(tstart)]

vectempl14<-vectempl4[1:NumSets]

vectempl24<-Var24[seq(NumGroups, length(Var14), NumGroups)]

write.table(vectempl14, "C:/Tempdata/Var14.txt", col.names=F, row.names=F)

write.table(vectempl24, "C:/Tempdata/Var24.txt", col.names=F, row.names=F)

SimF4<-rep(vectempl14,length(vectempl24))

SimG4<-rep(vectempl24, each=length(vectempl24))

SimFF4<-SimF4*1e6

SimGG4<-SimG4*1e6

LSimFF4<-(log10(SimFF4+1))


##Graphing

par(mfrow=c(11,11))

par(mar=c(0.2,0.2,0.2,0.2))


x0<- 0
```

```
xend<- EndTime^2     #can be changed to a number make plots better

y0<- 0

yend<-max(plate14S$OD)

#cropx=1                 #crop the plotted x axis

#cropy=1                 #crop the plotted y axis


for(i in 1:NumTempl){

  yi<- plate14S$OD[tstart[i]:tlast[i]]

  Yi<-yi[yi<delta]

  Tsq<-tsq[1:length(Yi)]

  regrCol<-lm(Yi~Tsq)

  #plot(Tsq,Yi,        col="red",        pch=20,xaxt="n",        yaxt="n",        xlim=c(x0,cropx*xend),
ylim=c(y0,cropy*yend))

  ##It is possible to change the plotting paramters here, x or y axis length etc

  #abline(regrCol)

  Res<-summary(regrCol)

  ODans<-Res$coef[2]

  ans<-signif(1e12*ODans/Bfact, digits=4)

  #text(cropx*xend/2, cropy*yend*0.9, ans)

  vect4s[i]<-ans

}

mat4s<- matrix(vect4s, byrow=TRUE, nrow=NumSets)
```

```
write.table(t(mat4s), "clipboard", sep="\t", col.names=F, row.names=F) # large datasets Clipboard overflows

write.table(mat4s, "C:/Tempdata/m.plateRes4.txt", sep="\t", col.names=F, row.names=F)

#Results are in m.plateRes4.txt and in clipboard for pasting

#print(round(mat4s, digits=3))


##Interperlation


library(lattice)

library(akima)

gran<-25    # granularity of projection (number of tiles in surfaces)

inter_data4<-interp(Lxxx4, yyy4, vect4,xo=seq(min(Lxxx4), max(Lxxx4), length = gran), yo=seq(min(yyy4), max(yyy4), length = gran),linear=T,duplicate=T)

inter_data3<-interp(Lxxx3, yyy3, vect3,xo=seq(min(Lxxx3), max(Lxxx3), length = gran), yo=seq(min(yyy3), max(yyy3), length = gran),linear=T,duplicate=T)

inter_sim3<-interp(LSimFF3, SimGG3, vect3s,xo=seq(min(LSimFF3), max(LSimFF3), length = gran), yo=seq(min(SimGG3), max(SimGG3), length = gran),linear=T,duplicate=T)

inter_sim4<-interp(LSimFF4, SimGG4, vect4s,xo=seq(min(LSimFF4), max(LSimFF4), length = gran), yo=seq(min(SimGG4), max(SimGG4), length = gran),linear=T,duplicate=T)


AY<-inter_data3

BE<-inter_sim3

max.z<-c(max(AY$z), max(BE$z))
```

```
min.z<-c(min(AY$z), min(BE$z))

max.allz<-max(max.z)

min.allz<-min(min.z)


##GRAPHS

##use this to generate a single big plot

#FigMid<-c(0.1, 0.90, 0.1, 0.90)

#par(fig=FigMid)

#image(AY,  col=heat.colors(2500))

#contour(AY,  nlevels=10,  lwd=1,  labcex=1.2,  method="flattest",  xlab="Fgn",  ylab="Pgn",
vfont=c("sans serif", "bold"),add=T)    #optional contours on heat map


##These commands generate a 4 panel plot

FigUL<-c(0.05,0.5,0.5,0.95)

FigLL<-c(0.1,0.47, 0.1,.5)

FigUR<-c(0.55,1, 0.5,0.95)

FigLR<-c(0.6,.95, 0.1,0.5)


#LEFT

par(fig=FigUL)

persp(AY,  xlab="Fgn",  ylab="Pgn",  zlab="Rate",  xlim=c(0,1.5),  zlim=c(min.allz,max.allz),
theta=-50, phi=20, col="lightblue")
```

```
#persp(AY, xlab="Fgn", ylab="Pgn", zlab="Rate", zlim=range(AY, finite=TRUE), theta=-40,
phi=30, col="lightblue")

#text(0,0.3, targetO3)    #include this line to print file names

par(fig=FigLL, new=T)

image(AY, xlim=c(0,1.5), col=heat.colors(2500))

contour(AY, nlevels=12, lwd=1, labcex=1.2, method="flattest", vfont=c("sans serif",
"bold"),add=T)    #optional contours on heat map


#RIGHT

#PHI<-50

par(fig=FigUR, new=T)

#persp(BE, xlab="Fgn", ylab="Pgn", zlab="Rate", zlim=range(BE, finite=TRUE), theta=-40,
phi=30, col="lightblue")

BEpersp<-persp(BE, xlab="Fgn", ylab="Pgn", zlab="Rate", xlim=c(0,1.5),
zlim=c(min.allz,max.allz), theta=-50, phi=20, col="pink")

#BEpersp

#text(0,0.3, targetO3)    #include this line to print file names


par(fig=FigLR, new=T)

image(BE,  xlim=c(0,1.5),col=heat.colors(2500))

contour(BE,    nlevels=10,  lwd=1,  labcex=1.2,  method="flattest",  vfont=c("sans serif",
"bold"),add=T)   #optional contours on heat map
```

```
##These commants generate an spinning 3d plot and a snapshot of the final position

##The  figure can be dragged and rotated by the mouse and new snapshots taken


setwd("C://Tempdata")

require(rgl)

z2<-seq(11,71,1)

dur<-z2

for(ii in 1:length(z2)){persp3d(inter_data3,  xlab="Fgn", ylab="Pgn", zlab="Rate",   zlim=c(-10,
300), theta=-60, phi=30, col="lightblue")

                  play3d(spin3d(rpm=1), duration=dur-10 )

                 print(z2[ii])

                  snapshot3d(paste("Figdat",z2[ii],".png",sep=""))}

##SHOULD BE AN EASIER WAY?

#rgl.open()

#movie3d(spin3d(), duration=3, convert=FALSE)
```